SHORT TERM CONTRACT FOR BIOLOGICAL STUDIES (ICCAT GBYP 09/2016) OF THE ATLANTIC-WIDE RESEARCH PROGRAMME ON BLUEFIN TUNA (GBYP Phase 6)

Final Report

for:

ICCAT

Scientific coordinator:

Dr. Haritz Arrizabalaga (AZTI-Tecnalia)

Pasaia, February 16th, 2017

PARTNERS:

Fundación AZTI-AZTI Fundazioa

Instituto Español de Oceanografía

IFREMER

Universitá di Genova

University of Bologna

COMBIOMA

National Research Institute of Far Seas Fisheries

INRH

AquaBioTech Ltd.

Texas A&M University

NECTON

GMIT

IPMA

ISTANBUL UNIVERSITY

SUBCONTRACTORS and COLLABORATORS:

Dr. Isik Oray

CNRS (France)

Univ. Arizona (USA)

Sgiker/Ibercron (EHU, Spain)

BMR Genomics

Dr. Toshihide Kitakado (Japan)

IZOR (Croatia)

CNAG (Spain)

INDEX:

EXECUTIVE SUMMARY:.....6
1. CONTEXT.....10
2. SAMPLING.....11
2.1. Sampling acomplished.....11
3. ANALYSES.....22
4. OTOLITH CHEMISTRY.....23
4.1. Determining nursery origin of bluefin tuna captured in the potential mixing zones.....24
4.2. Individual origin assignment.....30
4.3. Discrimination of nursery areas within the Mediterranean Sea by trace element and stable isotope composition in young-of-the-year bluefin tuna and origin assignation of individuals from Bay of Biscay.....32
5. GENETICS.....41
5.1. Origin assignment of juveniles and adults captured at feeding aggregations throughout the Atlantic and over different years (GBYPPh6-Task1).....41
5.1.1. Introduction.....41
5.1.2. Methods.....41
5.1.3. Results and discussion.....46
5.1.4. Conclusions.....53
5.1.5. Future analyses.....54
5.2. Microsatellite genotyping of reference samples in the Mediterranean (Task 2) 55
5.2.1. Backgrounds and Aims.....55
5.2.2. Experimental design, sample selection and DNA extraction of Mediterranean YOY.....56
5.2.3. Microsatellite loci selection and setup.....57
5.2.4. Microsatellite PCR amplification and genotyping.....61
5.2.5. Microsatellite data analysis.....61

6. OTOLITH SHAPE 75
6.1. Introduction 75
6.2. Methods 76
6.3. Results and Discussion 78
7. INTEGRATED APPROACH TO STOCK DISCRIMINATION 83
7.1. Introduction 83
7.2. Methods 83
7.3. Results and Discussion 84
8. AGE DETERMINATION ANALYSES 93
8.1. Introduction 93
8.2. Material and Methods 93
8.3. Results and Discussion 95
9. APPENDICES 104

EXECUTIVE SUMMARY:

The main objective of this project is to enhance knowledge about Atlantic bluefin tuna population structure and mixing, but also to focus on age dynamics.

During Phase 6, following sampling protocols agreed in earlier Phases, the consortium sampled a total of 2439 bluefin tuna (570 YOY, 69 juveniles, 253 medium sized fish and 1547 large fish) from different regions (140 from the East Mediterranean, 171 from the Central Mediterranean, 1052 from the Western Mediterranean, 200 from the North Sea, 50 from the East Atlantic - West African coast, 57 from the Northeast Atlantic, 719 from the Central North Atlantic, and 50 from the North-Western Atlantic). In total, 4092 biological samples were taken (1929 genetic samples, 1060 otoliths and 1103 spines). The consortium also received samples from other ICCAT contracts with tagging teams and farm operators. In total, the consortium handled 7352 samples from 3551 individuals.

Regarding otolith microchemistry, new carbon and oxygen stable isotope analyses were carried out in 145 otoliths of Atlantic bluefin tuna captured in the central Atlantic Ocean (both east of and west of 45ºW), Canary Islands and Morocco, to determine their nursery area. δ13C and δ18O values measured in otolith cores indicated that these samples were dominated by eastern origin individuals. The comparative analysis with previous Phases suggests that important interannual variations in the mixing proportions can be observed, especially in some areas (e.g. west of 45ºW and Morocco), which warrants year to year monitoring. Additional samples from the Central Atlantic are being processed in order to shed some more light on this issue. Finally, using the baseline produced in Phase 5 using trace element and stable isotope composition in young-of-the-year (YOY), juveniles from the Bay of Biscay (belonging to the 2011 cohort, n=53) were determined to be born predominantly (75%) in the western-central Mediterranean, with a lower contribution (25%) from the Levantine Sea spawning area. Additional work to expand the baseline to the 2013 cohort is presented.

Regarding genetic analyses, 354 reference samples have been used to validate the RADSeq SNP panel. Using 90% as a threshold, 71% of the samples of Gulf of Mexico and Mediterranean origin are correctly assigned and 13 and 2% are incorrectly assigned, respectively. Unassigned samples are 16 and 27% for Gulf of Mexico and Mediterranean respectively. Decreasing assignment score threshold to 70% reduces the number of unassigned samples (5 and 10% for Gulf of Mexico and Mediterranean respectively), but increases the number of incorrect assignments (to 17 and 6% respectively). 256 of these samples have been RAD-sequenced and will be added to the baseline to further improve the pannel. Finally, 940 samples from mixing aggregations are been analyzed to provide a map of Bluefin mixing. Results so far are consistent with previous knowledge, with extensive Mediterranean origin individuals spread throughout the Atlantic, and some non-negligible proportions of western Atlantic Bluefin tuna in the Northeast Atlantic.

Regarding microsatellite analyses (Genetic Task 2), 385 BFT YOYs collected over 4 areas of the Mediterranean in 2012 and 2013 have been genotyped at 33 BFT-specific microsatellite loci, most of them already used to genetically profile Gulf of Mexico reference samples during a NOAA Bluefin Tuna Research Program. The results of this genetic survey indicate irrefutably the lack of significant genetic differentiation in the Mediterranean YOY BFTs and this lead to propose a panmictic BFT population in the Mediterranean, at least in the four main spawning areas where the YOY samples were collected. The indication of panmixia we got with this robust and deep analysis is coherent with the patterns provided by SNP markers on the same samples and with the recent results obtained with similar markers on subadults and adults. The quality and robustness of genetic data obtained in this task allow them to be further exploited in a broader research framework to test and measure again the genetic divergence between the two well-defined but subtly differentiated BFT populations from Gulf of Mexico and Mediterranean. This will be addressed by combining the Mediterranean dataset with that independently obtained by US scientists on the Gulf of Mexico early stages, using an unprecedented joint dataset of highest quality for the experimental design. An intercalibration activity with US Scientists is already ongoing and it will allow the merging of Mediterranean and Gulf of Mexico genetic data.

Regarding otolith shape analyses, adult Bluefin tuna (>170cm) from the Gulf of Mexico and Mediterranean spawning areas (central, west and east) could be distinguished on the basis of otolith shape with a mean jack-knife classification accuracy of 78% (76% for Gulf of Mexico and 80% for Mediterranean). The lower classification success compared to that achieved using baseline samples from the Canadian fishery and Malta (82% in Brophy et al 2015) suggests otolith shape is a better marker of environmental history than of natal origin. Otolith shape analysis could be more effectively used to characterize feeding areas and combined with other markers of natal origin (chemistry and genetics) or tagging information could be used to estimate the proportions within each spawning area that feed in the east and west Atlantic.

Regarding the integrated approach to stock discrimination, adult bluefin tuna (>170cm) from the Gulf of Mexico and Mediterranean spawning areas could be distinguished on the basis of stable isotope measurements (d18O, d13C) with a mean jack-knife classification accuracy of 95%. Combining otolith shape with microchemistry gave an overall minor (0.4%) improvement in accuracy for the baseline samples but increased the uncertainty of population assignments for individuals of unknown natal origin (from Portugal, Morocco and Straits of Gibraltar). Combining two SNP Rad loci (Rad 213 and Rad26) slightly improved (1.1%) the accuracy of the classification and increased assignment probabilities of individuals from the Gulf of Mexico in a test sample by 6% and individuals from the Mediterranean by 0.92%. Thus, combining otolith stable isotope signatures and genetic markers improves estimation of natal origin while otolith shape could provide additional information about trans-Atlantic migrations.

Regarding the age determination analyses during Phase 6, age has been interpreted from 315 calcified structures, 135 otoliths and 180 spines. To the extent possible, individuals that had been identified as of Mediterranean origin were included in the analysis (besides other criteria). Age length keys (ALKs) were built for this sixth phase of the project and for all samples coming from 2012 which were analyzed in present and previous phases.

Most of the objectives of the Project were met. The analyses already started to provide important information that is relevant for Atlantic bluefin tuna management. As such, project results will continue to feed the upcoming stock assessment and Management Strategy Evaluation (MSE) process.

1. CONTEXT

On June 30th 2016, the consortium coordinated by Fundación AZTI-AZTI Fundazioa, formed by partners Fundación AZTI-AZTI Fundazioa, Instituto Español de Oceanografía, IFREMER, Universitá di Genova, University of Bologna, COMBIOMA, National Research Institute of Far Seas Fisheries, AquaBio Tech Ltd., INRH, GMIT, Texas A&M University, IPMA, Istanbul University and Necton, with subcontracted parties University of Pau, University of Arizona, SGiker/Ibercron, Dr. Isik Oray and BMR Genomics, and Dr. Toshihide Kitakado as Collaborator, presented a proposal to the call for tenders on biological and genetic sampling and analysis (ICCAT-GBYP 09/2016).

This proposal was awarded on July 22nd 2016 and the final contract between ICCAT and the consortium represented by Fundación AZTI-AZTI Fundazioa was signed on September 23rd 2016. This contract was amended on December 13th 2016.

According to the terms of the contract, a final report (Deliverable nº 5) needs to be submitted to ICCAT by February 16th, considering the comments provided by ICCAT on the draft final report submitted on January 31st. This report was prepared in response to such contractual requirement.

2. SAMPLING

The sampling conducted under this project follows a specific design, aimed primarily at contributing to knowledge on population structure and mixing. As such, the sampling conducted under this project is independent from other routine sampling activities for fisheries and fishery resources monitoring (e.g. the Data Collection Framework). Some of the sampling activities included in this report were conducted under other GBYP contracts (i.e. as part of the tagging programs, or through specific contracts to sample in farms). These other contracts required that the samples be sent to AZTI to be merged within the biological tissue bank handled within this contract.

2.1. Sampling acomplished

A total of 2439 bluefin tuna individuals have been sampled by the Consortium. Table 2.1a shows the number of bluefin tuna sampled by the Consortium in each strata (area/size class combination), and Table 2.2a provides summaries by main region and size class.

In addition, the Consortium received sampled from other teams contracted by ICCAT to conduct biological sampling in farms or while tagging. Altogether, the Consortium handled samples from 3551 individuals (Table 2.1b, Table 2.2b and Figure 2.1).

The original plan, according to the Consortium contract, was to acquire samples from 1375 individuals. Thus the overall current sampling status represents 177% of the target in terms of total number of individuals.

By size class, the objectives for juvenile, medium and large fish were accomplished (>100%, >100% and 344% of the target respectively), but the final sampling for age 0 remains only at 65% with respect to the original target (see Table 2.2). It is necessary to note that, with the expection of the Adriatic, no sampling for juveniles and medium size fish was planned, but some individuals have been finally sampled in the Levantine Sea, East of Sicily and Ionian Sea, Tyrrhenian, Portugal and the Central Atlantic. With respect to adults, the overall target has been exceeded. Although sampling in the Levantine Sea, East Sicily and Ionian Sea, Malta, Ligurian Sea, and the Canary Islands were below the target, this was compensated by other areas where the target was exceeded (Balearics, Southern Spain, Tyrrhenian, Norway,

Portugal, UK-Ireland and the Central Atlantic), as well as areas where no sampling of adults was originally planned but some samples were finally obtained (Norway and Canada).

Table 2.1. Number of bluefin tuna sampled by area and size class. Empty cells indicate that no sampling was planned in that stratum. a) Individuals sampled by the consortium. b) Total number of individuals sampled (including those of the consortium plus the ones sampled under other contracts and stored by the Consortium).

a)

		Age 0	Juveniles	Medium	Large	Total		
		<3 kg	3-25 kg	25-100 kg	>100 kg		Target	%
Eastern Mediterranean	Levantine Sea	36		95	9	140	350	40%
Central Mediterranean	East Sicily and Ionian	21		50	50	121	150	81%
	Adriatic Sea		50			50	50	100%
	Malta					0	150	0%
	Gulf of Gabes					0	0	
Western Mediterranean	Balearic	218				218	125	174%
	Southern Spain	68				68	0	>100%
	Ligurian	20				20	50	40%
	Sardinia					0	0	
	Tyrrhenian Sea	207	19	89	431	746	300	249%
North Sea	Norway				200	200	0	>100%
East Atlantic-West African coast	Morocco					0	0	
	Madeira, Canary Islands	0			50	50	100	50%
Northeast Atlantic	Portugal			3	52	55	50	110%
	UK, Ireland				2	2	0	>100%
Central North Atlantic	Central and North Atlantic			16	703	719	50	1438%
North-Western Atlantic	Canada (Gulf Saint Lawrence)				50	50	0	>100%
	TOTAL	**570**	**69**	**253**	**1547**	2439	1375	177%

b)

		Age 0	Juveniles	Medium	Large	Total		
		<3 kg	3-25 kg	25-100 kg	>100 kg		Target	%
Eastern Mediterranean	Levantine Sea	36		95	9	140	350	40%
Central Mediterranean	East Sicily and Ionian	21		50	50	121	150	81%
	Adriatic Sea	0	50		0	50	50	100%
	Malta	0			277	277	150	185%
	Gulf of Gabes	0			207	207	0	>100%
Western Mediterranean	Balearic	218			545	763	125	610%
	Southern Spain	68			0	68	0	>100%
	Ligurian	20			0	20	50	40%
	Sardinia	0		6	21	27	0	#¡DIV/0!
	Tyrrhenian Sea	207	19	89	431	746	300	249%
North Sea	Norway	0			200	200	0	>100%
East Atlantic-West African coast	Morocco	6			50	56	0	#¡DIV/0!
	Madeira, Canary Islands	0			50	50	100	50%
Northeast Atlantic	Portugal	0		3	52	55	50	110%
	UK, Ireland	0			2	2	0	>100%
Central North Atlantic	Central and North Atlantic	0		16	703	719	50	1438%
North-Western Atlantic	Canada (Gulf Saint Lawrence)	0			50	50	0	>100%
	TOTAL	**576**	**69**	**259**	**2647**	3551	1375	258%

Table 2.2: Number of bluefin tuna sampled *by main region and size class. Empty cells indicate that no sampling was planned in that strata. a) Individuals sampled by the consortium. b) Total number of individuals sampled (including those of the consortium plus the ones sampled under other contracts and stored by the Consortium).*

a)

	Age 0	Juvenile	Medium	Large	TOTAL	Target	%wrt targ
Eastern Mediterranean	36		95	9	140	350	40%
Central Mediterranean	21	50	50	50	171	350	49%
Western Mediterranean	513	19	89	431	1052	475	221%
North Sea				200	200	0	>100%
East Atlantic - West African coast				50	50	100	50%
Northeast Atlantic			3	54	57	50	114%
Central North Atlantic			16	703	719	50	1438%
North-Western Atlantic				50	50	0	>100%
TOTAL	570	69	253	1547	2439	1375	177%
Target	875	50	0	450	1375		
% wrt target	65%	>100%	>100%	344%	177%		

b)

	Age 0	Juvenile	Medium	Large	TOTAL
Eastern Mediterranean	36		95	9	140
Central Mediterranean	21	50	50	534	655
Western Mediterranean	513	19	95	997	1624
North Sea				200	200
East Atlantic - West African coast	6			100	106
Northeast Atlantic			3	54	57
Central North Atlantic			16	703	719
North-Western Atlantic				50	50
TOTAL	576	69	259	2647	3551

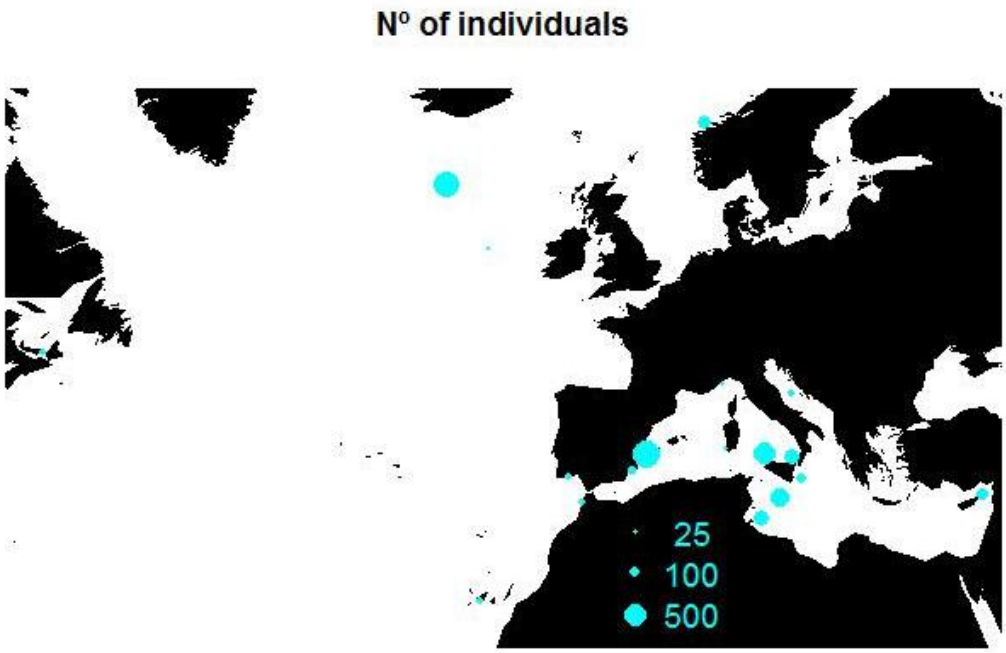

Figure 2.1: Total number of individuals sampled under all GBYP activities in Phase 6 in the Northeast Atlantic and Mediterranean, aggregated by main region. Positions of the dots are approximate averages across all samples.

The overall progress of the project was affected by the late award and signature of the contract, which came after many fisheries had already started or were already closed. Although members of the consortium tried to keep up with their tasks, the late signature of the contract affected mainly in those cases where travel, purchase and/or subcontracting costs were needed to accomplish the tasks. Yet, the sampling objectives were at least partially met.

In the Eastern Mediterranean, 40% of the target number of individuals (YOY and adults) has been sampled. The sampling for YOY in the Levantine Sea was below the original plan, with 36 individuals sampled (out of 50 planned) between July and September, mostly in the area near the Turkish-Syrian border. The lower than expected number of YOYs sampled this year is due to, under other potential reasons, the bad weather conditions and the prevailing disputes in Syria that did not allow normal fishing operations of small boats. Regarding adults, sampling conducted during tagging operations by Istanbul University was limited to three individuals dead during fishing operations. The majority of the sampling was scheduled for November-December, but there were problems to access the farms where the tagging operations were conducted. This required to reschedule the sampling in another farm (Group Sagun), in Cesme area, which started late January. Moreover, the success rate of getting

otoliths from these fish is very low far), due to the way they kill them (bullets seem to break them into many pieces).

As for the Central Mediterranean, 49% of the target number of individuals was sampled. The Univ. of Bologna sampled 21 (out of 150 planned) young of the year in East of Sicily and Ionian Sea, between September 2016 and January 2017. IZOR provided samples of 50 juveniles from the Adriatic. Regarding Malta, the national permit to get samples of young of the year through observers was delayed beyond August (the start of the dolphin fish fishing season when YOY can be caught). Moreover, bad weather conditions limited the number of trips where sampling was actually possible. As a result, no single YOY (out of 150 planned) were sampled in Malta. The sampling of adult fish in Malta and Gulf of Gabes (under a separate contract) worked succesfully, with several hundreds of fish being sampled in farms. These important samples have not phisically arrived yet, thus the numbers are subject to some modification.

In the Western Mediterranean, 221% of the target number of individuals was sampled, including fish from all sizes, but predominantly YOY and large fish. This year, the sampling in the Balearics and Southern Spain worked particularly well. The sampling of YOY by IEO was much better than expected (286 individuals sampled and 125 planned). In the southern Tyrrhenian, Necton has sampled 88 YOY in 2016 and provided additional individuals of all year classes from 2015. The Univ. of Bologna sampled additional 94 individuals. Likewise, in the Ligurian Sea, in the period from August to October, 20 YOY out of a target of 50 were sampled by the University of Genoa. The total sampling was not accomplished due to problems with weather conditions and reduced presence of YOY in the area. Regarding adults, NECTON sampled 50 medium and large adults in East of Sicily and Ionian Sea.

Under a separate contract, COMBIOMA provided some samples during their tagging survey in Sardinia (although below expectation), while ABT (through a separate ICCAT contract) sampled 484 individuals. In the Balearics, Taxon S.L. and Balfego Group sampled 283 and 262 adult individuals of Balearic origin in Spanish farms. Moreover, in this case the percent of otolith samples is high (399/545). From these, the percentage of whole otoliths is also high (around 67%), considering the size of the fish and the way they kill them.

In the East Atlantic-West African coast, 50% of the target number of individuals was sampled. Sampling of adults in the Canary Islands went as planned, but only 6 YOY (out of 50 planned) could be sampled in this region. The albacore fishery closure towards the end of the year 2016

kept most boats in port, and no signal of Bluefin YOY was detected after they returned to sea. In Morocco, the collaboration with tagging teams (INRH) went well and sampling of adult fish was conducted (under a separate contract).

In Portugal, IPMA, in collaboration with observers and Tunipex trap fishermen, conducted the sampling successfully. The objective was to sample 30 whole individuals, and on top of that, the tagging teams would provide 20 additional tissue samples. These objectives were met. Regarding otoliths, several (21/33) where broken by the bullet used to euthanize the fish, but all (33/33) contain the nucleus.

Furthermore, unexpected samples from Norway were obtained again (provided by IMR), as well as from the Gulf of Saint Lawrence (provided by collaborator J.L. Varela, Universidad de Cadiz/Universidad de Acadia).

In the Central Atlantic, the number of samples is much beyond the original expectation (n=719 compared to a target of n=50), most of them being large but including also some medium size fish, which will potentially allow for interesting insights into mixing of stocks.

Table 2.3: Number of samples collected by area and tissue type. a) Samples taken by the consortium. b) Total number of samples (including those of the consortium plus the ones taken under other contracts and stored by the Consortium).

a)

		Otolith	Spine	Muscle/Fin	Sampler
Eastern Mediterranean	Levantine Sea	41	140	133	ISTA/AZTI(Oray)
Central Mediterranean	East Sicily and Ionian	21	121	121	NECT/UNIB
	Adriatic Sea			50	AZTI(IZOR)
	Malta				ABT
	Gulf of Gabes				ABT
Western Mediterranean	Balearic	217	217	218	IEO/TAX/BALF
	Southern Spain	67	68	68	IEO
	Ligurian	19	20	20	UNIGE
	Sardinia				NECT/UNIM/UNIB
	Tyrrhenian Sea	218	309	309	ABT/COMBIOMA
North Sea	Norway		190	178	IMR
East Atlantic-West African coast	Morocco				INRH
	Madeira, Canary Islands	46		56	IEO
Northeast Atlantic	Portugal	33	38	55	IPMA
	UK, Ireland			2	IMR
Central North Atlantic	Central and North Atlantic	398		669	NRIFSF
North-Western Atlantic	Canada (Gulf Saint Lawrence)			50	UCA
	Total	**1060**	**1103**	**1929**	
			4092		

b)

		Otolith	Spine	Muscle/Fin	Sampler
Eastern Mediterranean	Levantine Sea	41	140	133	ISTA/AZTI(Oray)
Central Mediterranean	East Sicily and Ionian	21	121	121	NECT/UNIB
	Adriatic Sea			50	AZTI(IZOR)
	Malta	240		277	ABT
	Gulf of Gabes	151		207	ABT
Western Mediterranean	Balearic	616	755	760	IEO/TAX/BALF
	Southern Spain	67	68	68	IEO
	Ligurian	19	20	20	UNIGE
	Sardinia		22	27	NECT/UNIM/UNIB
	Tyrrhenian Sea	542	309	743	ABT/COMBIOMA
North Sea	Norway		190	178	IMR
East Atlantic-West African coast	Morocco	50		49	INRH
	Madeira, Canary Islands	46		56	IEO
Northeast Atlantic	Portugal	33	38	55	IPMA
	UK, Ireland			2	IMR
Central North Atlantic	Central and North Atlantic	398		669	NRIFSF
North-Western Atlantic	Canada (Gulf Saint Lawrence)			50	UCA
	Total	**2224**	**1663**	**3465**	
			7352		

Table 2.4: Number of samples by main region and tissue type. a) Samples taken by the consortium. b) Total number of samples (including those of the consortium plus the ones taken under other contracts and stored by the Consortium).

a)

	Otolith	Spine	Muscle/Fin	TOTAL
Eastern Mediterranean	41	140	133	314
Central Mediterranean	21	121	171	313
Western Mediterranean	521	614	615	1750
North Sea		190	178	368
East Atlantic - West African coast	46		56	102
Northeast Atlantic	33	38	57	128
Central North Atlantic	398		669	1067
North-Western Atlantic			50	50
TOTAL	**1060**	**1103**	**1929**	**4092**
Target	1305	1255	1375	3935
% wrt target	81%	88%	140%	104%

b)

	Otolith	Spine	Muscle/Fin	TOTAL
Eastern Mediterranean	41	140	133	314
Central Mediterranean	412	121	655	1188
Western Mediterranean	1244	1174	1618	4036
North Sea		190	178	368
East Atlantic - West African coast	96		105	201
Northeast Atlantic	33	38	57	128
Central North Atlantic	398		669	1067
North-Western Atlantic			50	50
TOTAL	**2224**	**1663**	**3465**	**7352**

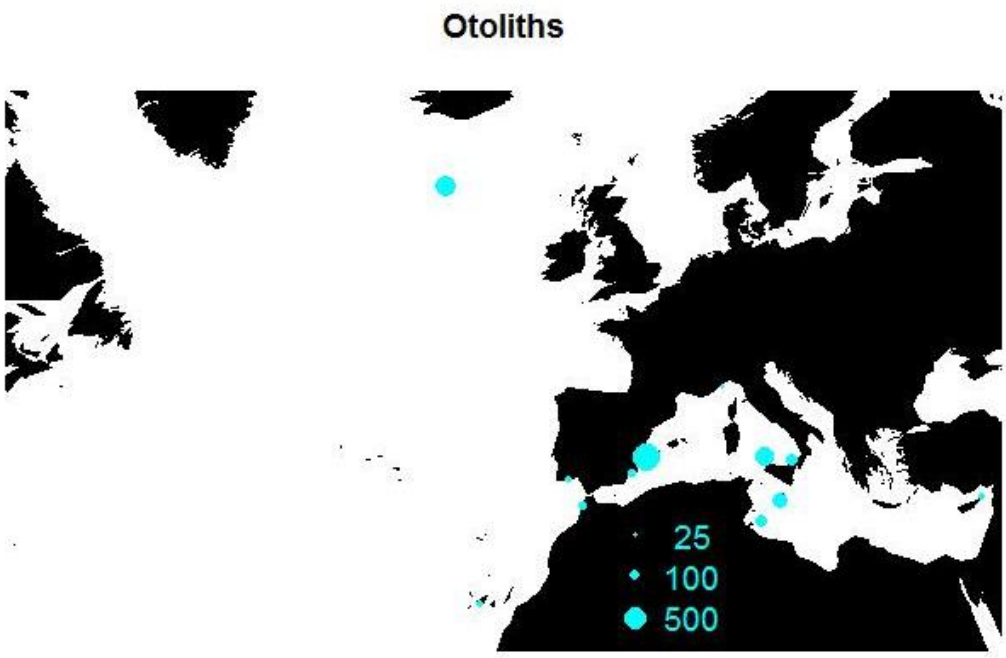

Figure 2.2: Total number of individuals with otolith sampling conducted under all GBYP activities in Phase 6 in the Northeast Atlantic and Mediterranean, aggregated by main region. Positions of the dots are approximate averages across all samples.

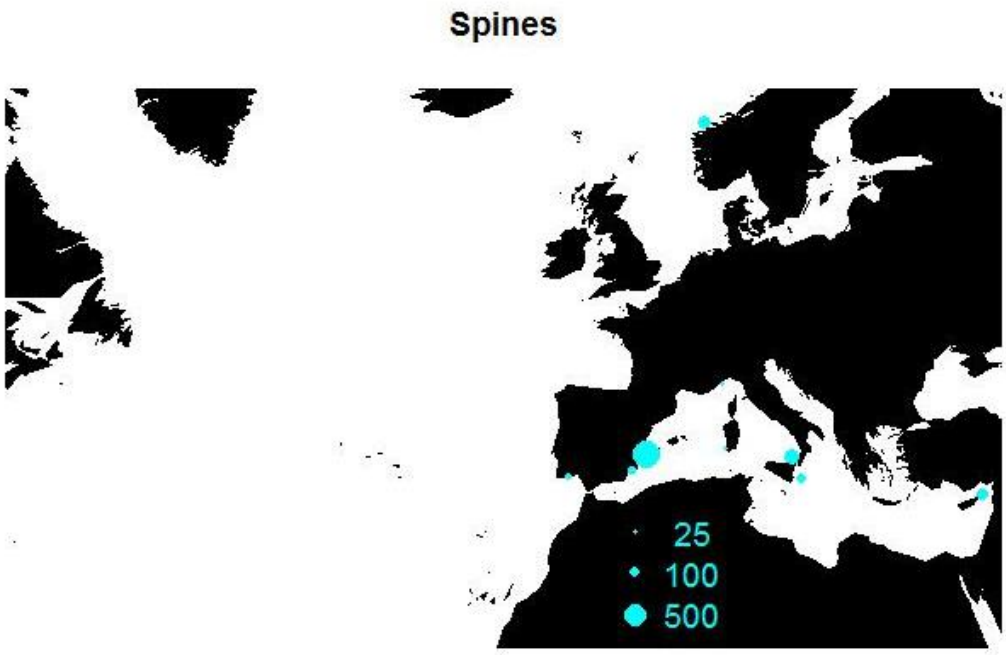

Figure 2.3: Total number of spines collected under all GBYP activities in Phase 6 in the Northeast Atlantic and Mediterranean, aggregated by main region. Positions of the dots are approximate averages across all samples.

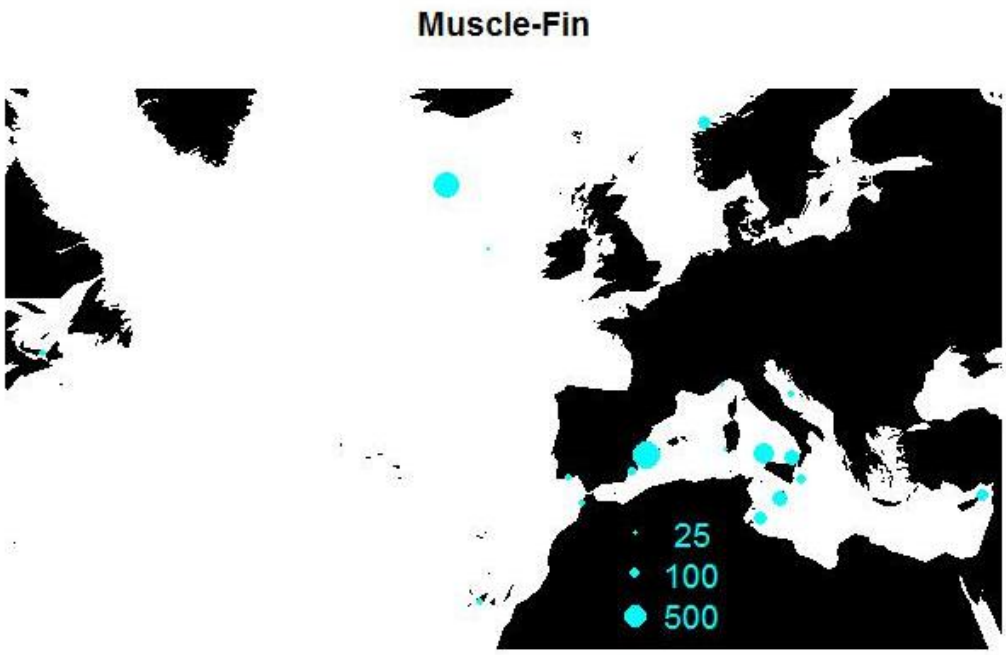

Figure 2.4: Total number of muscle or fin tissue samples collected under all GBYP activities in Phase 6 in the Northeast Atlantic and Mediterranean, aggregated by main region. Positions of the dots are approximate averages across all samples.

3. ANALYSES

In the proposal, the consortium proposed to conduct 200 stable isotope analyses on adult otoliths with subsequent individual assignments to origin, 140 trace element and stable isotope analyses on reference samples, 1334 genetic analyses with RAD-Seq, 320 genetic analyses with microsatellites, 300 otolith images for shape analyses and 300 age assignments.

As reflected in Deliverable 3, the late start of the contract affected the ability of some partners to conduct sampling in specific areas, send samples to AZTI, proceed with planned subcontracts, etc. Moreover, some technical difficulties (e.g. failure of the micromill and a saw used to slice the otoliths) further delayed some tasks. However, most of the tasks evolved quicker during the last weeks/months. The following sections reflect the status of analyses conducted by the consortium.

The consortium is also making every effort to contribute with new stock origin data to the next stock assessment as well as the Management Strategy Evaluation (MSE) process. For the purposes of this contribution, otolith microchemistry, genetic and otolith shape data, from previous Phases of the GBYP program, were made available to the Bluefin tuna working group and MSE developers (e.g. Tom Carruthers). The information obtained during this contract will also be made available for these efforts, interacting as necessary to make sure it is useful in the process.

4. OTOLITH CHEMISTRY

Task Leader: Igaratza Fraile (AZTI) & Jay Rooker (TAMU)

Participants:

AZTI: Igaratza Fraile, Haritz Arrizabalaga

TAMU: Jay Rooker

Otoliths of Atlantic bluefin tuna (*Thunnus thynnus*) have proven to be highly effective tools to study population structure and migratory pathways. Over fish's life, otoliths grow by accumulating new material in concentric layers around a central nucleus. Examining the chemical composition of different portions of otoliths informs about where fish have been at various life-stages. During GBYP Phase 6 we used otolith chemistry to answer different questions related with the ecology and stock structure of Atlantic bluefin tuna.

- We estimated mixed stock proportions of eastern and western populations throughout the North Atlantic Ocean (east and west of 45ºW in the North Atlantic Ocean, and west African coast) based on stable isotopic composition (Task 1)
- We assigned the nursery origin (East vs. West) to Atlantic bluefin tuna analyzed for stable isotopic composition in Task 1 at individual level (Task 2).
- We used otolith trace element and stable isotope composition in young-of-the-year (YOY, age-0) of the 2013 cohort to distinguish different nurseries within the Mediterranean Sea (Task 3a).
- We used otolith trace element and stable isotope composition in juvenile bluefin tuna of the 2011 cohort captured in the Bay of Biscay to assign origin within the Mediterranean Sea using the baseline generated in Phase 5 (Task 3b).

4.1. Determining nursery origin of bluefin tuna captured in the potential mixing zones

Introduction

The results from previous phases suggested that western origin contributions were negligible in the Mediterranean Sea, Bay of Biscay and Strait of Gibraltar, but mixing rates could be important in the central North Atlantic, Canary Islands and western coast of Morocco. In order to assess the spatial and temporal variability of mixing proportions, otoliths collected in areas with potential western contribution were analyzed for stable carbon and oxygen isotopes ($\delta^{13}C$ and $\delta^{18}O$).

Material and methods

In this section, we investigate the origin of bluefin tuna collected in the central North Atlantic Ocean (east and west of 45ºW) and the East Atlantic - West African coast (Canary Islands, Moroccan Coast) using stable $\delta^{13}C$ and $\delta^{18}O$ isotopes in otoliths. Samples utilized for this study (N=146 were collected under the GBYP program. In the western and central North Atlantic samples were captured from August to November 2014 by observers on board of Japanese longline vessels operating in the Atlantic Ocean (N=29). Samples from the west African coast were collected in May 2015 by Moroccan traps (N=50), off the African continent (35ºN, 6ºW approximately). Likewise, otoliths from Canary Islands were collected by bait boat fishery during March 2015 (N=23) and 2016 (N=44). (Figure 4.1).

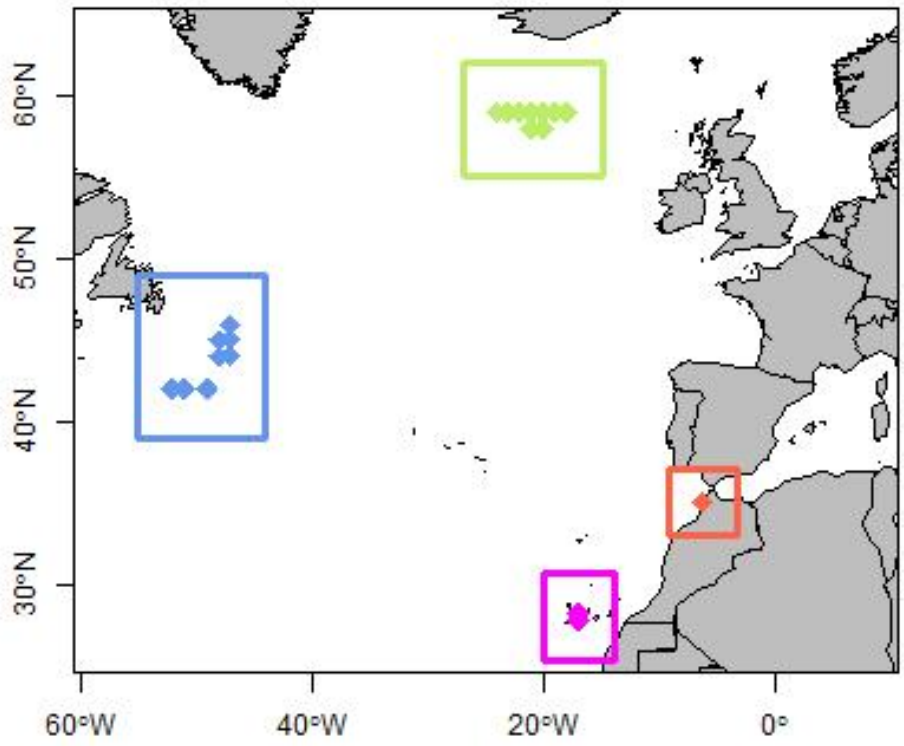

Figure 4.1: Study area in the North Atlantic Ocean. Otoliths collected in the central North Atlantic (west of 45°W, blue), central North Atlantic (east of 45°W, light green), Moroccan traps (orange), and Canary Islands (pink).

Otolith handling followed the protocols previously described in Rooker et al. (2008). Briefly, following extraction by GBYP participants, sagittal otoliths of bluefin tuna were cleaned of excess tissue with nitric acid (1%) and deionized water. One sagittal otolith from each bluefin tuna specimen was embedded in Struers epoxy resin (EpoFix) and sectioned using a low speed ISOMET saw to obtain 1.5 mm transverse sections that included the core. Following attachment to a sample plate, the portion of the otolith core corresponding to approximately the yearling periods of bluefin tuna was milled from the otolith section using a New Wave Research MicroMill system. A two-vector drill path based upon otolith measurements of several yearling bluefin tuna was created and used as the standard template to isolate core material following Rooker et al. (2008). The pre-programmed drill path was made using a 500 µm diameter drill bit and 15 passes each at a depth of 50 µm was used to obtain core material from the otolith. Powdered core material was transferred to silver capsules and later analyzed for $\delta^{13}C$ and $\delta^{18}O$ on an automated carbonate preparation device (KIEL-III) coupled to a gas-ratio mass spectrometer (Finnigan MAT 252). Stable $\delta^{13}C$ and $\delta^{18}O$ isotopes are reported

relative to the PeeDee belemnite (PDB) scale after comparison to an in-house laboratory standard calibrated to PDB.

Stable isotope signals of mixed stocks were compared with yearling samples from Mediterranean and Gulf of Mexico nurseries revised in GBYP-Phase 3 and presented in Rooker et al. (2014). HISEA software (Millar 1990) was used to generate maximum likelihood estimates (MLE) of mixed-stock proportions in each of the mixing zones.

Results

$\delta^{13}C$ and $\delta^{18}O$ were measured in the otolith cores of bluefin tuna from four locations in the Atlantic Ocean: 1) central North Atlantic Ocean (west of 45ºW), 2) central North Atlantic Ocean (east of 45ºW), 3) Atlantic coast of Morocco and 4) Canary Islands. Table 4.1 summarizes the attained results by region and sampling year. In the central North Atlantic mixing rates have varied over time. Based results shown by Rooker et al (2014), the majority of bluefin tuna captured west of 45°W are of western origin, whereas catches east of 45ºW are primarily from the eastern population. However, results found in previous GBYP phases indicated that mixing rates east of 45ºW during 2010 and 2013 were higher than in 2011 and 2012. During the current project we analyzed otoliths captured in 2014 at both sides of the 45ºW longitude. Mixed-stock analysis based on MLE indicated that catches in 2014 in the central North Atlantic Ocean (east of 45ºW) were almost exclusively from the eastern population (97%), whereas in the western North Atlantic a significant mixing of the two populations occurred (78% eastern vs. 22% western origin). Additional samples from the central North Atlantic are currently under analysis and will soon be incorporated.

Stable isotopic analyses indicated that mixing of eastern and western stocks occurred in the West African coast (Moroccan traps), although catches in 2015 were dominated by the Mediterranean population (84.3% of eastern origin fish). Mixing rates in the coast of Morocco varied considerably in preceding years, with catches in 2011 and 2014 dominated by the western population and catches in 2012 and 2013 comprised almost exclusively by the Mediterranean population. The results for 2015 confirm that mixing of the two populations occurs at variable rate (Table 4.2). Likewise, the presence of western migrants in the Canary Islands during 2015 and 2016 was also notable (Table 4.1). During these consecutive years the estimated mixing proportions for 2015 and 2016 were similar to those found in West African coast (14% and 19% of western contribution in 2015 and 2016 consecutively). Otoliths collected in previous GBYP phases revealed that bluefin tuna captured in 2014 in this region were exclusively originated in the Mediterranean Sea. In contrast, during the current project, the

data suggest that both eastern and western populations are the most likely to mix in the eastern North Atlantic Ocean, highlighting the importance of interannual variations in the spatial distribution of bluefin tuna.

Table 4.1. Maximum-likelihood predictions of the origin of bluefin tuna analyzed under the current contract. Estimates are given as percentages and the mixed-stock analysis (HISEA program) was run under bootstrap mode with 1000 runs to obtain standard deviations around estimated percentages (± %).

			Predicted Origin based on MLE			
Region	**Year**	**N**	**FL (cm)**	**% East**	**% West**	**% SD**
Central N. Atlantic (west of 45ºW)	2014	16	125-275	77.6	22.4	± 19.3
Central N. Atlantic (east of 45ºW)	2014	13	148-267	96.8	3.2	± 7.5
Morocco	2015	50	194-259	84.3	16.7	± 9.9
Canary Islands	2015	23	216-251	86.3	13.7	± 14.3
Canary Islands	2016	44	206-260	80.6	19.4	± 10.3

Table 4.2. Year to year variation of western contribution in bluefin tuna (Thunnus thynnus) catches by Japanese fisheries in the central North Atlantic (east and west of 45°W boundary), Moroccan traps and Canary Islands fisheries. Mixing proportions estimated by Maximum Likelihood Estimate using Hisea (Millar, 1990). Numbers highlighted in yellow correspond to analyses performed under the current contract.

Region	2010	2011	2012	2013	2014	2015	2016
C.N. Atl. (east)	43%	10%	17%	49%	3%		
C. N. Atl. (west)		30%	95%	74%	22%		
Morocco		74%	0%	2%	70%	16%	
Canary Islands				21%	0%	14%	19%

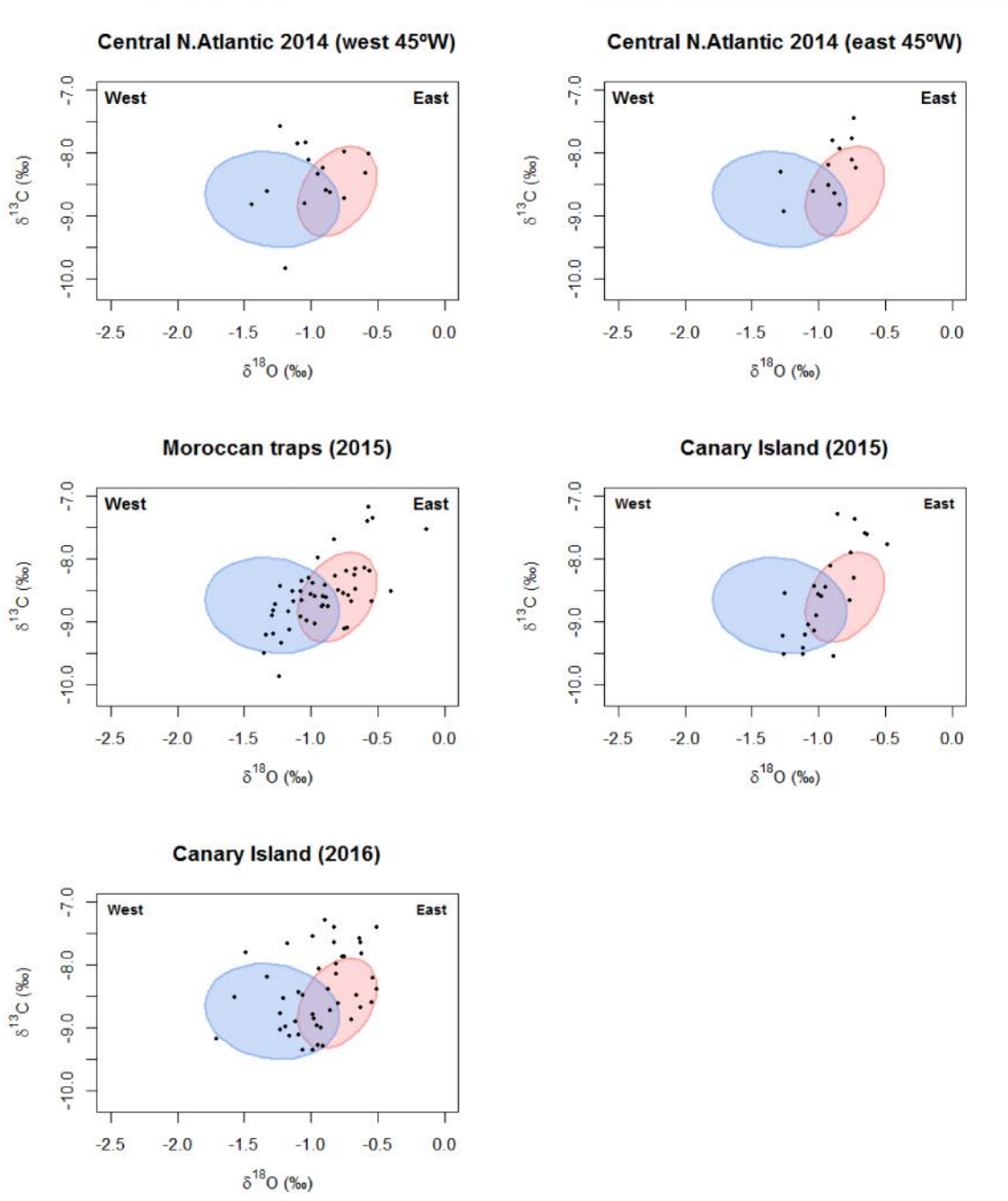

Figure 4.2: Confidence ellipses (1 SD or ca. 68% of sample) for otolith δ13C and δ18O values of yearling bluefin tuna from the east (red) and west (blue) along with the isotopic values (black dots) for otolith cores of bluefin tuna collected from central North Atlantic (west of 45ºW), central North Atlantic (east of 45ºW), Moroccan traps and Canary Islands.

4.2. Individual origin assignment

Introduction

During Phase 6, individual classification techniques were applied to $\delta^{13}C$ and $\delta^{18}O$ values to predict the origin of bluefin tuna at individual scale.

Samples analyzed in Task 1 were also assigned to origin individually, with associated levels of probability. The identification of individual origin is needed for at least two main reasons: the construction of stock-age-length-keys, and the comparison/improvement of individual assignments based on different types of markers (i.e. genetic, otolith shape and stable isotopes). Moreover, it allows to table the results according to any stratification that might be used during the stock assessment or MSE process.

Material and Methods

During the current project, 125 individual bluefin were assigned to their natal origin (Gulf of Mexico or Mediterranean Sea), including those from the central North Atlantic (west of 45ºW, N=16), Central North Atlantic (east of 45ºW, N=12), Morocco (N=50) and Canary Islands (N=67).

$\delta^{13}C$ and $\delta^{18}O$ values of bluefin tuna otoliths were statistically analyzed and individuals were assigned to source populations with associated levels of probability. Among the classification methods tested with the baseline dataset, it has been shown that Quadratic Discriminant Function Analysis (QDFA) performs the best attaining the highest classification accuracy (Fraile et al. 2015). Thus, QDFA was used to provide posterior probabilities for each pair of $\delta^{13}C$ and $\delta^{18}O$ values.

Results

Individual origin assignments based on QDFA suggest that population mixing occurs in all studied regions at variable rates. Overall, mixing proportions using QDFA yield higher western contributions than MLE with proportions from QDFA often varying by at least 10% from estimates generated with the MLE approach (Table 4.3). However, considering the confidence intervals around those averages (i.e. mean+-2*s.d), the results are generally concordant. Detailed individual classifications are provided in Appendix 1.

Table 4.3. Quadratic Discriminant Function Analyses predictions of the origin of bluefin tuna analyzed under the current contract. Estimates are given as percentages, and individual origin assignments were grouped into region and years.

	Predicted Origin based on QDFA			
Region	**Year**	**N**	**% East**	**% West**
Central N. Atlantic (west of 45°W)	2014	16	62.5	37.5
Central N. Atlantic (east of 45°W)	2014	13	84.6	15.4
Morocco	2015	50	70	30
Canary Islands	2015	23	73.9	26.1
Canary Islands	2016	44	72.7	27.3

.

4.3. Discrimination of nursery areas within the Mediterranean Sea by trace element and stable isotope composition in young-of-the-year bluefin tuna and origin assignation of individuals from Bay of Biscay

Introduction

The results from previous phases suggested that trace element composition might allow discriminating the Atlantic bluefin tuna from different spawning areas of the Mediterranean Sea. In 2011, YOY signatures were distinct among eastern and western nurseries within the Mediterranean, allowing discrimination of the two major Mediterranean basins.

Due to significant interannual variation in the chemical signatures in the Mediterranean Sea, our attempts to classify bluefin tuna from adjacent or combined year-classes will likely result in lower accuracy. Building a multiyear baseline for elemental signature is necessary when using trace element chemistry for classification of several year-classes. During this phase, stable isotope ($\delta^{13}C$ and $\delta^{18}O$) and trace element analyses have been carried out on young-of-the-year (YOY) fish captured in the Balearic Sea, southern Tyrrhenian Sea, east of Sicily and Levantine Sea during 2013. Additionally, we used the existing baseline to assign origin to 60 juvenile individuals of the 2011 cohort caught in the Bay of Biscay, for which otoliths are available. The results provide a first insight on which Mediterranean spawning area contributes to this important feeding area of the northeast Atlantic in the studied years.

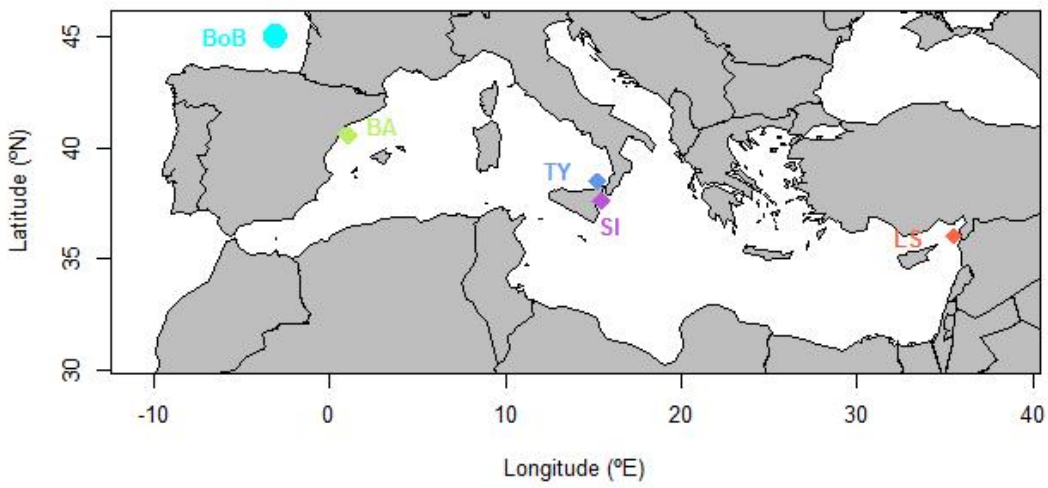

Figure 4.3: Sample collection in the Bay of Biscay (BoB), Balearic Sea (BA), south Tyrrhenian Sea (TY), east of Sicily and Ionian Sea (SI) and Levantine Sea (LS).

Material and methods

Young-of-the-year (YOY) bluefin tuna used in this study were collected during 2013 in the different spawning grounds within the Mediterranean Sea (Figure 4.3). Samples from the Bay of Biscay were collected between 2012 and 2013 by bait-boat fishery operating during summer months. Fork length of the juvenile bluefin tuna ranged from 57cm to 97cm (corresponding to ages 1 and 2 based on age-length key by Cort [1991]), and were estimated to be born in 2011. Sagittae otoliths were extracted from each YOY and juvenile fish using fine-tipped forceps, cleaned of excess tissue with nitric acid (1%) and deionized water and placed in plastic vials until further processing. Trace element and stable otolith measurements were performed on the same otolith.

For microchemistry analyses, whole otoliths were embedded in a mix of Araldite epoxy GY502 and hardener HY956 in a 5:1 weight ratio. After a block was removed from the mold, otolith cores from each bluefin tuna specimen were identified and marked under a light microscope. Then, otolith blocks were sanded until the core and polished using sandpaper of multiple grits. After polishing, otoliths were triple rinsed Milli-Q water and dried under a laminar air flow prior to the laser ablation-ICP-MS analysis.

Otolith samples were analyzed with an IR 1030 nm femtosecond laser (Alfamet-Novalase, France) in conjunction with an Elan DRC II (Perkin Elmer) located at the University of Pau, France. A rectangle of 250 µm x 200 µm was ablated in the first inflexion point of the otolith, and results over a whole ablated surface were analyzed for trace element concentration to get the signature of the post-larval live stage. This allows avoiding possible perturbations resulting from the contamination introduced by the Crystalbond throughout micro-cracks often occurring around the core, as well as incorporation of elements due to maternal transfer. A *pre-ablation* step was implemented to minimize potential surface contamination (rectangle of 300 µm x 250 µm). The laser beams operated at a repetition rate of 500 Hz. Three glass reference material (NIST 610, NIST 612 and NIST 616 (National Institute of Standards and Technology, USA)) and two fish otolith powder reference materials (FEBS-1 (National Research Council, Canada; Sturgeon 2005) and NIES No.22 (National Institute for Environmental Studies, Japan; Yoshinaga et al. 2000)) were used for laser ablation as calibration standards and quality control samples. Ten isotopes (Li^{7}, Mg^{24}, Ca^{43}, Mn^{55}, Fe^{56}, Co^{59}, Ni^{60}, Cu^{63}, Zn^{66}, Sr^{88} and Ba^{138}) were measured in each otolith by the LA-ICP-MS system. All the reference materials were measured at the beginning and the end of the session, for calibration and drift correction. ^{43}Ca was used as an internal standard for each ablation to check for variation in ablation yield. Elemental concentrations were standardized to calcium (i.e. Sr:Ca and Ba:Ca) based on the stoichiometry of calcium carbonate (380.000 µg Ca g^{-1} otolith). The data processing proceeds by identifying the background and signal windows for each measurement. Each measurement is defined here as the acquisition of data from one complete rectangle. The background signal is defined as the period during which only the carrier gas composition is measured, prior to the laser firing. The background signal was used to calculate the limit of detection (LOD) and the limit of quantification (LOQ), which was calculated as the mean background level plus 3 and 10 times standard deviation respectively. Concentrations below LOQ were not included in the statistical analysis.

Once trace element analyses were completed, stable isotope analyses were performed on the same otolith following a similar procedure described in Task 1. Embedded otolith blocks were first attached to a microscope slide and then to a sample plate using thermostatic glue (Crystalbond). The portion of the otolith core corresponding to approximately the first two to three month of live of bluefin tuna was milled from the otolith section using a New Wave Research MicroMill system. A two-vector drill path based upon otolith measurements of several yearling bluefin tuna was created and used as the standard template to isolate core material. The pre-programmed drill path was made using a 300 µm diameter drill bit and 10 passes each at a depth of 50 µm was used to obtain core material from the otolith. Powdered

core material was transferred to plastic vials and later analyzed for $\delta^{13}C$ and $\delta^{18}O$ on an automated carbonate preparation device (KIEL-III) coupled to a gas-ratio mass spectrometer (Finnigan MAT 252). Stable $\delta^{13}C$ and $\delta^{18}O$ isotopes are reported relative to the PeeDee belemnite (PDB) scale after comparison to an in-house laboratory standard calibrated to PDB.

Multivariate statistics were used to determine the "within Mediterranean" nursery origin of bluefin tuna captured in the Bay of Biscay. HISEA software (Millar et al. 1990) was used under bootstrap mode with 1000 runs to generate maximum likelihood estimates of mixed-stock proportions in the Bay of Biscay.

Table 4.3: Number of YOY and juvenile Bluefin tuna otoliths successfully analyzed for near-core trace element concentration. Juvenile signatures were compared to YOY signatures of their corresponding year-class (2011). YOY signatures will be used to build a baseline for discrimination of nurseries within the Mediterranean Sea: Levantine Sea (LS), southern Tyrrhenian Sea (TY), east Sicily (SI) and Balearic Sea (BA).

Region	N samples	Size-range (cm)	Category
Levantine Sea (LS)	20	21-26	2013 baseline
Tyrrhenian Sea (TY)	17	17-21	2013 baseline
Ionian Sea (SI)	20	30-42	2013 baseline
Balearic Sea (BA)	20	32-41	2013 baseline
Bay of Biscay (BoB)	60	57-97	Origin assigned

Results

Reference samples

Previous results suggest that in population structure studies within the Mediterranean Sea, it might be necessary to match adult signature to the appropriate year class when predicting the natal origin of adult bluefin tuna. YOY bluefin tuna captured in 2011 in the Levantine Sea reflected a distinct chemical signature compared to those captured in the central and western Mediterranean Sea (Figure 4.4). However, the chemical signature of bluefin tuna captured in Balearic Sea, Tyrrhenian Sea and Ionian Sea was similar and discriminating among these nursery grounds was difficult. Thus, central and western nursery areas were merged together dividing the Mediterranean in two major basins.

In 2013, significant differences were found in otolith Li, Mg, Mn, Fe, Zn, Sr, and Ba concentrations among the Levantine, Ionian, Tyrrhenian and Balearic Sea nursery grounds (MANOVA, $p > 0.05$). Linear Discriminant Analysis (LDA) was performed to check for the differences in chemical signatures among the sampling localities, to describe the differences among predefined groups and to determine which elements were responsible for dissimilarities among the groups. Optimal combination of elements to discriminate among the four groups was comprised by Mg, Mn, Sr and Zn; with a classification accuracy of 76% (Table 4.4)

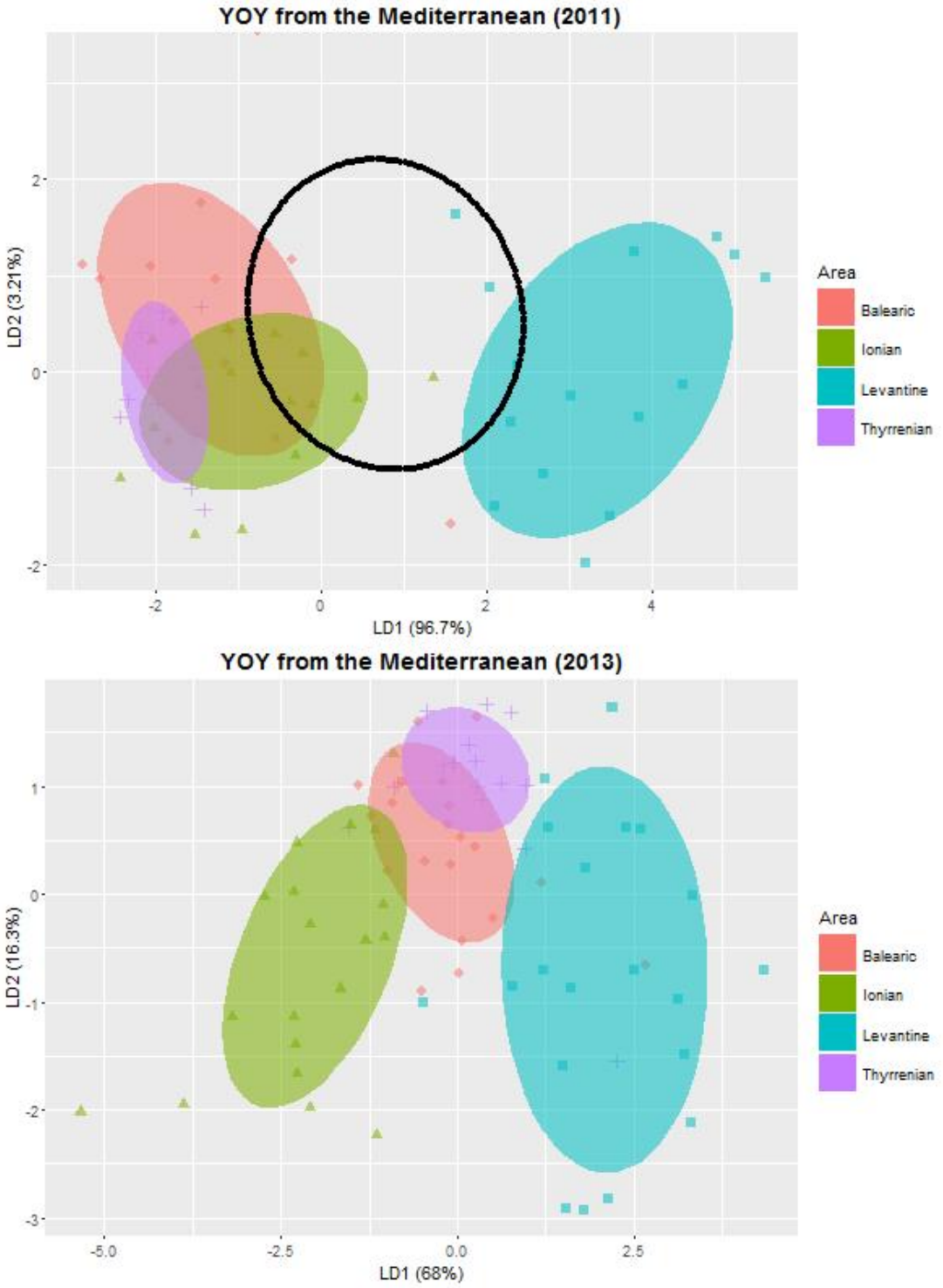

Figure 4.4:. Discriminant analysis of otolith trace element concentration in otoliths of young-of-the-year bluefin tuna (Thunnus thynnus) from the Mediterranean nursery grounds along with otolith near-core signature from juvenile bluefin tuna (2011 year-class) of unknown origin collected in the Bay of Biscay (black circle). The ellipses mark 1 SD (67%) confidence levels for the underlying populations.

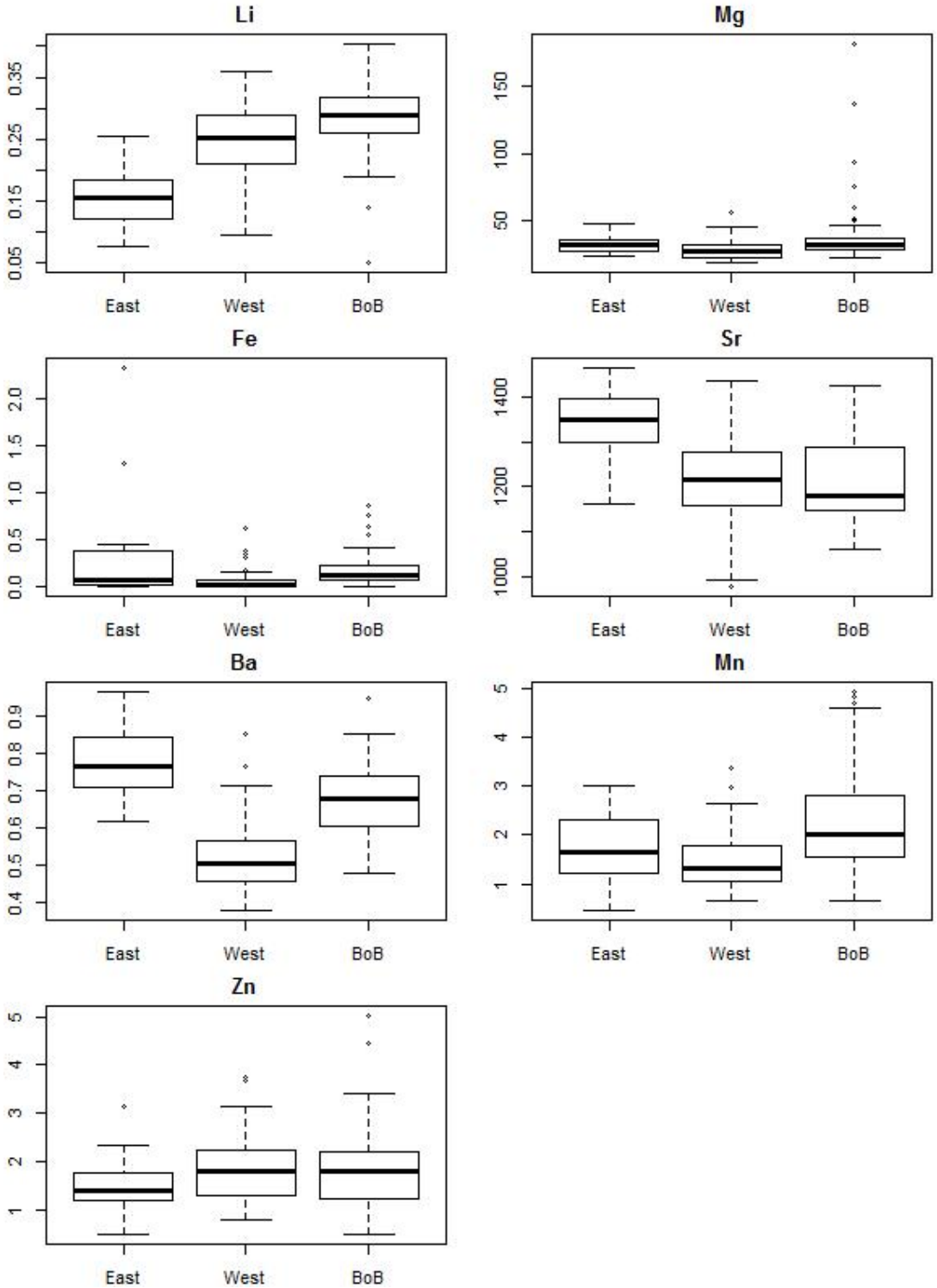

Figure 4.5: Boxplot of elemental concentration (ppm) measured in YOY bluefin tuna captured in the spawning grounds in the eastern and western Mediterranean Sea compared to juvenile bluefin tuna of the same cohort captured in the Bay of Biscay.

Origin assignment

During the current project, otolith near-core values of trace elements (corresponding to the post-larval stage) were used to assess the origin of juvenile bluefin tuna from the Bay of Biscay. Age-length key was used to determine the birth year of juvenile bluefin tuna, ensuring that all otoliths included in the study were born in 2011. A total of 53 otoliths from the Bay of Biscay corresponding to the 2011 cohort were successfully analyzed for trace element composition and compared to YOY elemental signature used as a baseline dataset (Figure 4.5). The remaining 7 otoliths were discarded due to irregular chemical signals, probably related to sample contamination. The results suggest different nursery grounds may be contributing to the Bay of Biscay bluefin tuna fishery. Mixed-stock analysis based on MLE indicated that bluefin tuna captured in the Bay of Biscay were mostly comprised by individuals from the central or western Mediterranean spawning grounds (75% vs. 25% from the Levantine Sea). This could also result from the fact that our baseline samples are not a complete representation of the nursery grounds, since generally YOY fish have been collected in a very short time frame and limited geographic area. Alternatively, additional nursery areas not included in the baseline dataset may be contributing to juvenile aggregations in the Bay of Biscay.

Additional analyses (carbon and oxygen stable isotopes) on otoliths of YOY bluefin tuna from Balearic Sea, southern Tyrrhenian Sea, Ionian Sea and Levantine Sea from 2013 are currently ongoing and will be soon incorporated to the existing baseline.

Given that stable isotopic analyses are not included in this report, these results should be considered as preliminary.

Table 4.4: Optimal combination of elements and classification accuracy (estimated by LDA) of young-of-the-year bluefin tuna otoliths for 2011 and 2013 cohorts. Area codes correspond to Levantine Sea (LS), southern Tyrrhenian Sea (TY), east Sicily (SI) and Balearic Sea (BA).

Group division	Optimal combination of elements	Year	Classification accuracy
East (LS) / West (BA, TY, SI)	Ba + Li + Mg	2011	100%
East (LS) / West (BA, TY, SI)	Ba + Li + Mn + Sr	2013	91%*
LS / SI / TY / BA	Mg + Mn + Sr + Zn	2013	76%*

* Preliminary results prior to incorporating stable isotopic data

Conclusions

The results of this research show that discrimination of nursery grounds within the Mediterranean Sea is possible using otolith chemistry. However, given interannual variability in the oceanographic conditions, discrimination capability may vary from year to year. Therefore, the origin determination should be adapted to each of the reference years. Bluefin tuna from the 2011 cohort can be assigned to the two major Mediterranean basins, whereas discrimination among the four main nursery grounds is possible for bluefin tuna born in 2013.

Our preliminary results (prior to including stable isotopic data) suggest that the majority of bluefin tuna captured in the Bay of Biscay were originated in the central or Western Mediterranean Sea. Nevertheless, this hypothesis is based on a very limited number of analyses, and it is likely that the total number of contributing sources is not included in the baseline nursery signature, and/or that the baseline does not fully characterize the variability of each nursery ground. Thus, we suggest extending this work by expanding the baseline in number of individuals and including additional nursery grounds for which YOY otoliths are available (e.g. Ligurian Sea and Maltese waters).

We have created the tool to be able to start discerning different behaviors throughout the life history of Bluefin tuna born in different spawning areas, and additional analyses can reveal the potential importance of differential behavior.

References

Millar RB (1990). Comparison of methods for estimating mixed stock fishery composition. Canadian Journal of Fisheries and Aquatic Sciences, 47, 2235-2241.

Cort, J.L., 1991. Age and growth of the bluefin tuna, Thunnus thynnus (L.) of the Northeast Atlantic. Collect Vol Sci Pap ICCAT 35:, 213-230.

Sturgeon RE, SN Willie, L Yang, R Greenberg, R O Spatz, Z Chen, C Scriver, V Clancy, J W Lam and S Thorrold (2005). Certification of a fish otolith reference material in support of quality assurance for trace element analysis. Journal of Analytical Atomic Spectrometry, 20, 1067-1071.

Yoshinaga J, A Nakama, M Morita, JS Edmonds (2000). Fish otolith reference material for quality assurance of chemical analyses. Marine Chemistry, 69, 91-97.

5. GENETICS

5.1. Origin assignment of juveniles and adults captured at feeding aggregations throughout the Atlantic and over different years (GBYPPh6-Task1)

Task Leader: Naiara Rodriguez-Ezpeleta (AZTI)

Participants: Iñaki Mendibil, Natalia Diaz-Arce, Haritz Arrizabalaga

5.1.1. Introduction

GBYPPh6-Task1 consists on deciphering the map ABFT mixing in the Atlantic. Two main activities were planned: 1) assessing the validity of the optimal minimal SNP panel developed in Phase 5 on spawning adult reference samples, which includes calculating correct assignment rates of currently available panel and developing a strategy to improve these assignments, and 2) genotyping the minimal best available SNP panel in adults from feeding aggregations, which includes DNA extraction of about 1000 individuals and processing in a Fluidigm Assay.

Note that the selection of the RAD-seq derived 96 SNP described here corresponds to analyses performed within Phase 5 that could not be included in Phase 5 report for being still in progress.

5.1.2. Methods

A schematic view of the SNP selection procedure and samples used at each step of the process is provided in Figure 5.1.

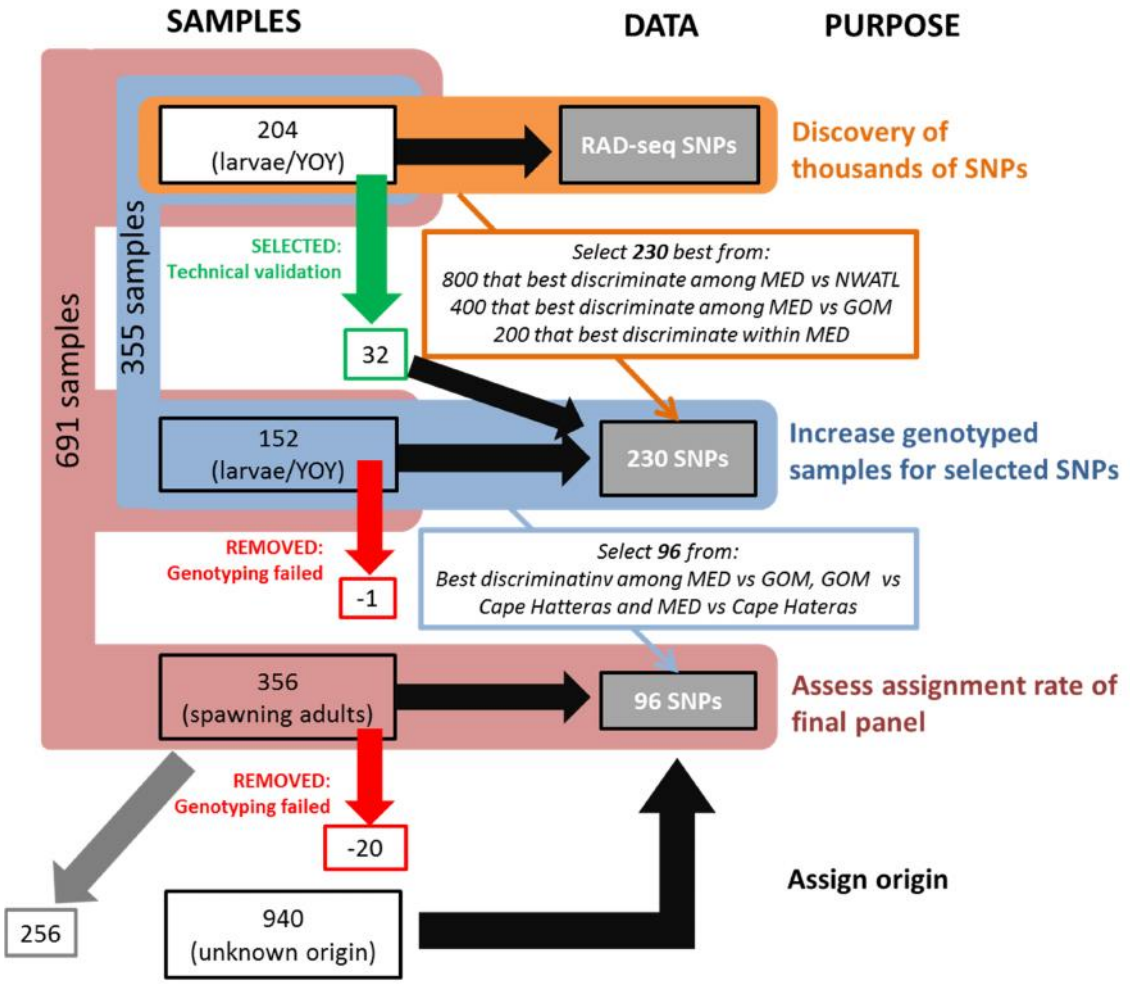

Figure 5.1: Schematic representation of the procedures followed. First, thousands of SNP markers are discovered using RAD- seq on 204 samples (orange). From those, the 230 most discriminant (based on genotypes of 204 samples) SNPs are selected and genotyped in 32 already used and 152 new samples (blue). From those, the 96 most discriminant (based on genotypes of 204 + 152 -1 samples) are selected and genotyped in 356 new samples (pink). Finally, 940 samples of unknown origin are genotyped for 96 SNPs and assignment calculated on a baseline of 204 + 152 -1 + 356 – 20 samples.

Samples

Reference samples analyzed for assessing the validity of the panel

355 reference samples (10 larvae and 181 spawning adults from the Gulf of Mexico and 164 spawning adults from the Mediterranean) were genotyped in Phase 5. The obtained genotypes have been analyzed to calculate the assignment power of the currently available RAD-seq derived panel.

Reference samples analyzed for improving the panel

256 of the spawning adult samples used to assess the validity of the panel (179 from the Gulf of Mexico and 87 from the Mediterranean) were RAD-sequenced in order to increase the reference baseline of the Gulf of Mexico from which candidate traceability suitable SNPs are selected. Table 5.1 shows the distribution of samples per location and age class including the 240 previously available.

Table 5.1: Samples to be used for the new RAD-seq based analyses

	Larvae	YOY	Spawning adult	TOTAL
NWATL		13		13
GOM	38		179	217
MED	71	118	77	266
TOTAL	109	131	256	**496**

Feeding aggregate samples used for origin assignment

940 samples of unknown origin were selected covering, to the extent possible, the spatial distribution of the specie, several years and several age classes (Table 5.2).

Table 5.2: Samples selected for the ABFT mixing analysis. L M and J denote Large, Medium and Juvenile respectively

	Size Class		J	M		L					
	Year		2012	2011	2012	2011	2012	2013	2014	2015	2016
AREA	GSL	G. Sait Lawrence	0	0	0	0	0	23	0	0	30
	NL	Newfoundland	0	0	0	0	0	9	0	0	0
	NS	Nova Scotia	0	0	0	0	0	17	0	0	0
	CA	Central Atlantic	0	13	14	53	54	59	24	30	0
	UI	UK Ireland	0	0	0	0	0	0	0	0	2
	GI	Gibraltar	0	0	28	0	0	0	0	0	0
	MC	Madeira/Canarias	0	0	0	0	0	30	0	23	48
	MO	Morocco	0	0	0	30	14	30	30	28	30
	MS	Mauritania	0	0	0	0	0	23	0	0	0
	BB	Bay of Biscay	30	0	29	28	0	0	0	0	0
	PO	Portugal	0	0	0	0	25	0	0	0	0
	NW	Norway	0	0	0	0	0	1	0	22	163

DNA extraction

For those samples for which no DNA was already available, DNA was extracted using the Wizard® Genomic DNA Purification kit (Promega, WI, USA) following manufacturer´s instructions for "Isolating Genomic DNA from Tissue Culture Cells and Animal Tissue". The starting material was approximately 20 mg of tissue or whole larvae and after extraction all samples were suspended in equal volumes of Milli-Q water. DNA quantity (ng/µl) was evaluated on the Qubit® 2.0 Fluorometer (Life Technologies) and DNA integrity was assessed by electrophoresis.

SNP selection and genotyping

From the four RAD-seq catalogs including all samples generated in Phase 5, in a first instance the 200 SNPs with the highest F_{ST} values among Northwest Atlantic (including Gulf of Mexico larvae and Cape Hatteras young of the year) and Mediterranean larvae and young of the year were selected; in a second instance, assuming that Cape Hatteras individuals might not be representatives of Gulf of Mexico spawning ground (see Phase 5 report and Richardson et al. 2016), the 100 SNPs with the highest F_{ST} values among Gulf of Mexico larvae and Mediterranean samples were selected. Additionally from the four catalogs based on only the Mediterranean samples, the 30 SNPs with the highest F_{ST} values among each pair of intra Mediterranean areas (West, Central and East) were retrieved, and from those, the 50 SNPs that provided the highest sum of pairwise F_{ST}s were selected. Using an in-house script, the flanking regions of the 1,400 selected SNPs were obtained by matching their corresponding tags against the Atlantic Bluefin Tuna reference genome (generated during GBYP Phases 2 and 3). Obtained sequences were submitted to the Assay Design Group at Fluidigm Corporation (South San Francisco, CA, USA), and from the ones fulfilling the Fluidigm design criteria, the 230 most discriminant were selected and sent for design and manufacture of primers for a SNPtype™ genotyping panel. Genotyping of 184 larvae and young of the year samples, including 32 already genotyped with RAD-seq, was performed on the Biomark™ HD platform using Flex Six™, 48.48 and 96.96 Dynamic Array IFCs, and the resulting data was analyzed with the Fluidigm Genotyping Analysis Software. Genotypes derived from RAD and Fluidigm were combined for the 230 SNPs to make

a dataset of 355 individuals (one was removed for having low genotyping rate). Successfully genotyped SNPs were ranked according to the average F_{ST} values for each of the following pairs: Gulf of Mexico larvae *vs.* Mediterranean samples, Gulf of Mexico larvae *vs.* Cape Hatteras young of the year, and Cape Hatteras young of the year *vs.* Mediterranean samples. Within Mediterranean comparisons were excluded based on previous results suggesting no differentiation within this area (see Results). SNPs were checked for linkage disequilibrium using *Genepop 4.3* (Rousset 2008), and only one per linked group (p-value < 0.001) and/or per genome contig (genome region constructed by overlapping genome sequence fragments) was selected to complete a set of 96 most discriminant SNPs. For validation and origin assignment respectively, 356 spawning adults from the Gulf of Mexico and Mediterranean and additional 940 samples of unknown origin were genotyped for the 96 selected SNPs using 96.96 Dynamic Array IFCs, and the resulting data was analyzed with the Fluidigm Genotyping Analysis Software.

Assignment

The Fluidigm and RAD-seq derived genotypes for the 32 repeated samples were merged using *PLINK* to assess technical reproducibility. Assignments were performed with *GENECLASS2* (Piry *et al.* 2004) using the Rannala and Mountain (1997) criterion (0.05 threshold) considering two populations (Gulf of Mexico and Mediterranean) as baseline. For each individual, assignment scores, *i.e.* probability of belonging to each of the baseline populations, was calculated. For panel validation, assignment scores were calculated for the new 356 reference samples on 96 SNP using a leave-one-out approach with a baseline of 690 individuals, that is, 355 previously genotyped plus 336 newly genotyped individuals (356 genotyped minus 20 that failed) excluding the one being assigned. For determining origin of mixed samples, assignment scores were calculated for the 96 SNP set on 940 samples using the combined set of 691 reference samples (246 from the Gulf of Mexico and 435 from the Mediterranean) as baseline; results are provided considering both 70% and 90% thresholds as "unassigned".

RAD-seq library preparation and sequencing

RAD-seq libraries were constructed following the protocol from Etter et al. (2011) with some modifications. Briefly, starting DNA (ranging from 250 to 750ng, depending on integrity) was digested with the SbfI restriction enzyme and ligated to modified Illumina P1 adapters containing 5bp unique barcodes. Pools of 33 individuals were sheared using the Covaris® M220 Focused-ultrasonicator™ Instrument (Life Technologies) and size selected to 300-500 bp by cutting agarose migrated DNA. After Illumina P2 adaptor ligation, each library was amplified using 14 PCR cycles. Each pool was paired-end sequenced (100 bp) on an Illumina HiSeq2000. Quality filtering and demultiplexing was performed with the process_radtags module of Stacks v. 1.32 (Catchen et al. 2013) with default parameters and keeping only the highest quality 90 positions of the reads.

5.1.3. Results and discussion

Development of a 96 SNP assignment panel

1400 selected SNPs were successfully mapped to the Bluefin Tuna reference genome, 929 remained after removing duplicates (those matching to the same contig on the same position), and 423 of them fulfilled Fluidigm specifications. From those, 230 where selected: the 144 that most discriminate between Northwest Atlantic *vs.* Mediterranean samples, the 38 that most discriminate between Gulf of Mexico larvae *vs.* Mediterranean samples, and the 48 that most discriminate among Mediterranean locations. All subsets had SNPs that originated from the 8 catalogs. Genotyping failed for 15 SNPs, and one sample failed for more than 23% of the SNPs and was removed for subsequent analyses. Genotyping rate of remaining SNPs and individuals is 99% and average validation rate (calculated from the 32 individuals genotyped with both technologies) is 98%. Most of the mismatches between RAD-seq and Fluidigm derived genotypes are due to homozygous calls in RAD-seq that are heterozygous in Fluidigm, effect that is slightly more pronounced in SNPs originating from catalogs from which clones were not removed.

Assignments of new Mediterranean samples based on the 48 SNPs that best differentiate among Mediterranean areas resulted in 15-25% correct assignment rate (Figure 5.2), confirming that finding SNPs that distinguish the Mediterranean

locations is difficult as suggested by the non-genetic differentiation within the Mediterranean observed in previous studies (see Phase 5 report as well as Task 2 below). For this reason, SNPs that differentiate among Mediterranean areas were not included in subsequent steps.

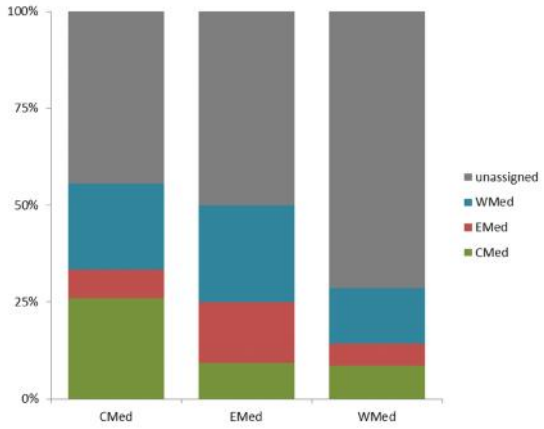

Figure 5.2: Assignment rates of 114 newly genotyped individuals for 46 SNPs (48 selected to differentiate among Mediterranean populations minus 2 that failed). Individuals with assignment score lower than 90% are considered unassigned.

Also, for the selection of final 96 SNP set, only those that discriminate among Gulf of Mexico and Mediterranean where considered; Cape Hatteras samples (only 16 young of the year) were excluded for being slightly different from the Gulf of Mexico (see report of Phase 5) and for having chances from arising from another spawning ground (see Richardson et al. 2016). Additional analyses including larvae from Cape Hatteras are required to solve the question of the origin of samples collected in this area.

Genotyping of the final set of 96 SNPs in 356 spawning adult samples resulted in 20 samples failing for more than 50% of the SNPs. Average genotyping rate in remaining individuals and SNPs of 99%.

Assignment power of the RAD-seq derived 96 SNP panel

The set of the best 96 SNPs derived from the RAD-seq analyses was validated in 336 (356 minus 20 whose genotyping failed) newly genotyped spawning adults from the main spawning areas. Using these adults as new reference test samples, new assignment rates were calculated (Figure 5.3).

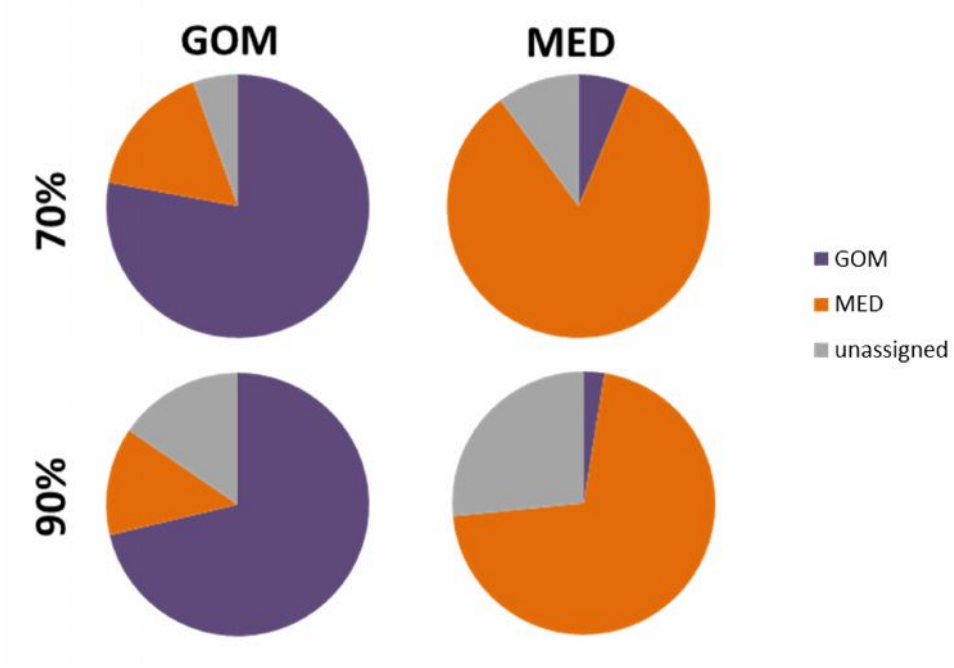

Figure 5.3. Assignment of Gulf of Mexico (GOM) and Mediterranean (MED) samples based on the best performing 96 RAD-seq derived SNPs panel when samples with assignment scores higher than 70% (above) or 90% (below)

Using 90% as a threshold, 71% of the samples of Gulf of Mexico and Mediterranean origin are correctly assigned and 13 and 2% are incorrectly assigned, respectively. Unassigned samples are 16 and 27% for Gulf of Mexico and Mediterranean respectively. Decreasing assignment score threshold to 70% reduces the number of unassigned samples (5 and 10% for Gulf of Mexico and Mediterranean respectively), but increases the number of incorrect assignments (to 17 and 6% respectively).

Implications in assignments of samples of unknown origin

From these results and under the hypothesis of only two possible origins (Gulf of Mexico and Mediterranean), it can be derived that in an assay with samples of unknown origin i) from those assigned to the Gulf of Mexico, 3-6% would come from the Mediterranean, ii) from those assigned to the Mediterranean, 18% would come from the Gulf of Mexico and iii) from those considered unassigned, 40% and 60% would come from the Gulf of Mexico and the Mediterranean respectively (Figure 5.4).

This means that, among the assigned individuals, there will be a slight undersetimation of the proportion of GOM origin.

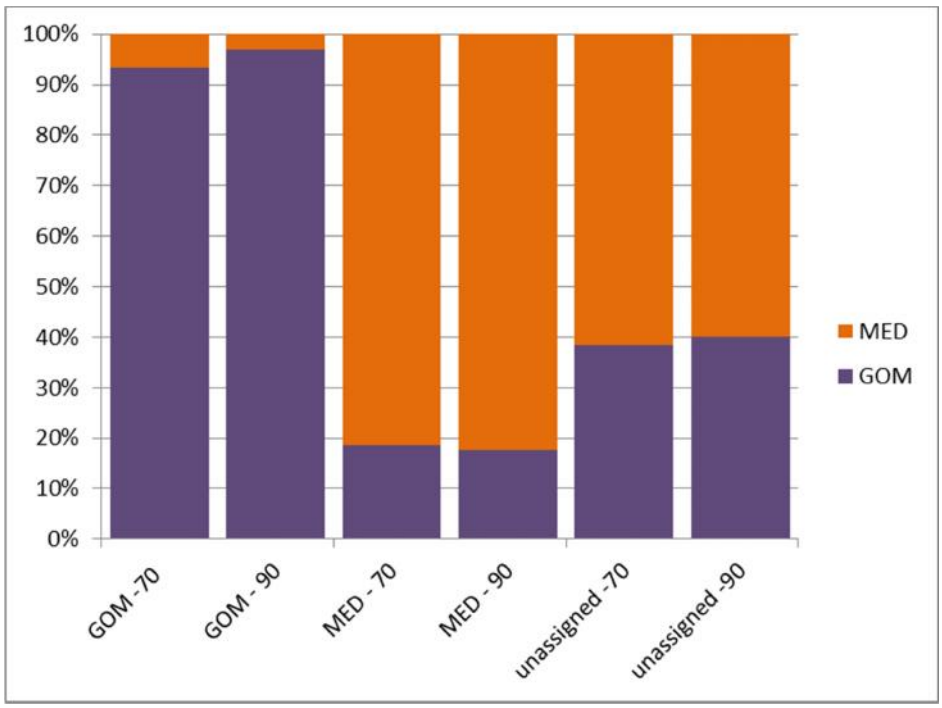

Figure 5.4. Percentage of real origin in a set of samples assigned as "Gulf of Mexico" (GOM), "Mediterranean" (Med) or "Unknown" (unassigned) when assignment score threshold is set to 70 or 90%.

Need for improving current assignments

These assignments, which are similar although slightly better than the ones obtained from the GBS analyses, are not optimal and they should be improved. From the population structure analyses (see Phase 5), we can conclude that genetic diversity within each spawning ground is high and that genetic differentiation among spawning grounds is small. This implies that the set of diagnostic SNPs should be large (a few tens of SNPs) and that finding diagnostic SNPs should be based on a large number of individuals. The fact that assignments based on smaller (see above) or larger set of SNPs (the subset of 230 SNPs was tested on a small set of samples) do not provide higher assignment rates suggests that selecting more SNPs from the ones available will not result in higher assignment rates and that selecting new SNPs based on a

larger number of reference samples is needed. Yet, in both, the GBS and RAD-seq analyses, the number Gulf of Mexico reference samples used for SNP selection was low, meaning that discriminant SNPs were being selected from a few individuals that do not capture the whole genetic diversity of the species. Indeed, self-assignments (that is, assignments on the samples used for SNP selection and or as baseline) provide very high assignment rates (>98% success in the case of RAD-seq) suggesting that the SNPs selected are very good at assigning the samples that were used to select them, but not that good for assigning new samples. This also highlights that reliable assignment success rates should be calculated in new samples, that is, those not used for SNP selection or as baseline. Additionally, the recent discovery of potential new spawning grounds (e.g. see Richardson et al. 2016) could make the assignment to origin even more complicated. Analyses based on more reference samples including larvae and young of the year from Cape Hatteras could shed light in this issue.

RAD-seq analyses of new reference samples

RAD-seq libraries from 256 spawning adults have been generated and sequenced successfully. Sequencing read quality is excellent and number of reads per individual is in general above 1 million. Merging this data with previously available RAD-seq data (see Phase 5) is currently underway.

Map of ABFT mixing in the Atlantic

Genomic DNA was successfully extracted from 940 individuals, which have been genotyped and assigned to origin. Samples from twelve different locations throughout the Atlantic have been analyzed (Table 5.3, Figure 5.5). These include mixing areas previously identified by other studies (e.g. Central Atlantic), as well as some areas close to the distribution limit of the specie that have not been analyzed previously (e.g. Norway and Mauritania). Results show a longitudinal gradient in the mixing proportions of both stocks, with some exceptions. Samples captured east of the 45ºW meridian are mostly of Mediterranean origin; yet a small percentage of Gulf of Mexico samples is also observed. Individuals caught in Norway and Mauritania seem to be mostly of Mediterranean origin, and the proportion of western origin fish in the other

regions (Bay of Biscay, Morocco, Canary Islands, Strait of Gibraltar and Portugal) is comparable to previous estimates using microchemistry.

West of 45ºW, the proportion of Mediterranean origin individuals is quite variable between regions. This proportion is highest in the Central Atlantic (yet west of 45ºW) and lowest in Newfoundland-Labrador. However, the Gulf of Saint Lawrence shows a surprisingly high proportion of Mediterranean origin individuals.

a)

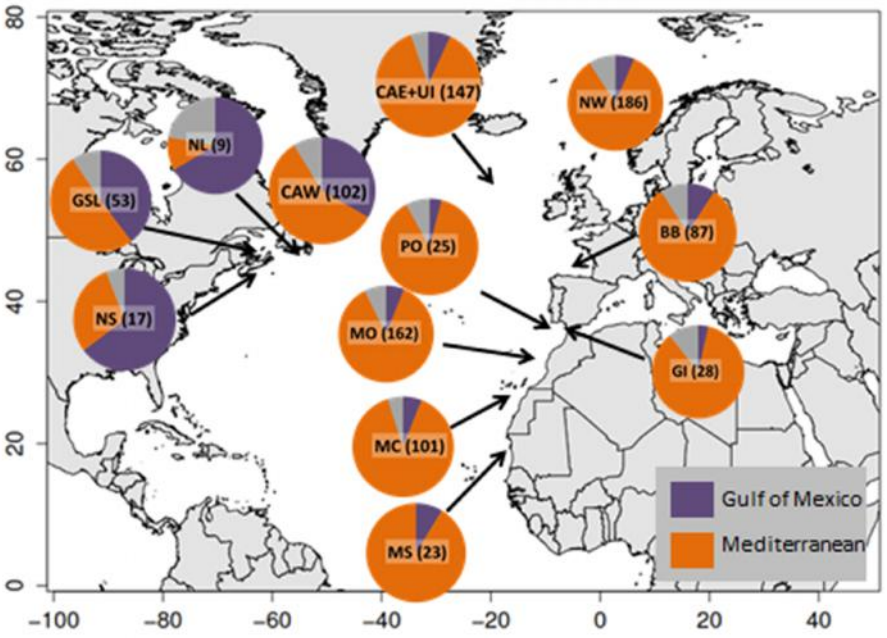

b)

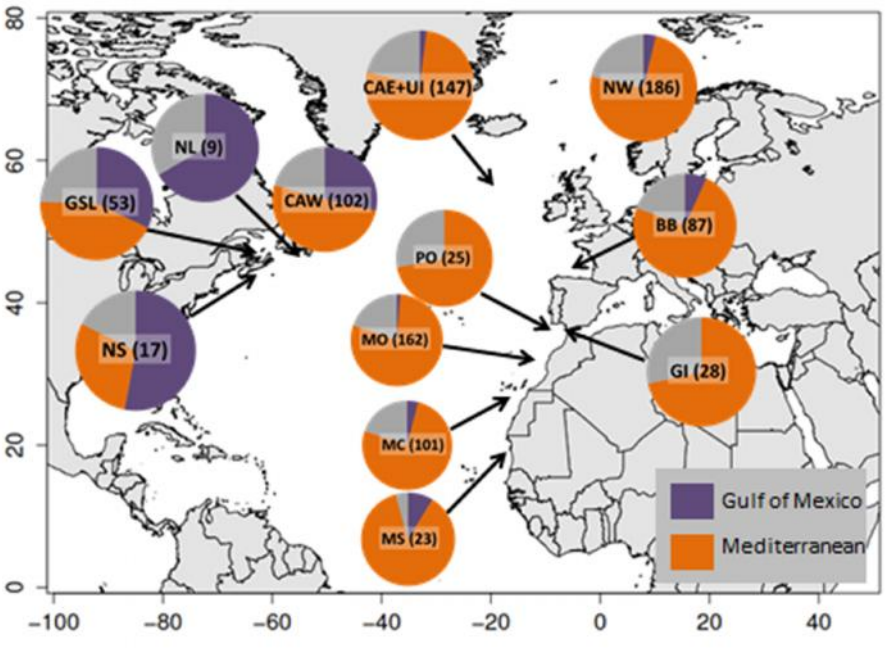

Figure 5.5. Percentage of samples belonging to each spawning component from the ones captured in each location, with assignment scores of 70% (pannel a) and 90% (pannel b); numbers in parenthesis indicate number of samples per location: Norway (NW), Bay of Biscay (BB), Portugal (PO), Strait of Gibraltar (GI), Morocco (MO), Canarias (MC), Mauritania (MS), Central Atlantic (east of 45ºW, CAE), Central Atlantic (west of 45ºW, CAE), Newfoundland (NL), Gulf of Saint Lawrence (GSL), Nova Scotia (NS).

Table 5.3. Number of samples belonging to each spawning component from the ones captured in each location, with assignment scores of 70% (pannel a) and 90% (pannel b); Norway (NW), Bay of Biscay (BB), Portugal (PO), Strait of Gibraltar (GI), Morocco (MO), Canarias (MC), Mauritania (MS), Central Atlantic (east of 45ºW, CAE), Central Atlantic (west of 45ºW, CAE), Newfoundland (NL), Gulf of Saint Lawrence (GSL), Nova Scotia (NS).

a)	GOM	MED	Unknown	TOTAL
BB	8	71	8	87
MS	2	21	0	23
GSL	21	27	5	53
NL	6	1	2	9
NS	11	5	1	17
MC	6	90	5	101
GI	1	24	3	28
NW	12	157	17	186
UI	0	2	0	2
MO	10	140	12	162
PO	1	22	2	25
CAE	10	129	8	147
CAW	34	59	9	102

b)	GOM	MED	Unknown	TOTAL
BB	6	64	17	87
MS	2	20	1	23
GSL	17	23	13	53
NL	6	0	3	9
NS	9	5	3	17
MC	4	77	20	101
GI	0	20	8	28
NW	7	139	40	186
UI	0	2	0	2
MO	2	128	32	162
PO	0	18	7	25
CAE	3	113	31	147
CAW	29	52	21	102

5.1.4. Conclusions

- We have assessed the assignment power of the 96 RAD-seq derived SNP panel, which is established in 61% and 89% correct assignment for Gulf of Mexico and Mediterranean samples and 19 and 1% incorrect assignment respectively.

- We have determined provenance of 374 samples of unknown origin resulting in a larger proportion of Mediterranean and Gulf of Mexico origin in samples captured in Eastern and Western Atlantic locations respectively.

- There is evidence that the samples used for SNP selection do not represent the whole genetic diversity of the Gulf of Mexico spawning components and new analyses to overcome this issue have been started.

- The uncertainty about the relatedness of the new spawning ground found in the Slope Sea (near Cape Hatteras) with the Gulf of Mexico and other possible Atlantic spawning areas makes interpretation about assignments more complicated.

5.1.5. Future analyses

Due to an identified need to include more Gulf of Mexico samples in the SNP discovery pipeline, Phase 6 included the generation of new RAD-seq libraries of Gulf of Mexico and Mediterranean spawning adults. These libraries have been generated and sequenced, thus, the tasks we committed to within this Phase have been completed. Despite this phase of the project being concluded, we will continue with the analyses which will include i) generating new libraries of Slope Sea larvae, ii) merging the three RAD-seq datasets (initial, spawning adults, Slope Sea larvae) into a complete dataset, iii) perform population genomics analyses on reference samples (including the Slope Sea); iv) extracting the best diagnostic SNPs (some will be new and some will be already among the 96 already used); v) constructing a new set of 96 most discriminant SNPs; vi) validating these new 96 SNPs in samples not used for SNP selection.

5.2. Microsatellite genotyping of reference samples in the Mediterranean (Task 2)

Task Leader: Fausto Tinti (UNIBO)

Participants: Alessia Cariani (UNIBO), Rita Cannas and Riccardo Melis (COMBIOMA)

Subcontractor: BMR Genomics

5.2.1. Backgrounds and Aims

Task 2 aims to provide a clear-cut evidence for BFT population structure fulfilling the gap represented by the microsatellite genotyping of reference samples in the Mediterranean at an extensive spatial scale and across a short-term temporal scale to check interannual stability of genetic structure. In fact, previous microsatellite analyses on BFT (Carlsson et al. 2004, 2006, 2007, Riccioni et al. 2010, 2013) have never been conducted on experimental designs accomplishing simultaneously the use of reference samples (Larvae or Young-of-the-Year) collected during the same spawning season (from June to September) of multiple consecutive years in the same Mediterranean spawning subareas.

In addition, the Task 2 aims to overwhelm the methodological constraints represented by the use of a limited number of microsatellite loci (< 20) in the previous analyses and by the use of panels of microsatellites largely different among studies carried out including both the Mediterranean and Gulf of Mexico samples that prevent any fully reliable comparative issue. Thus, a pan-Atlantic study based on a large panel of microsatellite loci (> 20) used to genotype reference samples from both ascertained spawning areas is considered necessary to assess genetic differences within and between each area and provide clear-cut evidence for population structure both in the Mediterranean and in the Gulf of Mexico.

To accomplish such aims a Research Collaborative Agreement between scientists of UNIBO-COMBIOMA (GBYP Consortium Partners) and of Stanford University – Marine Hopkins Station (B. Block and C. Reeb) has been formally activated to exchange genetic resources (primer sequences and PCR conditions for 18 microsatellite loci newly developed by Stanford University researchers and already used to type Gulf of Mexico reference samples and 10 reference gDNAs from Gulf of Mexico for genotype intercalibration) and merge genetic data (Mediterranean and Gulf of Mexico intercalibrated genotypes) to achieve a pan-Atlantic BFT population structure pattern.

5.2.2. Experimental design, sample selection and DNA extraction of Mediterranean YOY

The original experimental design included 320 samples. The refined experimental design includes the comparative genotype analysis of eight YOY reference strata samples (N = 480) collected from three grand-areas of the Mediterranean (Western Mediterranean, WMED; Central Mediterranean, CMED; Eastern Mediterranean, EMED) and four subareas corresponding to the most known spawning areas in the Mediterranean (Balearic Islands, BA; Southern Tyrrhenian Sea, TY; Sicilian Channel, SI; Levantine Sea, LS). Each subarea was represented by statistically-representative YOY samples (N ≥ 50) collected over two consecutive years (2012 and 2013). An additional Maltese YOY sample (MA, n=26) collected in 2013 in SI, CMED was added to this experimental design to deeply focus spatio-temporal BFT dynamics in this transition Mediterranean area. We selected N > 50 individuals from both EMED strata (2012 and 2013) because this is a crucial area within the Mediterranean and we would like to cover the entire batch of individuals previously analyzed with the other genetic markers and techniques (2012, RAD: 21 individuals; 2013, RAD: 33 individuals and GBS: 40 individuals).

Such an experimental design can be fully accomplished by muscle tissue specimens archived in the GBYP database deposited at AZTI. When possible, YOYs already typed for GBS/RAD-derived SNP were selected for microsatellite analysis to make possible the comparison with SNP-based results (Phases 5 and 6). Finally, 445 YOY muscle tissue specimens were retrieved from the GBYP database by AZTI and delivered to UNIBO for analyses (Table 5.4). Such specimens were organized in five 96-well plates for automated genomic DNA extraction at BMR Genomics.

Table 5.4: The reference samples (YOY) of the Mediterranean used for the DNA extraction.

GRAREA	SUBAREA	YEAR	N
WMED	BA	2012	50
WMED	BA	2013	50
WMED	TY	2012	50
WMED	TY	2013	50
CMED	SI	2012	44
CMED	SI/MA	2013	74
EMED	LS	2012	55
EMED	LS	2013	75
3	**4**	**2**	**445**

5.2.3. Microsatellite loci selection and setup

After reviewing literature and primer databases (e.g. http://tomato.bio.trinity.edu) as well as by contacting US and EU scientists, 33 BFT-specific microsatellite loci already used to genetically profile Gulf of Mexico, Atlantic and Mediterranean reference and non-reference samples have been selected. The setup of laboratory protocols for multiplexed PCR and genotyping conditions has been realized in silico and hence experimentally tested at the BMR-genomics service provider. Seven multiplexed PCRs containing from four to six microsatellite loci each have been set up. A reduced set of samples is analysed at first stage to assess outcomes and better tackle possible troubleshooting. Then GBYP samples are processed with the BMR-genomics automated and ISO certified system in batch of 96 samples to shorten lab time.

The description of the seven multiplexed PCR reactions is summarized in Figure 5.4, while the detailed list of identified loci is reported in Table 5.5.

Figure 5.4: Graphical description of the seven multiplexed PCR reactions. Microsatellite loci detailed in Table 5.5.

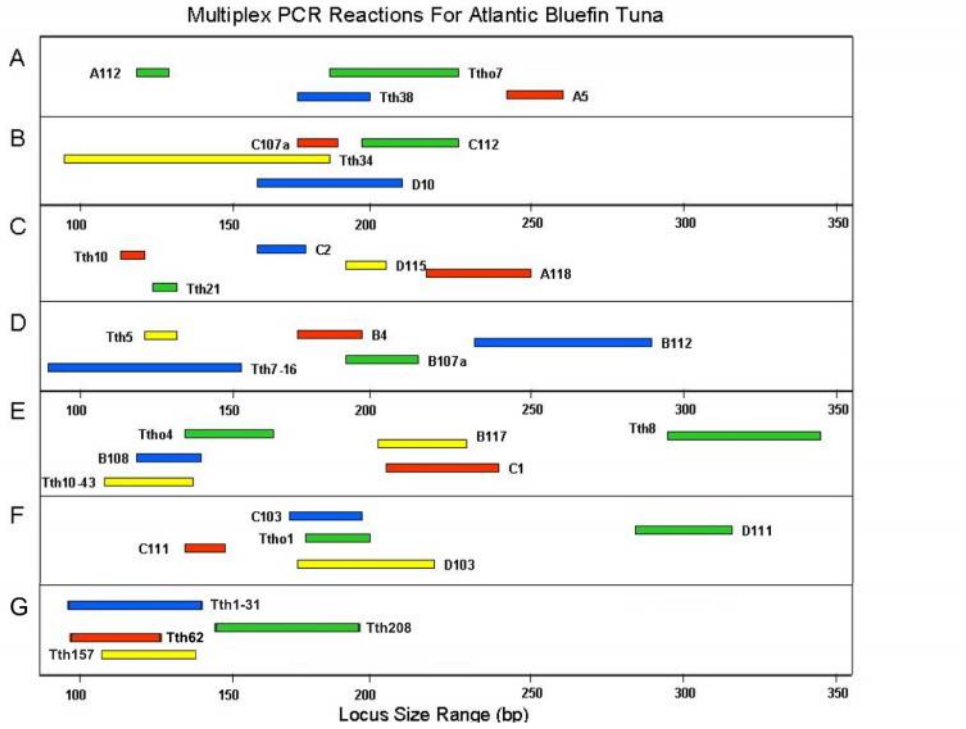

Table 5.5: Detailed list of the 33 microsatellite loci selected.

Locus N°	Reference	Primer	Sequence	Label	Tm (°C)	RANGE (bp)	Repeat
1	NA	ABFT_ A5_F	Carol Reeb personal communication	PET	56	250 - 259	(GA)5+(GTT)8
		ABFT_ A5_R	Carol Reeb personal communication		57		
2	NA	ABFT_ A112_F	Carol Reeb personal communication	VIC	58	121 - 130	(TTG)7
		ABFT_ A112_R	Carol Reeb personal communication		57		
3	NA	ABFT_ A118_F	Carol Reeb personal communication	PET	57	215 - 248	(CAA)14
		ABFT_ A118_R	Carol Reeb personal communication		57		
4	NA	ABFT_ B4_F	Carol Reeb personal communication	PET	57	175 193	(TCA)10
		ABFT_ B4_R	Carol Reeb personal communication		56		
5	NA	ABFT_ B107a_F	Carol Reeb personal communication	VIC	58	184 - 205	(TCA)8
		ABFT_ B107a_R	Carol Reeb personal communication		58		
6	NA	ABFT_ B108_F	Carol Reeb personal communication	6FAM	56	121 - 142	(ATG)8
		ABFT_ B108_R	Carol Reeb personal communication		56		
7	NA	ABFT_ B112_F	Carol Reeb personal communication	6FAM	59	253 - 268	(CAT)8
		ABFT_ B112_R	Carol Reeb personal communication		59		
8	NA	ABFT_ B117_F	Carol Reeb personal communication	NED	59	214 - 238	(CAT/C)17
		ABFT_ B117_R	Carol Reeb personal communication		57		
9	NA	ABFT_ C1_F	Carol Reeb personal communication	PET	56	206 - 238	(TGGA)8
		ABFT_C1_R	Carol Reeb personal communication		56		
10	NA	ABFT_ C2_F	Carol Reeb personal communication	6FAM	59	159 - 187	(TCCA)6
		ABFT_C2_R	Carol Reeb personal communication		60		
11	NA	ABFT_ C103_F	Carol Reeb personal communication	6FAM	58	166 194	(TCCA)9
		ABFT_C103_R	Carol Reeb personal communication		57		
12	NA	ABFT_ C107a_F	Carol Reeb personal communication	PET	59	172 - 188	(TGGA)6
		ABFT_C107a_R	Carol Reeb personal communication		59		
13	NA	ABFT_ C111_F	Carol Reeb personal communication	PET	59	134 - 147	(TCCA)8
		ABFT_C111_R	Carol Reeb personal communication		59		
14	NA	ABFT_ C112_F	Carol Reeb personal communication	VIC	56	183 -220	(TCCA)6
		ABFT_C112_R	Carol Reeb personal communication		56		
15	NA	ABFT_ D10_F	Carol Reeb personal communication	6FAM	59	159 207	(TCTA)14
		ABFT_D10_R	Carol Reeb personal communication		59		
16	NA	ABFT_ D103_F	Carol Reeb personal communication	NED	57	176 - 212	(GATA)11
		ABFT_D103_R	Carol Reeb personal communication		57		
17	NA	ABFT_ D111_F	Carol Reeb personal communication	VIC	55	287 - 319	(GATA)15
		ABFT_D111_R	Carol Reeb personal communication		55		
18	NA	ABFT_ D115_F	Carol Reeb personal communication	NED	56	189 - 205	(TATC)7

Table 5.5 Continued: Detailed list of the 33 microsatellite loci selected.

Locus N°	Reference	Primer	Sequence	Label	Tm (°C)	RANGE (bp)	Repeat
19	McDowell 2002	Tth 38_F	ACAAGCAGCCATAGAGCAGCAC	6FAM	65	170 - 206	(GACA)4
		Tth 38_R	CAACAAGCAAAATGACCGCC		60		
20	McDowell 2002	Tth 10_F	GCTGAGCACGCATTTACTGTAG	PET	63	112 - 128	(GACA)6
		Tth 10_R	CGTCACAACCTTCCAACTCG		63		
21	McDowell 2002	Tth 8_F	CCTGTTTGAGTGTTTATCTGTGCG	VIC	63	294 - 346	(CTGT)10
		Tth 8_R	GGTGTTGGCTATTGAGGAAATGC		63		
22	McDowell 2002	Tth 21_F	GACAGAGAGACAGAGAGAAGGGGAG	VIC	68	125 - 133	(GACA)5
		Tth 21_R	CACAGAGTTGATAACAGCGGCAG		65		
23	McDowell 2002	Tth 34_F	GATGCCATTTCTCTGTCTATCTG	NED	61	99 - 175	(CTGT)7
		Tth 34_R	AAGCCGTTCCCTCAGTGTC		62		
24	McDowell 2002	Tth 5_F	AGGGGGTGGACAAAATAAAAGG	NED	61	125 - 133	(CTGT)4
		Tth 5_R	TGGGAGTGGAGAATGACAGGAGAG		66		
25	Clark 2004	Tth 716_F	TTCCTTCAGGACCAATAAAGTATC	6FAM	59	86 - 170	(TATC)17
		Tth 716_R	TCAGAGCTGCTAGCATGTATGTAG		63		
26	Clark 2004	Tth 1043_F	ATTTTTACCTGGCTACATCTATCT	NED	58	109 - 137	(TCTA)9
		Tth 1043_R	CACACCGGCGATTTTGAG		60		
27	Takagi 1999	Ttho 1_F	AAACGCTCCAGGCAAATGAC	VIC	61	177 - 213	(GT)
		Ttho 1_R	CATAGCACACCCATAGACAC		61		
28	Takagi 1999	Ttho 4_F	CCTTCATCTTCAGTCCCATC	VIC	61	128 - 188	(CA)
		Ttho 4_R	CTGTTCATCTGTTCGCCC		61		
29	Takagi 1999	Ttho 7_F	ACTGGATGAAAGGCGATTAC	VIC	61	180 - 226	(CA)
		Ttho 7_R	ACAGAGGAGCATAACAGAAAC		61		
30	Clark 2004	Tth157_F	CAAGAGGCTTAAAGCAAACTC	NED	60	116-130	(CA)13
		Tth157_R	CATGAATGGGTTCCTTCATC		60		
31	Clark 2004	Tth208_F	GAGAGGGAAAGCAAAGAAG	VIC	60	140-198	(GA)18
		Tth208_R	GTTGAGCTGCTGACACAGA		60		
32	Clark 2004	Tth1-31_F	ATGCACAAGTCATTTATCACCT	6FAM	60	91-133	(AC)11
		Tth1-31_R	AGATGCATGGATTACATTCTACC		60		
33	Clark 2004	Tth62_F	GGTATATGTGTTTGTAGGCGTGTG	PET	60	90-124	(GT)16
		Tth62_R	TTTTCCCAATGCGACTGATGA		60		

5.2.4. Microsatellite PCR amplification and genotyping

Preliminary optimization tests

A total of 16 samples (2 for each of the YOY reference strata samples) have been amplified using all the 33 primers pairs described in Table 5.5.

Multiplex A, B, C, F, G were successfully amplified. Problems arose with Multiplex D and E; in particular loci Tth5 and Tth10-43 failed to amplify or gave inconsistent results. Further optimization steps allowed recuperating all the loci and allowed to include loci Tth5 and Tht10-43 of Multiplex D and E.

Amplification and genotyping.

Alleles were scored using the software Genemarker v1.75 (Softgenetics). The PCR amplification success was calculated with in Genalex 6.5 using the 'Check raw data option' (Peakall and Smouse, 2006; 2012).

Allele scoring was completed for samples included in preliminary tests and 4 out of the 5 plates (see previous paragraph on DNA extraction) for a total of 388 individuals (so beyond the original 320 individuals in the original plan), and 33 loci. The microsatellite genotyping of additional 24 Maltese YOY and 35 Levantine Sea YOY will be performed in the next weeks to get more experimental data on these areas, which provided in the past spotted and subtle genetic divergences (Report of GBYP Phase 4; Riccioni et al. 2013).

5.2.5. Microsatellite data analysis

Check of raw data

Individual genotypes were further checked for genotype quality, and 3 of them were excluded because they failed to amplify for more than 5 loci. All the other specimens had unique multi-locus genotype (MLG); therefore, the subsequent analyses were conducted considering a data set composed by 385 individual MLGs (Table 5.6).

Table 5.6 List of the 385 specimens analysed.

Strata	N° analysed
WMED_BA_2012	49
WMED_BA_2013	46
WMED_TY_2012	50
WMED_TY_2013	50
CMED_SI_2012	44
CMED_SI_2013	50
EMED_LS_2012	55
EMED_LS_2013	40
	385

Materials and methods

Statistical methods for the stock genetic structure and differentiation analyses: ARLEQUIN v.3.5.1.3 (Excoffier and Lischer, 2010) was used to measure genetic differentiation, computing overall as well as pairwise FST, and the exact test of differentiation between all pairs of samples. To correct for multiple comparisons, a false discovery rate FDR correction (Benjamini and Hochberg, 1995) was performed using SGoF+ v3.8 (Carvajal-Rodriguez, and de Uña-Alvarez 2011), whenever necessary. Principal coordinate analysis (PCoA) was calculated with Genalex from covariance matrices with data standardization using FST.

Statistical methods for the clustering analyses: Bayesian Markov Chain Monte Carlo programs with different algorithms and assumptions were used to infer population structure of the studied populations. In all approaches, individuals are assigned probabilistically to one subpopulation or jointly to two or more subpopulations if their genotypes indicate that they are admixed. Firstly, the population structure was investigated with STRUCTURE v2.3.4 (Falush, et al 2003; Falush et al, 2007; Hubisz, et al 2009; Pritchard, et al 2000), using directly the admixture model with correlated alleles frequencies between clusters and LOCPRIOR option (Hubisz, et al 2009). Ten different runs from K=1 to K= 9 of 100000 burn-in followed by 500000 iterations were computed for each K value. To determine the most appropriate value

of K, ΔK statistic developed by (Evanno et al., 2005) calculated using Structure Harvester (Earl and vonHoldt, 2012).

Secondly, the software BAPS v.6 (Bayesian Analysis of Population Structure) was used to cluster specimens into genetically homogenous groups. In BAPS, clustering analysis started with a mixture analysis to determine the most probable number of clusters (K) given the data. The number and composition of clusters was estimated considering upper limit of K at 9. We ran 10 repetitions for each K. Using the groups identified in the mixture analysis, we conducted an admixture analysis with 1000 realizations from the posterior of the allele frequencies. The number of reference individuals from each population was 200 and 15 iterations were used to estimate the admixture coefficients for these reference individuals. The admixture analysis was repeated five times to confirm consistent results. The model estimates the posterior mean probability of an individual with a given multilocus genotype.

Finally, the Discriminant Analysis of Principal Components (DAPC), implemented in the Adegenet R packages (Jombart, 2008), was used since it provides an efficient description of genetic clusters using a few synthetic variables (called the discriminant functions). It maximizes differences between groups while minimizing variation within clusters, and it provides an "assignment measure" of individuals to predefined groups, comparable with ancestry value derived by the Structure analysis. In DAPC analyses, the number of retained PCs has been chosen after the calculation of the α-score.

Results

Large allele dropout and scoring errors (due to stutters) were checked using MICROCHECKER v.2.2.3 (Van Oosterhout, et al 2004). No evidence of stuttering or scoring errors was detected in any locus. All the 33 microsatellite loci we used were polymorphic, and hence used for the following analyses.

The pairwise comparisons showed very low, and mostly not significant, differentiation among the samples (F_{ST}: 0.00–0.003; Table 5.7) with an overall F_{ST} value of 0.0006 (not significant). Out of 28 pairwise F_{ST} comparisons, only one (WMED_TY_2012 vs WMED_TY_2013) resulted significant, but not after FDR correction (Table 5.7 and Figure 5.5). The PCoA analysis confirmed the low level of differentiation among samples and showed WMED_TY_2012 and WMED_TY_2013 as the most divergent samples (Figure 5.6).

Table 5.7 Pairwise F_{ST} values (below the diagonal) and probability values (above the diagonal). The underlined values were not significant after FDR correction.

	WMED_BA_2012	WMED_BA_2013	WMED_TY_2012	WMED_TY_2013	CMED_SI_2012	CMED_SI_2013	EMED_LS_2012	EMED_LS_2013
WMED_BA_2012		0.71582+-0.0119	0.55273+-0.0156	0.46973+-0.0121	0.19629+-0.0103	0.95508+-0.0066	0.83203+-0.0148	0.64258+-0.0143
WMED_BA_2013	-0.00035		0.39844+-0.0155	0.98926+-0.0033	0.90234+-0.0108	0.48047+-0.0156	0.43945+-0.0140	0.94141+-0.0065
WMED_TY_2012	0.00028	0.00084		0.03809+-0.0053	0.31055+-0.0135	0.65137+-0.0146	0.22656+-0.0132	0.24902+-0.0141
WMED_TY_2013	0.00065	-0.00266	0.00318		0.11230+-0.0089	0.05957+-0.0070	0.05469+-0.0064	0.17383+-0.0107
CMED_SI_2012	0.00187	-0.00150	0.00111	0.00239		0.31055+-0.0163	0.55566+-0.0127	0.69238+-0.0148
CMED_SI_2013	-0.00170	0.00059	-0.00021	0.00289	0.00118		0.48047+-0.0138	0.35742+-0.0134
EMED_LS_2012	-0.00078	0.00074	0.00151	0.00288	0.00028	0.00051		0.89453+-0.0111
EMED_LS_2013	0.00006	-0.00193	0.00169	0.00222	-0.00030	0.00104	-0.00123	

Figure 5.5: Matrix of pairwise F_{ST} calculated with the software Arlequin.

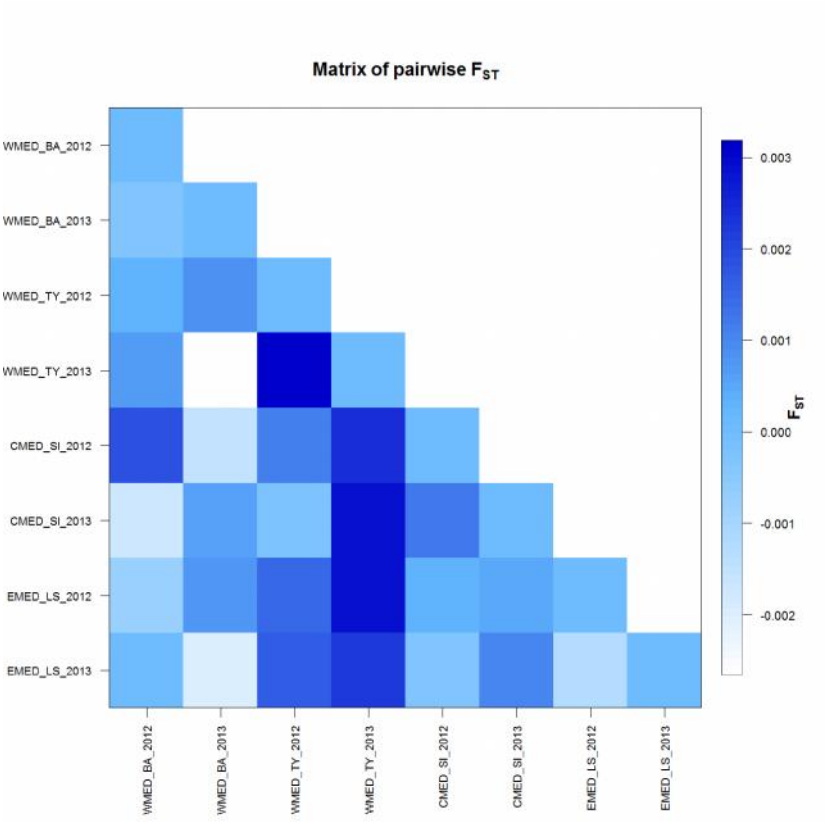

Figure 5.6: Results of the Principal Coordinate Analysis performed with Genalex.

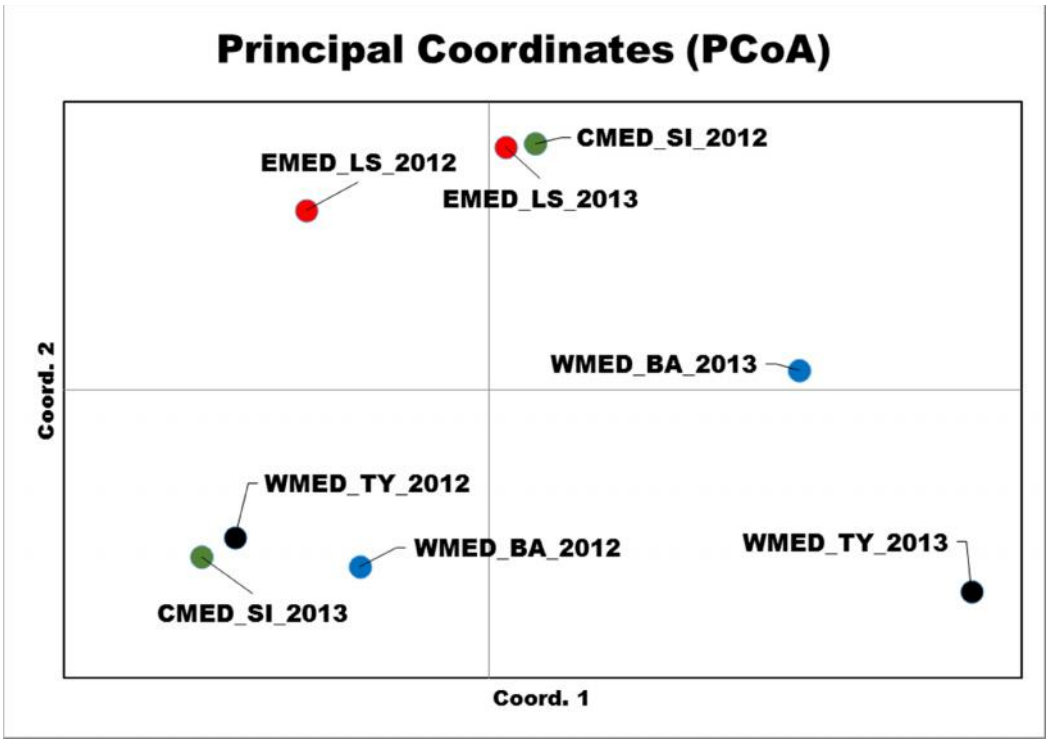

The overall (P value = 0.48094 ± 0.01673) and pairwise Exact tests (data not shown) indicated a total lack of differentiation between all samples.

In the Structure analysis, the ΔK statistics showed a maximum at K=2 (Figure 5.7, upper panel). Therefore, K=2 was retained as the optimal number of clusters in the dataset. The inferred proportional membership to each colony for K=2 (Fig. 5.7, lower panel), clearly indicated that all samples are attribute to the same genetic cluster.

Figure 5.7: Results of the Bayesian clustering realized with Structure.

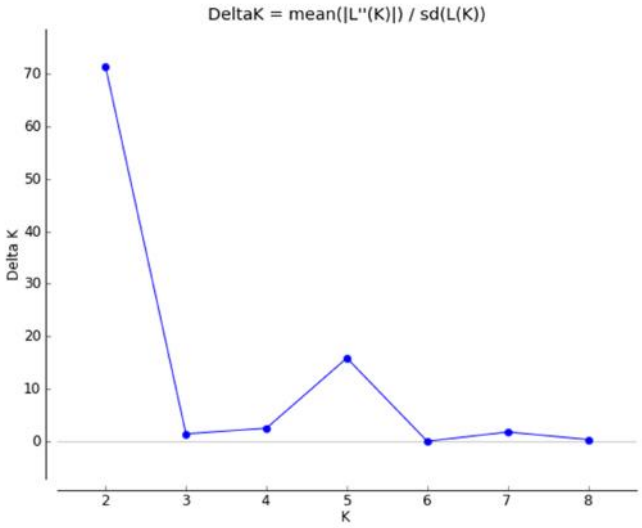

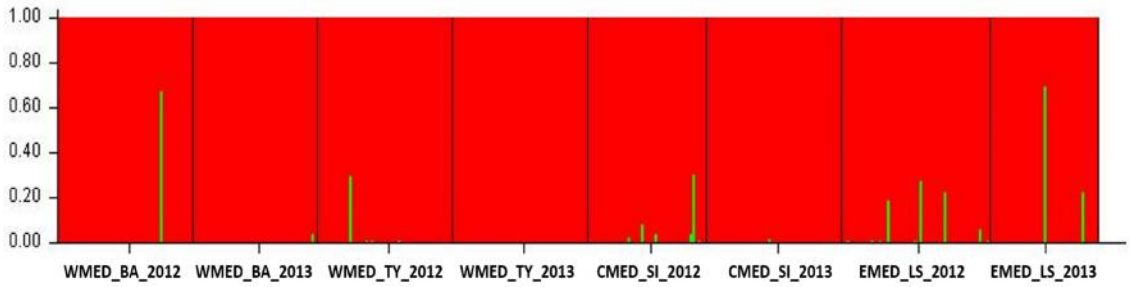

The Bayesian approach implemented in BAPS found a probability of 100% in K=1 for being the correct number of cluster (Figure 5.8).

Figure 5.8: Results of the admixture analysis realized with BAPS.

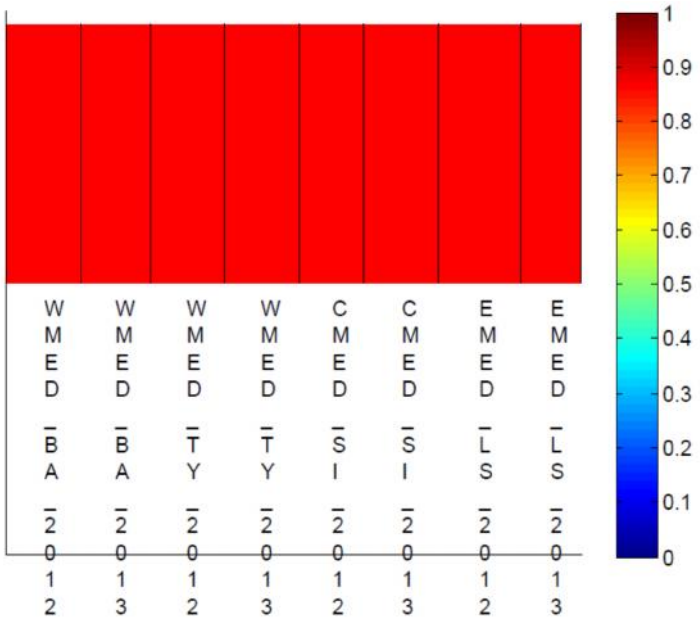

The lack of differentiation was again confirmed by the results of DAPC (Figure 5.9).

Figure 5.9: Results of the DAPC analysis performed with Adegenet.

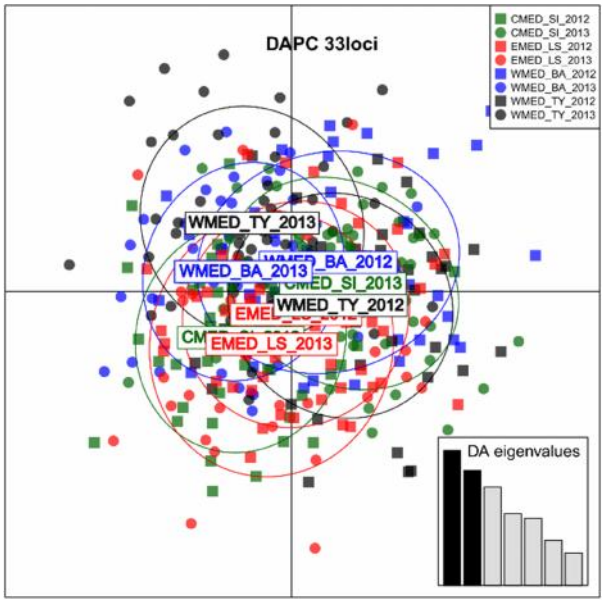

At the end, also the AMOVA analyses displayed the lack of genetic structuring; they indicated that the largest part of the genetic variance is to be attributed to differences among individuals within samples (>99%). No significant differentiation was retrieved when samples were grouped according to the year of collection (2012 vs 2013) or the area of sampling (WMED-BA, WMED-TY, CMED-SI, and EMED-LS) (Table 5.7).

Table 5.7 Results of the analysis of molecular variance (AMOVA).

Source of variation	% of variance	F index	P-value
2clusters			
(WMED_BA_2012+WMED_TY_2012+CMED_SI_2012+EMED_LS_2012)/(WMED_BA_2013+WMED_TY_2013+CMED_SI_2013+EMED_LS_2013)			
among clusters	0.01	F_{CT} = 0.00060	0.48387+-0.01965
Among samples within clusters	0.06	F_{SC} = 0.00055	0.49756+-0.01874
Among individuals within samples	99.94	F_{ST} = 0.00005	0.47605+-0.01547
4clusters			
(WMED_BA_2012+WMED_BA_2013/WMED_TY_2012+WMED_TY_2013/CMED_SI_2012+CMED_SI_2013/EMED_LS_2012+EMED_LS_2013)			
among clusters	-0.02	F_{CT} = -0.00017	0.57674+-0.01380
Among samples within clusters	0.07	F_{SC} = 0.00072	0.42326+-0.01436
Among individuals within samples	99.94	F_{ST} = 0.00056	0.49658+-0.0135

5.2.5. Discussion and future implements.

The results obtained with the present experimental design are straightforward to affirm that *T. thynnus* in the Mediterranean is spatially and temporally structured in a panmictic population with high level of genetic connectivity. The analysis of samples of YOY collected over the four main areas of spawning and density of early life stages (e.g. larvae and small-sized YOY: WMED: Balearic Islands; CMED: South Tyrrhenian and Sicilian Channel; EMED: Levantine Sea) and over two consecutive years (2012 and

2013) represents the most solid genetic survey carried out since now for testing the population structure in the Mediterranean BFT using polymorphic species-specific microsatellite loci. This type of molecular markers has proven to be of high resolving power in detecting subtle genetic differentiation in marine fish (see Hauser et al. 2008). All the statistical tests performed, robustly and consistently indicated that genetic differences in BFT Mediterranean reference samples were null or near null. The spotted and subtle signals of genetic differentiation obtained in the previous analyses using YOY (Carlsson et al. 2004, 2007) and the marked genetic differences detected using juvenile, medium and large BFTs (Riccioni et al. 2010, 2013) could be caused by sampling bias, small number of markers analysed (≤ 9 microsatellite loci), and ecological genetic drift rather than to effective reproductive barriers among groups of subpopulations in the Mediterranean BFT. The lack of genetic heterogeneity recently revealed by the genetic survey carried out by Antoniou et al. (2017) combining data from 16 microsatellite loci and hundreds of genome-wide SNPs obtained from adult farmed BFT collected over Western, Central and Eastern Mediterranean, and by Riccioni et al. (2017) using EST-linked microsatellite loci on medium and large BFTs from the same areas are coherent with the pattern here obtained and with the null genetic heterogeneity detected. However, it has to be stressed that both these studies (Antoniou et al. 2017; Riccioni et al. 2017) targeted adult or subadult BFT individuals whose ecological and behavioural traits enhance gene flow through high potential of migration. On the contrary, obtaining similar homogenous genetic patterns using larvae and/or small-sized YOY BFT individuals, whose ecological and behavioural traits tend to diminishing the potential of dispersal and migration, speaks in favour of large scale reproductive dynamics of *T. thynnus* in the whole Mediterranean.

The use in the present analysis of a large proportion of YOY individuals already genotyped by SNP markers within this and the previous Phases of the GBYP Project (41% and 55% in RAD and GBS genotyping technologies, respectively) makes robust comparison between the results of the present investigation (microsatellite-based) and those obtained from the previous SNP-based genetic investigations. All studies substantially agreed in indicating a genetic homogeneity of the Mediterranean BFT; the feeble signs of temporal heterogeneity detected by previous SNP analyses in the CMED-SI Maltese area (see genetic results of the GBYP phase 4) could not be here verified because we could not include a statistically robust (N ≥ 40) Maltese YOY sample (MA) collected in 2013 in the same area (CMED-SI).

The quality and robustness of genetic data obtained in this task allow them to be further exploited in a broader research framework to test and measure the genetic divergence between the two well-defined but subtly differentiated BFT populations from the Gulf of Mexico and the Mediterranean Sea. This will be addressed by combining the Mediterranean dataset here obtained with that independently obtained by US scientists of the Stanford University at the Marine Hopkins Station (B. Block and C. Reeb) on the Gulf of Mexico early stages. To have an unprecedented joint dataset of highest quality for the experimental design, an intercalibration task between the datasets will be realized using 10 BFT individual gDNAs recently provided by US scientists, and genotyped with independent financial resources.

References

Antoniou A, Kasapidis P, Kotoulas G, Mylonas CC, Magoulas A: Genetic diversity of Atlantic Bluefin tuna in the Mediterranean Sea: insights from genome-wide SNPs and microsatellites. J Biol Res (Thessalon) 2017, 24:3.

Benjamini, Y., and Y. Hochberg, 1995 Controlling the False Discovery Rate: A Practical and Powerful Approach to Multiple Testing. Journal of the Royal Statistical Society. Series B (Methodological) 57: 289-300.

Carlsson, J., J. R. McDowell, et al. (2004). "Microsatellite and mitochondrial DNA analyses of Atlantic bluefin tuna (*Thunnus thynnus thynnus*) population structure in the Mediterranean Sea." Molecular Ecology 13(11): 3345-3356.

Carlsson, J., J. R. McDowell, et al. (2006). "Genetic heterogeneity of Atlantic bluefin tuna caught in the eastern North Atlantic Ocean south of Iceland." Ices Journal of Marine Science 63: 1111-1117.

Carlsson, J., J. R. McDowell, et al. (2007). "Genetic identity of YOY bluefin tuna from the eastern and western Atlantic spawning areas." Journal of Heredity 98(1): 23-28.

Carvajal-Rodriguez, A., and J. de Uña-Alvarez, 2011 Assessing Significance in High-Throughput Experiments by Sequential Goodness of Fit and *q*-Value Estimation. PLoS One 6: e24700.

Earl, D.A. & vonHoldt, B.M. Conservation Genet Resour (2012) 4: 359. doi:10.1007/s12686-011-9548-7

Evanno, G., S. Regnaut & J. Goudet, 2005. Detecting the number of clusters of individuals using the software STRUCTURE: a simulation study. Molecular ecology 14(8):2611-2620 doi:DOI 10.1111/j.1365-294X.2005.02553.x.

Excoffier, L., and H. E. Lischer, 2010 Arlequin suite ver 3.5: a new series of programs to perform population genetics analyses under Linux and Windows. Mol Ecol Resour 10: 564-567.

Falush, D., M. Stephens and J. K. Pritchard, 2003 Inference of population structure using multilocus genotype data: Linked loci and correlated allele frequencies. Genetics 164: 1567-1587.

Falush, D., M. Stephens and J. K. Pritchard, 2007 Inference of population structure using multilocus genotype data: dominant markers and null alleles. Molecular Ecology Notes 7: 574-578.

Hauser L, Waples RS, Carvalho GR: Special Issue: Advances in Marine Fish and Fisheries Genetics. Fish and Fisheries 2008, 9(4):331-332.

Hubisz, M. J., D. Falush, M. Stephens and J. K. Pritchard, 2009 Inferring weak population structure with the assistance of sample group information. Mol Ecol Resour 9: 1322-1332.

Jombart Thibaut (2008). Adegenet: a R package for the multivariate analysis of genetic markers. Bioinformatics; 24 (11): 1403-1405. doi: 10.1093/bioinformatics/btn129

Peakall, R., and P. E. Smouse, 2006 GENALEX 6: genetic analysis in Excel. Population genetic software for teaching and research. Molecular Ecology Notes 6: 288-295.

Peakall, R., and P. E. Smouse, 2012 GenAlEx 6.5: genetic analysis in Excel. Population genetic software for teaching and research—an update. Bioinformatics 28: 2537-2539.

Pritchard, J. K., M. Stephens and P. Donnelly, 2000 Inference of population structure using multilocus genotype data. Genetics 155: 945-959.

Riccioni, G., M. Landi, et al. (2010). "Spatio-temporal population structuring and genetic diversity retention in depleted Atlantic Bluefin tuna of the Mediterranean Sea." ProcNatlAcadSci U S A 107(5): 2102-2107.

Riccioni, G., M. Stagioni, et al. (2013). "Genetic Structure of Bluefin Tuna in the Mediterranean Sea Correlates with Environmental Variables." PLoS ONE 8(11): e80105.

Riccioni G, Cariani A, Ferrara G, Cannas R, Melis R, Stagioni M, Addis P, Tinti F: Evolutionary constraints limiting the variation of Expressed Sequence Tag-

linked microsatellite loci, prevent the detection of local adaptation in Mediterranean Bluefin tuna. Fisheries Research 2017, 190:157-163.

Van Oosterhout, C., M. K. Van Heuven and P. M. Brakefield, 2004 On the neutrality of molecular genetic markers: pedigree analysis of genetic variation in fragmented populations. Mol Ecol 13: 1025-1034.

6. OTOLITH SHAPE

Task: Otolith shape analysis

Task leader: Deirdre Brophy (GMIT)

Participants:

GMIT: Deirdre Brophy, Roxanne Duncan, Aaron Hickey

AZTI: Haritz Arrizabalaga, Igaratza Fraile

6.1. Introduction

Brophy et al (2015) showed that variation in otolith shape is useful for discriminating between adult (>200cm) bluefin tuna from the eastern and western Atlantic. The baseline samples used in that study comprised of 50 adult fish from the Canadian fishery (Gulf of St Lawrence, Newfoundland and the Scotian Shelf) and 50 adult fish from the central Mediterranean (Malta) collected during the spawning season. Previous evidence from otolith stable isotope signatures indicated that the vast majority (99%) of the bluefin caught in the Gulf of St Lawrence and adjacent areas had originated from nursery areas in the western Atlantic (Schloesser et al. 2010), justifying the choice of samples for the western baseline. However, a more recent study (Hanke et al 2016) has shown that catches of bluefin from the Gulf of St Lawerence fishery can contain individuals of Mediterranean origin (up to 35%). Therefore, the western baseline may have contained some individuals that belonged to the eastern spawning population. In addition, the eastern baseline samples all came from the same location and may not have been fully representative of the Mediterranean spawning population. Otolith shape is under both genetic and environmental influence (Vignon and Morat 2010) and is likely to reflect migration history as well as natal origin. To determine if otolith shape descriptors can be used to accurately assign individuals to spawning populations (rather than just capture

locations), samples of spawning adults collected from known spawning grounds should be used to characterise the stocks. An objective of GBYP Phase 5 and 6 was to refine the baselines used to characterise the western and eastern stocks by including adults from the Gulf of Mexico spawning grounds and adults from a wider geographical range within the Mediterranean collected during the spawning season (May and June). The sampling also targeted a broader size range of fish (>170cm). The task aimed to use shape analysis of otolith outlines to distinguish between the two spawning populations to determine if otolith shape descriptors provide a reliable marker of spawning origin and to use this classification to determine the likely origin of estimate stock composition of mixed samples collected in the Atlantic in 2011, 2012 and 2013.

6.2. Methods

Baseline samples

The western baseline comprised of 104 otoliths from bluefin collected from the Gulf of Mexico between 2009 and 2014 that were sourced through collaboration with Robert Allman and John Walter (NOAA). The eastern baseline samples included 118 otoliths from bluefin captured from five locations in the Mediterranean during the spawning season as part of the GBYP sampling programme in 2011, 2012, 2013 and 2015 (Table 6.1).

Mixed samples

Seventy nine samples of unknown spawning origin were obtained from the GBYP database. These fish were collected from three locations in the eastern Atlantic: the straits of Gibraltar (GI), the coast of Portugal (PO) and Morocco in 2011, 2012 and 2013 (Table 6.2). These individuals were chosen for inclusion in this analysis because stable isotope measurements were also available allowing comparison of assignments in the subsequent integrated analysis task. The classification functions developed from the baseline samples were used to assign these individuals to one of the two spawning populations.

Image capture and extraction of shape variables

Otolith images were captured using a stereomicroscope connected to a digital camera with a PC interface. Otoliths were photographed as a white object on a black background in a standard orientation. The right otolith was used where possible. When the right otolith was unavailable the left otolith was photographed and the image was rotated. Otoliths were excluded from shape analysis when their outline was obscured by breakage or adhering dirt/tissue.

Bluefin otolith images were converted to 8 bit and the otolith outline was created by intensity thresholding in Image J (Version 1.50i). Seven shape indices were obtained: Circularity, (4π * (Area/Perimeter2)), Aspect ratio, (the ratio of the major and minor axes of the ellipse which binds the outline), Roundness, (4 *(Area/π * (Major axis2)) and Solidity, (Area/Convex area), Ellipticity, ((Feret Length – Feret Width) – (Feret Length + Feret Width)), Form factor, (4pi*area/ (perimeter) 2), and Squareness, (Area / (Feret Length x Feret Width)). The XY coordinates for each otolith were saved for subsequent extraction of the Elliptical Fourier coefficients. The elliptical Fourier analysis was conducted using the statistical program, R (Version 3.3.2). Using the Momocs package (Version 1.1.0), the coordinates of each otolith were centred, scaled and aligned to a consistent orientation. A Fourier power test was performed and the first twelve harmonics were shown to describe 99% of the cumulative variability of the otolith shape. Since each harmonic consists of four coefficients and the first three were used for standardisation; altogether, 52 variables (45 coefficients and 7 shape indices) were used in the analysis.

Data analysis

All the variables were tested for normality and homogeneity of variance and were transformed when necessary. Variables significantly correlated with fish length were standardised using the common within-group slope from an analysis of covariance (ANCOVA) with population included as a factor and fish length as a covariate. Any variables with a significant interaction term between fish length and population could not be corrected with the within-group slope and were therefore removed from the analysis. After standardisation, 24 (23 elliptical

coefficients and 1 shape index) were found to be significantly different between populations and were kept for further analysis. Within each population, variation in the shape descriptors between sampling years was also investigated.

A correlation plot was created to identify multicollinearity among the selected variables. Where strong correlations ($r>0.7$) were detected, variables were omitted from the analysis. The variables were included in a stepwise forward variable selection discriminant analysis. Variables which showed significant differences between sampling years were removed and the stepwise DFA was repeated.

The final sets of variables from the DFA were then used in a random forest analysis (randomForest package in R) and the probability of group membership was estimated for each individual in the mixed sample.

6.3. Results and Discussion

Baseline analysis

Nine shape descriptors (A2, A3, B2, B4, B10, C4, D2, D5, and circularity) were retained in the DFA by stepwise selection producing one canonical function that distinguished between otoliths from east Atlantic and west Atlantic fish ($P<0.0001$). The canonical function distinguished between fish of eastern and western origin with a mean jack-knife classification success rate of 78% (Table 6.3a). Three shape descriptors (circularity, B10 and A2) showed significant differences between years. Removal of these descriptors from the variable selection process produced a slightly different classification model (A3, A9, B5, B9, C4, C9, D2, D5, D9) but the same overall classification success (Table 6.3b).

Brophy et al (2015) discriminated between bluefin from the western (Canada) and eastern Atlantic (Malta) with a classification success of 82% (83% for the western samples and 82% for the eastern samples). In this analysis using baseline samples from the Gulf of Mexico spawning grounds and additional sites within the Mediterranean, the classification success decreased to 76% for the western Atlantic and 80% for the Mediterranean. The original baseline samples

from Canada and Malta (Brophy 2015) may have had more distinct environmental histories (e.g. have resided in the west or east Atlantic for the majority of their lives) compared to the more extensive baselines used in the current analysis. Although there is significant variation in otolith shape between the Gulf and Mexico and the Mediterranean spawning populations, a classification function based on otolith shape descriptors alone provides only moderate discrimination between the groups.

Mixed analysis

The misclassification rate (out of bag error) associated with the random forest model was 28%. When individuals in the mixed samples were assigned to populations using the random forest model of shape descriptors, the percentage of fish that were estimated to be of Mediterranean origin was lower than that previously reported by Brophy et al (2015) (Table 6.2). The probabilities of group membership was <70% for the majority (73%) of the individuals. The analysis of the refined baseline samples confirms that there is considerable overlap in otolith shape between the two spawning populations. On its own, otolith shape does not provide a sufficiently reliable marker of spawning origin and estimates of stock composition based on otolith shape are subject to a large degree of error. It appears that due to the strong influence of environmental history on otolith shape, the technique may be a more powerful for characterising contingents within both populations that follow different migration pathways. Otolith shape analysis could be used together with stable isotope measurements and genetic markers to characterise stock contingents at feeding areas in the western Atlantic and Mediterranean. The stable isotope and genetic markers would provide a marker of natal origin while otolith shape could be used to characterise the feeding area. This could be used to estimate the relative proportions of four contingents: 1) bluefin of Mediterranean origin that feed in the western Atlantic; 2) bluefin of Mediterranean origin that remain resident, 3) bluefin that originate from the western spawning grounds and feed in the Atlantic 4) bluefin of western origin that remain in the western Atlantic.

Table 6.1: Summary of bluefin tuna (>170 fork length (cm)) baseline samples used to characterise the eastern and western spawning populations with otolith shape analysis. Mean lengths (cm) are shown in regular font followed by the range (in italics) and the number of fish used in the analysis (in bold)

	Sampling year							
Region	**2009**	**2010**	**2011**	**2012**	**2013**	**2014**	**2015**	**Total**
GoM	253.7	246.0	-	248.4	244.3	225.3	-	
	205-288	*212-280*	-	*230-273*	*227-281*	*181-259*	-	
	44	**24**	**0**	**10**	**14**	**12**	**0**	**104**
LS	-	-	-	-	-	-	231.3	
	-	-	-	-	-	-	175-272	
	0	**0**	**0**	**0**	**0**	**0**	**23**	**23**
MA	-	-	225.8	225.8	-	-	-	
	-	-	*220-230*	*184-270*	-	-	-	
	0	**0**	**4**	**63**	**0**	**0**	**0**	**67**
SA	-	-	-	214.9	-	-	184.0	
	-	-	-	*204-252*	-	-	*184-184*	
	0	**0**	**0**	**15**	**0**	**0**	**1**	**16**
SY	-	-	-	-	-	-	195.2	
	-	-	-	-	-	-	*170-237*	
	0	**0**	**0**	**0**	**0**	**0**	**11**	**11**
TY	-	-	-	-	215.0	-	-	
	-	-	-	-	*215-215*	-	-	
	0	**0**	**0**	**0**	**1**	**0**	**0**	**1**

Table 6.2: Summary of bluefin tuna mixed samples that were assigned to putative populations using a classification function based on otolith shape descriptors

	Sampling year				
Region	**2011**	**2012**	**2013**	**% east new baselines**	**% east Brophy et al 2015**
GI	198.5 - **1**			100	94.3*
MO	230.5 *220-241* **2**	209.9 *187-225* **18**	214 *176-236* **30**	66.0	78.6
PO	207 *183-235* **16**	210.8 *191-281* **12**	- - **0**	78.6	91.4

*****from sample of 17 fish

Table 6.3: Jack-knife classification matrix from the discriminant function analysis, using a) nine otolith shape descriptors (A2, A3, B2, B4, B10, C4, D2, D5, and circularity) and b) nine otolith shape descriptors that showed no significant variation between sampling years (A3, A9, B5, B9, C4, C9, D2, D5, D9) to discriminate between adult bluefin tuna (>170cm FL) from spawning populations in the Gulf of Mexico and the Mediterranean.

a)

True origin	**GoM**	**Med**	**%correct**
GoM	77	27	74
Med	22	96	81
Total	99	123	78

b)

True origin	**GoM**	**Med**	**%correct**
GoM	79	25	76
Med	24	94	80
Total	103	119	78

7. INTEGRATED APPROACH TO STOCK DISCRIMINATION

Task leader: Deirdre Brophy (GMIT)
Participants:
GMIT: Deirdre Brophy, Roxanne Duncan, Aaron Hickey
AZTI: Haritz Arrizabalaga, Naiara Rodriguez Ezpeleta, Igaratza Fraile

7.1. Introduction

Various genotypic (Carlsson et al. 2007; Boustany et al. 2008; Dickhut et al. 2009; Albaina et al. 2013) and phenotypic (Brophy, et al. 2015; (Rooker et al. 2003; Rooker et al. 2008; Dickhut et al. 2009; Fraile et al. 2014) population markers have been used to distinguish between bluefin from the eastern and western Atlantic. However, there is a degree of uncertainty associated with each method of population assignment. In GBYP Phase 5, comparisons of individual assignments using genetics, isotopes and otolith shape methods revealed disagreement between the three methods. It may be possible to improve overall accuracy of stock assignment by using a combination of population markers in an integrated stock mixture analysis (Smith and Campana 2010). This task employs the data and material produced by the integrated analysis task from Phase 5 and additional data generated by other tasks in Phase 6 to develop a multi-marker method for discriminating between bluefin tuna from the Gulf of Mexico and Mediterranean spawning populations.

7.2. Methods

Combining chemistry and shape

For the baseline samples and the mixed samples used in the otolith shape analysis task, stable isotope (d13C, d18O) measurements from the natal portion of the otolith were provided through collaboration with NOAA and from additional analysis conducted during GBYP Phase 6. Random forest machine learning algorithms were used to classify the baseline fish (table 7.1, otolith shape task) based on a) shape only b) chemistry only and c) chemistry and shape.

The classification error associated with each model was compared using out of bag estimates of error rates.

The same models were then used to assign probabilities of group membership to the 79 individuals in the mixed sample (table 7.2, otolith shape task). Individual assignments were compared between the three models and levels of agreement were examined.

Combining chemistry, shape and genetics

In the baseline samples, 57 of the Gulf of Mexico fish and 102 of the Mediterranean fish were analysed using chemistry (d13C, d18O), shape and genetics. For the genetic analysis nucleotide sequences were available for 48 individual SNP loci. Gene frequencies were compared between the two populations using Chi square analysis. Loci which varied between populations were included as categorical predictors in three classification models using random forest: a) genetics only; b) chemistry and genetics; c) chemistry, shape and genetics. The classification error associated with each model was compared using out of bag estimates of error rates.

The mixed sample had not been analysed using SNP loci so individual assignments could not be compared between the various models. To examine the effect of combining genetic and otolith data on individual assignments, the baseline data set was split into a train (50 Mediterranean and 50 Gulf of Mexico) and a test (7 Gulf of Mexico, 52 Mediterranean) set. The classification models were built again using the training set and probabilities of group membership was estimated for each individual in the test set. The individual assignment probabilities for the test sample were also compared between the chemistry only model and the integrated models.

7.3. Results and Discussion

Combining chemistry and shape

The baseline samples could be classified to population of origin with a high degree of accuracy using stable isotopes (95% accuracy, Table 7.1). There was a

comparatively high error rate associated with the shape only model (28%). Combining shape descriptors and chemistry produced only a slight improvement in classification success for fish of Mediterranean origin (98% compared to 97%, Table 7.1) and the variable influence plot showed that the model was largely driven by d18O followed by d13C and D5 (Figure 7.1).

Individual assignment of the mixed sample resulted in 39% disagreement between the shape only and chemistry only models and 10% disagreement between the chemistry/shape combined model compared to the chemistry model. The percentage of individuals that were assigned to the Mediterranean sample varied between each model, particularly for the sample from Morocco (Table 7.2). Mean individual assignment probabilities for the mixed sample were highest for the chemistry model (GoM 79.9%, Med 92.8%) compared to the shape model (GoM 67%; Med 64%) and the combined chemistry/shape model (GoM 76%; Med 80%). In other words, combining chemistry and shape data increased the uncertainty of the individual assignments compared to the chemistry only model. Otolith shape appears to reflect environmental history rather than natal origin and thus does not complement stable isotope measurements in a discrimination of adults from the two spawning populations. A better way to combine otolith shape and chemistry data may be to characterise resident and migrant groups at feeding grounds in the western and eastern Atlantic.

The classification success achieved here using adult spawning fish as the baseline samples is higher than that reported by Rooker et al (2014) (Figure 7.2). In that study stable isotope signatures discriminated between yearlings from western and eastern nursery areas with a success rate of 73% and 90% respectively. The isotope data from the two studies are directly comparable; the same portion of the otolith was analysed in both cases using the same techniques and the same machine. The fact that the adult spawning assemblages in the Gulf of Mexico and the Mediterranean are much more distinct than the yearlings from the two areas may indicate that some transfer of fish from the eastern to the western Atlantic occurs after the natal signature was laid down and before the

yearlings were captured (i.e. between 12 and 18 months after hatching) or alternatively that there is a third spawning component at nursery areas in the west Atlantic. It should also be considered that the higher degree of overlap between the two populations in the yearling baseline may be explained by inter-annual variability, if more year-classes are represented in the yearling baseline compared to the adult baseline. Finally, the adult baseline does not yet include samples from the Balearic Islands in the Western Mediterranean. If the natal stable isotope signature of bluefin spawning in this area is less distinct from the Gulf of Mexico baseline than bluefin from other parts of the Mediterranean, this would increase the overlap between the two adult baselines. Further analysis to resolve the observed differences between the yearling and adult baselines is ongoing. The outcome of those investigations will establish if population assignments of bluefin captured in mixing areas could be improved by using adult rather than yearling baseline signatures.

Combining chemistry, shape and genetics

The chi square analysis revealed significant differences in frequencies at nine loci (Rad213, Rad26, Rad207, Rad109, Rad47, Rad96, Rad117, Rad55, Rad78). When gene frequencies at these 9 loci were included in a random forest model, the baseline samples were classified to population of origin with a classification success of 68% and 80% for the Gulf of Mexico and Mediterranean populations respectively (Table 7.1, Table 7.3). The 9 loci were then included with d13C and d18O in a combined classification model. On examination of the variable influence plot (Figure 7.1), the model was rerun using the main contributory variables (d18O, Rad213, d13C and Rad26. This produced the lowest error rate of all models tested (3.8%, Table 7.4). The three way integrated model (chemistry, shape and genetics) did not improve the classification success (error rate 5.1%; Table 7.3). This again suggests that the otolith shape measurements do not provide complementary information about natal origin but may provide an alternative indicator of migratory history.

Combining chemistry and genetics improved the mean individual assignment probabilities by 6% for the Gulf of Mexico samples and 0.92% for the Mediterranean samples compared to the chemistry only model. Improvements relative to the genetics only model were 14% for the Gulf of Mexico samples and 20% for the Mediterranean samples (Table 7.4). This shows that Rad SNP genotypes can complement stable isotope measurements and improve the accuracy of natal origin estimates. The baseline samples used in this analysis showed relatively large differences in stable isotope measurements with little overlap between the Gulf of Mexico and Mediterranean samples. Greater improvements in accuracy may be possible for samples that are more difficult to discriminate using stable isotope measurements (as has been reported in previous studies, eg Rooker et al 2014). The genetics only model is included here for comparative purposes. It is important to note that higher rates of classification success could be achieved using a greater number of genetic markers.

Of the 59 individuals in the test sample, 58 were assigned to the same group using both models. One individual from the Mediterranean population was incorrectly assigned to the Gulf of Mexico population based in stable isotopes, although the assignment probability was borderline (0.52). This individual was correctly assigned to the Mediterranean population using the combined model and the assignment probability increased to 0.68. This illustrates the potential usefulness of combining stable isotope and genetic markers for individuals of uncertain origin.

Table 7.1: Confusion matrix from the random forest analysis, using a) d18O and d13C stable isotope measurements b) a combination of stable isotope measurements and shape descriptors (d18O, d13C, D5, C4, A3, B2, D2, D9) and c) a combination of otolith chemistry and genetics (d18O, d13C, Rad213, Rad26) d) 9 SNP Rad loci (Rad213, Rad26, Rad207, Rad109, Rad47, Rad96, Rad117, Rad53, Rad 78) to discriminate between adult bluefin tuna (>170cm FL) from spawning populations in the Gulf of Mexico and the Mediterranean.True origin indicated in first column. Assignements to Gulf of Mexico and Mediterranean in the second and third columns.

a)

True origin	GoM	Med	%correct
GoM	97	7	93
Med	4	114	97
Total	101	121	95

b)

True origin	GoM	Med	%correct
GoM	97	7	93
Med	3	115	98
Total	100	122	95

c)

True origin	GoM	Med	%correct
GoM	53	2	96
Med	4	98	96
Total	57	100	97

d)

True origin	GoM	Med	%correct
GoM	39	18	68
Med	14	88	86
Total	53	106	80

Table 7.2: Comparison of population assignments of the mixed sample using chemistry and shape

		% eastern (Mediterranean) origin		
Region	**N**	**shape**	**chemistry**	**chem-shape**
GI	1	100	100	100
MO	50	66	72	70
PO	28	78.6	71.4	75

Table 7.3: Comparison of classification accuracy achieved across the final random forest models

Model	**Variables used**	**Error estimate**
Shape	D5+C4+A3+B2+D2+A2+B10+B4	28%
Chemistry	D18o+d13C	4.9%
Genetics	Rad26+Rad213+Rad207+Rad109+Rad47+Rad96+Rad117+Rad53+Rad78	20.1%
Shape and chemistry	d18o+d13c+D5+C4+A3+B2+D2+D9	4.5%
Chemistry and genetics	d18o+d13c+Rad26+Rad213	3.8%
Shape and genetics	Rad26 + Rad213 + D5 + C4 + A3 + B2 + D2 + D9	18.8%
Chemistry, shape and genetics	d13c+d18o+Rad26+Rad213+D5+C4+A3+B2+D2+D9	5.1%

Table 7.4 Average improvement in individual population assignment probabilities for each of the combined models compared to the chemistry only model using a test sample of the baseline.

Population	chem-shape vs chem	chem-gen vs chem	Chem-gen vs genetics		chem-shape-gen vs chem
GoM	0.34%	6.05%	14.4%		-2.50%
Med	-8.28%	0.92%	20.4%		-6.56%
Overall	-7.26%	1.53%	20%		-6.08%

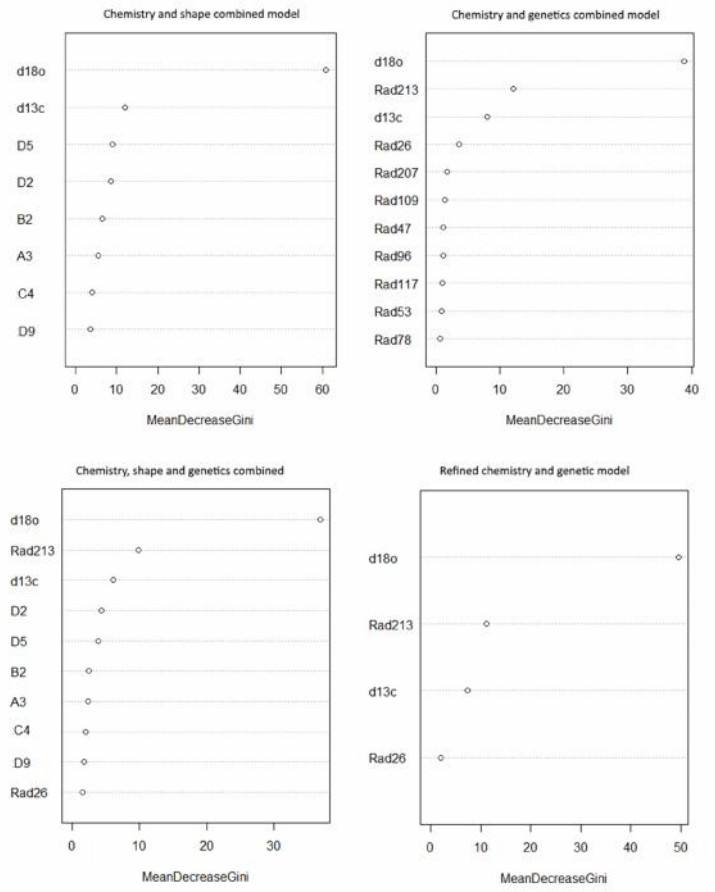

Figure 7.1: Variable influence plots showing the relative importance of each of the variables in the combined chemistry and shape model (top left), the combined chemistry and genetic model (top right), the combined chemistry, shape and genetics model (bottom left) and the final refined chemistry and genetic model which produced the lowest error rate (bottom right).

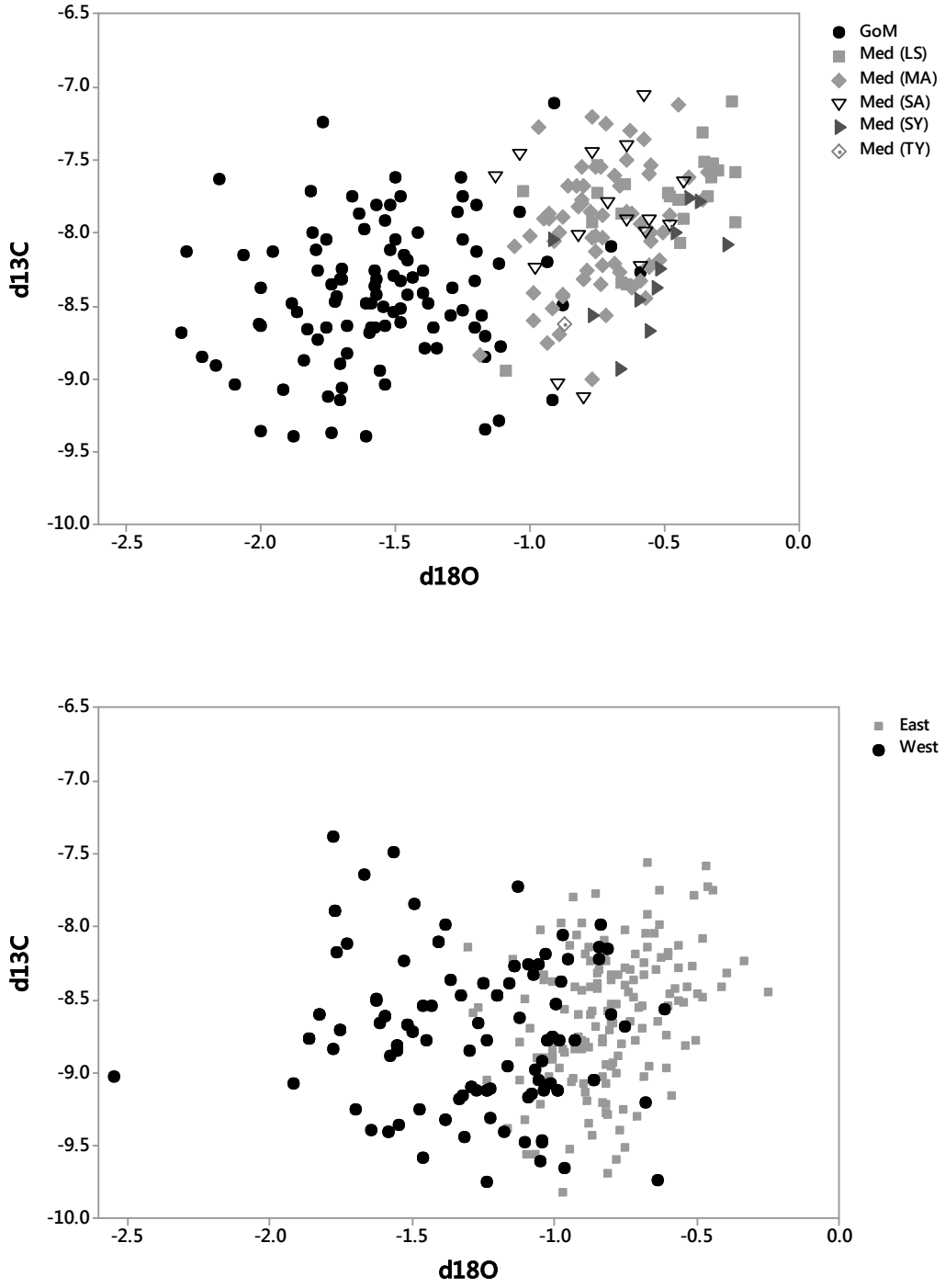

Figure 7.2. Plot showing the distributions of d13C and d18O measurements for a) the adult baseline samples from the Gulf of Mexico (GoM) and five locations (Levantine Sea (LS); Malta (MA); Sardinia (SA); Gulf of Syrta (SY); Tyrrhenian Sea (TY)) in the Mediterranean (Med) used in this analysis and b) the yearling baseline samples from the east and west Atlantic used in Rooker et al (2014).

References

Brophy Deirdre, Haynes P, Arrizabalaga H, Fraile I, Fromentin JM, Garibaldi F, Katavic I, Tinti F, Karakulak FS, Macías D, Busawon D, Hanke A, Kimoto A, Sakai O, Deguara S, Abid N, Santos MN (2015) Otolith shape variation provides a marker of stock origin for north Atlantic bluefin tuna (Thunnus thynnus). Marine and Freshwater Research **67**, 1023-1036.

Hanke A, Busawon D, Rooker JR, and Secor DH (2016) Estimates of stock origin for bluefin tuna caught in western Atlantic fisheries from 1975 to 2013. Collect. Vol. Sci. Pap. ICCAT, 72(6): 1376-1393 SCRS/2015/041

Rooker JR, Arrizabalaga H, Fraile I, Secor DH, Dettman DL, Abid N, Addis P, Deguara S, Karakulak FS, Kimoto A, Sakai O, Macias D, Santos MN (2014) Crossing the line: migratory and homing behaviors of Atlantic bluefin tuna. Marine Ecology Progress Series 504: 265-276 doi 10.3354/meps10781

Schloesser RW, Neilson JD, Secor DH, Rooker JR (2010) Natal origin of Atlantic bluefin tuna (Thunnus thynnus) from Canadian waters based on otolith delta C-13 and delta O-18. Canadian Journal of Fisheries and Aquatic Sciences 67: 563-569 doi 10.1139/f10-005

Vignon M, Morat F (2010) Environmental and genetic determinant of otolith shape revealed by a non-indigenous tropical fish. Marine Ecology Progress Series 411: 231-241 doi 10.3354/meps08651

8. AGE DETERMINATION ANALYSES

Task Leader: Enrique Rodriguez-Marin (IEO)

Participants

IEO: Pablo Quelle, Marta Ruiz and Elvira Ceballos.

8.1. Introduction

The biological analysis of this project includes direct ageing to obtain age composition of Atlantic bluefin tuna (ABFT) catches and age composition of the population structure samples. The bluefin tuna Species Group has emphasized the need for annual age-length keys (ALKs) (ICCAT, 2015b; 2016). Rodriguez-Marin et al. (2009) found that cohorts of bluefin tuna can be more easily detected and followed when annual ALKs were used.

In previous phases of the project, a stratified sampling by size class, geographical location, month of harvest and fishing gear was used in the selection of samples to obtain a robust ALK for 2011. In this sixth phase of the project it was proposed that the activity of aging be carried out on the available hard parts already collected in 2012. Thus two annual ALKs with good sampling coverage would be available. In the sixth phase we propose to complete the 2012 ALK, which has currently 239 calcified structures read in previous phases, with the analysis of 325 new ones.

8.2. Material and Methods

The selection of samples included the following strata: 10 cm size bins (straight fork length, SFL), east Atlantic Ocean and Mediterranean Sea, and type of calcified structure (otoliths and fin spines). A total of 325 hard parts were selected with an approximately equal number of samples from the Atlantic Ocean and Mediterranean Sea, and type of calcified structure, otoliths and spines (Table 8.1). The most commonly used fishing gear for catching the tuna from which the samples originated was bait boat, followed by long line, trap and purse seine. Some samples were obtained from specimens caught in 2012 but harvested in 2013 (n=11).

Otoliths were prepared and interpreted following the methodology described in Secor et al. (2014) and Busawon et al. (2015). Whole otolith image was captured for otolith shape analysis. Then, otolith was used to obtain three sections: two thin sections (≈ 0.5 mm) for age estimates and a thick section (≈ 2 mm) for natal origin analyses. Images of sanded sections were taken under reflected light and opaque bands were counted. Spines were prepared and read following the methodology described in Rodriguez-Marin et al. (2012) and Luque et al. (2014), therefore, transmitted light was used and translucent bands were counted. The age interpretation of both structures was performed on digitally enhanced images.

Otoliths were read once by two experienced readers, each reader read half of the set of otoliths. When sample reading was difficult and the ager was unsure with the age estimation, a 2nd reading was conducted by the other reader. If the readings differed by 1 year, the most experienced ager reading was used as the final age and if the readings differed by 2 or more years, a 3rd reading was conduct with knowledge of the prior readings to reach a consensus final age. Spine readings were conducted independently by two experienced readers; both readers aged all the samples. When differences appeared in the readings, a 3rd reading of consensus was made.

Final age was adjusted for both structures to account for the date of harvesting and the timing of bands formation throughout the year: otoliths final age was adjusted by adding 1 year to the age when the fish was caught between January 1 and the assumed time of the opaque band formation (June 1) (Rodriguez-Marin et al., 2016b); spines final age was adjusted by subtracting 1 year to the age when the fish was caught between June 1 and December 31 and the edge of the structure was translucent (Luque et al., 2014).

Diagnosis of paired age agreement was evaluated for spines by precision indices through Average Percent Error (APE) and Coefficient of Variation (CV), and tests of symmetry (Campana et al., 1995; McBride, 2015). Precision was not estimated for otoliths, since there was only time to make a single reading of each otolith (the samples were received in October 2016 due to the delay in signing the contract).

Age length keys (ALKs) were built for this sixth phase of the project and for all samples coming from 2012. Samples were grouped by calcified structure and geographical origin (Atlantic Ocean and Mediterranean Sea). Both calcified structures readings were combined to build these last ALks, but spines aged older than 13 years were not included (Rodriguez-Marin et al., 2016a).

8.3. Results and Discussion

In the sixth phase of the project, age has been interpreted from 315 calcified structures, 135 otoliths and 180 spines. Some structures, 4 otoliths and 6 spines, were discarded because of the difficulty in reading, sampling data inconsistencies or being damaged. Precision for spine agers was high and no bias was detected (Table 8.2). Both structures were represented in a wide size range in both ALKs (Table 8.3). In the otoliths based ALK, the samples of 8 and 9 years of age with sizes from 130 to 150 cm SFL are striking. These unusual sizes for 8 and 9 years old specimens can also be appreciated in the spines based ALK (Table 8.3).

In the 2012 ALKs, built with the otolith samples analyzed in the current phase and in previous ones, sizes unusually low for ages 8 and 9 are also observed (Table 8.4). Those age readings were reviewed and confirmed. It could have been a mistake in the size sampling, but they are too many samples to discard them (n = 14) and come from different catch locations, most of them from the Mediterranean Sea (86%), although the two specimens of the Atlantic come from the Strait of Gibraltar and the Gulf of Cadiz, locations very close to the Mediterranean Sea. This fact is also observed in the spine ALK (Table 8.4). And those spines also come from the Mediterranean. Those specimens correspond to the 2002/2003 year classes, which have been considered to be extraordinary abundant (ICCAT, 2015a). This lower length at age may be related to an effect of density-dependence and/or to a lower growth in the Mediterranean bluefin tuna (Hearn and Polacheck, 2003; Santamaria et al., 2009). No differences were observed in the mean SFL by age for both structures based ALKs, although the otoliths ALK presented greater length variability by age (Table 8.4). Mean lengths at age from both structures ALKs showed similar values with the ICCAT currently adopted growth curve (Cort, 1991), but from age 8 ALK values are slightly higher (Figure 8.1).

The ALKs by ocean/sea present also some variability of sizes by age and numerous length bins without age (Table 8.5). It is necessary to analyze a greater number of samples so that the annual keys by ocean/sea have an adequate number of samples per size. Mean length at age differences were observed for ages 6 to 9 between both ALKs and with ICCAT adopted growth curve, with higher values for the Atlantic Ocean based ALK (Table 8.5, Figure 8.1). Also appeared a high standard deviation at ages 8 and 9, notably in the Mediterranean ALK (Table 8.5).

References

Busawon, D.S., Rodriguez-Marin, E., Luque, P.L., Allman, R., Gahagan, B., Golet, W., Koob, E., Siskey, M,, Ruiz, M., Quelle, P. 2015. Evaluation of an Atlantic bluefin tuna otolith reference collection. Collect Vol Sci Pap ICCAT 71: 960-982

Campana, S.E., Annand, M.C., Mcmillan, J.I. 1995. Graphical and statistical methods for determining the consisteny of age determinations. T Am Fish Soc.. 124:131-138

Cort, J.L., 1991. Age and growth of the bluefin tuna, Thunnus thynnus (L.) of the Northeast Atlantic. Collect Vol Sci Pap ICCAT 35:, 213-230.

Hearn, W.S., Polacheck, T., 2003. Estimating long-term growth-rate changes of southern bluefintuna (Thunnus maccoyii) from two periods of tag-return data. Fish. Bull. 101: 58-74.

ICCAT, 2015a. Report of the 2014 Atlantic bluefin tuna Stock Assessment Session (Madrid, September 2014). Collect. Vol. Sci. Pap. ICCAT, 71(2): 692-945

ICCAT. 2015b. Report of the 2015 ICCAT Bluefin Data Preparatory Meeting (Madrid, March 2015).

ICCAT. 2016. Report of the 2016 ICCAT Bluefin Data Preparatory Meeting (Madrid, July 2016).

Luque, P.L., Rodriguez-Marin, E., Ruiz, M., Quelle, P., Landa, J., Macias, D., Ortiz deUrbina, J.M. 2014. Direct ageing of Thunnus thynnus from the east Atlantic and western Mediterranean using dorsal fin spines. J. Fish. Biol. 84, 1876–1903.

McBride. R.S. 2015. Diagnosis of paired age agreement: a simulation of accuracy and precision effects. ICES Journal of Marine Science; doi:10.1093/icesjms/fsv047.

Rodriguez-Marin, E., Luque, P.L., Ruiz, M., Quelle, P., Landa, J., 2012. Protocol for sampling, preparing and age interpreting criteria of Atlantic bluefin tuna (Thunnus thynnus) first dorsal fin spine sections. Collect. Vol. Sci. Pap. ICCAT 68 (1): 240–253.

Rodriguez-Marin, E., Ortiz de Urbina, J.M., Alot, E., Cort, J.L., De la Serna, J.M., Macias, D., Rodríguez-Cabello, C., Ruiz, M., Valeiras, J., 2009. Tracking bluefin

tuna cohorts from east Atlantic Spanish fisheries since the 1980s. Collect. Vol. Sci. Pap. ICCAT 63, 121-132.

Rodriguez-Marin, E., Quelle, P, Ruiz, M., Busawon, D., Golet, W., Dalton, A., Hanke, A. 2016a. Updated comparison of age estimates from paired calcified structures from Atlantic bluefin tuna. ICCAT SCRS/2016/134

Rodriguez-Marin, E., Quelle, P., Ruiz, M., Luque, P., 2016b. Standardized age-length key for east Atlantic and Mediterranean bluefin tuna based on otoliths readings. Collect. Vol. Sci. Pap. ICCAT 72: 1365-1375.

Santamaría, N., Bello, G., Corriero, A., Deflorio, M., Vassallo-Agius, R., Bök, T., Metrio, G.D., 2009. Age and growth of Atlantic bluefin tuna, Thunnus thynnus (Osteichthyes: Thunnidae), in the Mediterranean Sea. J Apple. Ichthyol 25, 38-45.

Secor, D.H., Allman, R., Busawon, D., Gahagan, B., Golet, W., Koob, E., Luque, P.L., Siskey, M. 2014. Standardization of otolith-based ageing protocols for Atlantic bluefin tuna. Collect. Vol. Sci. Pap. ICCAT 70: 357-363

Table 8.1. Number of selected calcified structures for ageing analyses for the sixth phase of the biological project Numbers by 10 cm length class (straight fork length, SFL), ocean / sea (Atlantic NE and Mediterranean) and fishing gear (bait boat, long line, purse seine, trap, troll and hand line).

Size bin (SFL, cm)	Spines				Otholits		
	2012		2013	Total	2012		Total
	AtlNE	Med	Med		AtlNE	Med	
40-49		14		14		6	6
50-59	6			6		1	1
60-69	8			8	6		6
70-79	7	6		13	3	3	6
80-89	6	6		12	3	2	5
90-99	7	2		9	3		3
100-109	6	6		12	2	3	5
110-119	4	1		5			
120-129	6			6	2	3	5
130-139	6			6	3	12	15
140-149	4	5		9	2	11	13
150-159	6	11		17		14	14
160-169	5	4	1	10		3	3
170-179	6	4	4	14	3		3
180-189	4	1	3	8	3	3	6
190-199	5	3		8	3	8	11
200-209	6	2		8	5	5	10
210-219	10	1		11	9	3	12
220-229	3			3	6		6
230-239					3	1	4
240-249		1		1		2	2
250-259			1	1		1	1
260-269	1	2		3	1		1
270-279			2	2		1	1
Fish. gear							
BB	70	11		81	28	5	33
LL	9	30		39	3	41	44
PS		10	11	21		9	9
TRAP	27	17		30	26	24	50
TROL / HAND		1		1		3	3
Total	106	69	0 11	186	57	82	139

Table 8.2. Diagnosis of paired age agreement for spines. Precision indices: CV = Coefficient of Variation, APE = Average Percent Error and tests of symmetry. Symmetry tests: df = degrees of freedom, chi.sq = chi-squared test, p = p-value. MRS, ECR correspond to readers' initials.

Spines ageing error	Precision		Symmetry tests			
	CV	APE		df	chi.sq	*p*
Both readers (n=180)	2.68	1.90		-		
MRS vs consensus (n=180)	1.20	0.85	EvansHoenig	3	1.286	7.33E-01
			Bowkers	10	11.667	3.08E-01
ECR vs consensus (n=180)	1.48	1.05	EvansHoenig	2	2.882	2.37E-01
			Bowkers	11	11.476	4.04E-01

Table 8.3. Atlantic bluefin age-length key built up with samples coming from sixth phase of the project. Numbers by 10 cm length class (straight fork length, SFL). Upper table for otoliths and bottom table for spines.

Otoliths Estimated age

SFL (cm)	0	1	2	3	4	5	6	7	8	9	10	11	12	13	14	15	16	17	18	Total n
40-50	6																			6
50-60			1																	1
60-70		5	1																	6
70-80		1	2	3																6
80-90			1	3																4
90-100			2	1																3
100-110			1	3	1															5
110-120																				0
120-130					1	3	1													5
130-140				1	1	2	6	2	2	1										15
140-150					1		2	2	4	4										13
150-160					1	3	3	5	2											14
160-170								2			1									3
170-180								1	1	1										3
180-190								1	1	1		1	1							5
190-200								1	3	4	3									11
200-210								1	2	5		1								9
210-220								2	3	3	1	2	1							12
220-230									1	3		2								6
230-240												1	1			1				3
240-250																	1		1	2
250-260														1						1
260-270																			1	1
270-280																1				1
Total	6	6	8	11	5	8	12	17	19	22	5	7	3	1	0	2	1	0	2	135

Spines Estimated age

SFL (cm)	0	1	2	3	4	5	6	7	8	9	10	11	12	13	14	15	16	17	18	Total n
40-50	13	1																		14
50-60	1	5																		6
60-70		7																		7
70-80			13																	13
80-90		1	8	3																12
90-100			2	7																9
100-110			1	9	2															12
110-120				3	2															5
120-130					5	1														6
130-140					3	3														6
140-150					1	3	4													8
150-160						8	5	3	1											17
160-170							6	1	1	1										9
170-180							5	5	3	1										14
180-190							3	3	1											7
190-200								2	2	3	1									8
200-210									6	1		1								8
210-220									1	8	1			1						11
220-230									1	1	1									3
230-240																				0
240-250															1					1
250-260																				0
260-270														1	2					3
270-280														1						1
Total	14	14	24	22	13	15	23	14	16	15	3	1	0	3	3	0	0	0	0	180

Table 8.4. Age length key for Atlantic bluefin caught in 2012 built up with samples coming from several phases of the project. Numbers represent percent by number by 10 cm length class (straight fork length, SFL). Upper table for otoliths and bottom table for spines. Mean SFL and standard deviation (SD) by age are shown.

Otoliths Estimated age

SFL (cm)	0	1	2	3	4	5	6	7	8	9	10	11	12	13	14	15	16	17	18	Total n
40-50	100																			6
50-60			100																	1
60-70		83	17																	6
70-80		17	33	50																6
80-90			40	60																5
90-100			67	33																3
100-110			17	50	33															6
110-120					60	20	20													5
120-130					14	57	29													7
130-140				5	14	23	36	9	9	5										22
140-150					11	6	11	17	33	22										18
150-160					5	15	30	40	10											20
160-170							15	46	31		8									13
170-180								44	22	22	11									9
180-190								25	17	8	17	25	8							12
190-200								4	30	43	17	4								23
200-210								6	16	32	16	16	4	8	2					50
210-220								11	11	20	18	31	4	2		2				45
220-230									8	16	20	44	8	4						25
230-240									18	6	18	29	6	6	6	12				17
240-250									7	21	14		29		7		14		7	14
250-260													25	50	25					4
260-270													33		33				33	3
270-280																100				1
280-289																		100		1
Total	6	6	9	11	12	14	21	35	44	51	34	42	14	9	5	4	2	1	2	322
Mean SFL	41	65	81	94	127	136	142	173	188	201	211	215	229	222	237	237	245	281	256	
SD SFL	0.8	5.6	16	17	16	11	14	24	31	24	17	12	23	22	23	25	1.7		9.7	

0-20%
20-50%
50-100%

Spines Estimated age

SFL (cm)	0	1	2	3	4	5	6	7	8	9	10	11	12	13	14	15	16	17	18	Total n
40-50	93	7																		14
50-60	17	83																		6
60-70		100																		12
70-80			100																	13
80-90		8	67	25																12
90-100			29	57	14															14
100-110			8	69	23															13
110-120				38	46	15														13
120-130				6	65	29														17
130-140				5	18	55	23													22
140-150					12	35	41	6	6											17
150-160						33	41	19	7											27
160-170							38	31	15	15										13
170-180							23	31	38	8										13
180-190							20	40	10	30										10
190-200								19	38	25	19									16
200-210								3	38	41	7	10								29
210-220									5	55	27	5		9						22
220-230									11	33	56									9
230-240											17	67	17							6
240-250											20	40	20	10	10					10
250-260												50					50			2
260-270														25	75					4
270-280																				0
Total	14	19	26	27	28	34	33	22	30	37	19	13	3	4	4	0	1	0	0	314
Mean SFL	42	63	82	103	121	139	153	173	191	204	217	230	240	236	258		251			
SD SFL	4.7	6.4	7.5	11	13	12	14	16	20	15	13	17	4.9	26	8.8					

Table 8.5. Age length key for Atlantic bluefin caught in 2012 built up with samples coming from several phases of the project. Estimated ages from otoliths and spines were combined (spines aged older than 13 years were not used). Numbers represent percent by number by 10 cm length class (straight fork length, SFL). Upper table for Atlantic Ocean and bottom table for the Mediterranean Sea. Mean SFL and standard deviation (SD) by age are shown.

Atlantic Otoliths & spines estimated age

SFL (cm)	0	1	2	3	4	5	6	7	8	9	10	11	12	13	14	15	16	17	18	Total n
40-50																				0
50-60	17	83																		6
60-70		92	8																	13
70-80		10	90																	10
80-90		13	75	13																8
90-100			30	70																10
100-110			11	67	22															9
110-120				43	43	14														7
120-130					56	33	11													9
130-140					33	44	22													9
140-150						43	29		14	14										7
150-160						67	33													6
160-170							46	38	15											13
170-180							25	33	17	17	8									12
180-190								50	20		20	10								10
190-200								7	21	50	14	7								14
200-210								7	14	26	16	21	5	9	2					43
210-220								10	10	24	22	24	5	2		2				41
220-230									9	23	14	45	5	5						22
230-240									25	8	17	25	8	0	8	8				12
240-250										25	13		38		13		13			8
250-260														50	50					2
260-270													33		33				33	3
270-280																				0
280-289																		100		1
Total	1	19	20	17	13	15	16	22	25	39	27	34	10	7	5	2	1	1	1	275
Mean SFL	58	64	82	101	122	139	155	187	201	207	212	215	230	216	237	220	244	281	263	
SD SFL		6	8.8	7.7	9.3	13	15	17	24	18	15	10	21	20	23	14				

0-20%
20-50%
50-100%

Mediterranean Otoliths & spines estimated age

SFL (cm)	0	1	2	3	4	5	6	7	8	9	10	11	12	13	14	15	16	17	18	Total n
40-50	93	7																		14
50-60			100																	1
60-70																				0
70-80			67	33																9
80-90			44	56																9
90-100			43	29	29															7
100-110			11	67	22															9
110-120				25	50	13	13													8
120-130				7	50	36	7													14
130-140				7	11	29	36	7	7	4										28
140-150					14	10	14	19	29	14										21
150-160					4	13	33	38	13											24
160-170							9	45	27	9	9									11
170-180								50	33	17										6
180-190										25		50	25							4
190-200								9	36	27	27									11
200-210									40	50	10									10
210-220								17	17			67								6
220-230											50	25	25							4
230-240											20	40		20		20				5
240-250									17	17	17		17				17		17	6
250-260													50	50						2
260-270														100						1
270-280																100				1
Total	13	1	15	21	22	19	24	25	26	16	9	9	4	3	0	2	1	0	1	211
Mean SFL	41	48	81	100	124	135	141	160	173	184	210	214	226	252		254	246		249	
SD SFL	1		12	17	16	11	13	17	30	29	24	17	31	17		24				

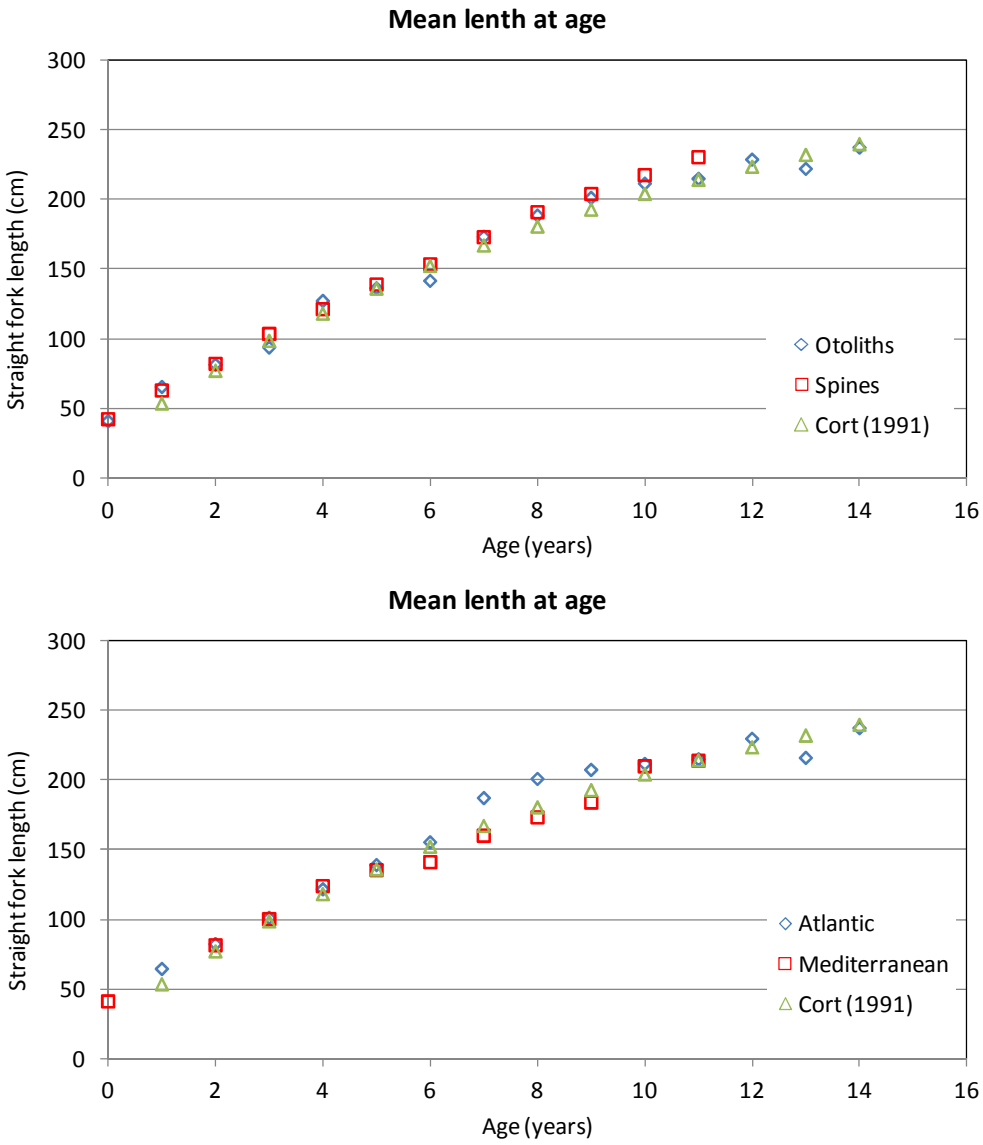

Figure 8.1. Mean length at age from present study 2012 ALKs and from the growth curve currently adopted by ICCAT (Cort, 1991). Are only shown mean lengths at age for ages with at least 5 samples read.

9. APPENDICES

APPENDIX 1. Individual probabilities of belonging to the western population based on QDFA analysis of otolith stable isotope composition.

general ID	FISHING GEAR	Date [dd/mm/yyyy]	Latitude	Longitude	Subyear	ICCAT Area	prob (0-1) Western QDFA (80%)
INRH-MO-L-247	TRAP	4/5/15	35.12	-6.28	2	SE_ATL	0.198
INRH-MO-L-248	TRAP	4/5/15	35.12	-6.28	2	SE_ATL	0.505
INRH-MO-L-249	TRAP	4/5/15	35.12	-6.28	2	SE_ATL	0.077
INRH-MO-L-250	TRAP	4/5/15	35.12	-6.28	2	SE_ATL	0.100
INRH-MO-L-251	TRAP	4/5/15	35.12	-6.28	2	SE_ATL	0.083
INRH-MO-L-252	TRAP	4/5/15	35.12	-6.28	2	SE_ATL	0.089
INRH-MO-L-253	TRAP	4/5/15	35.12	-6.28	2	SE_ATL	0.014
INRH-MO-L-254	TRAP	4/5/15	35.12	-6.28	2	SE_ATL	0.091
INRH-MO-L-255	TRAP	4/5/15	35.12	-6.28	2	SE_ATL	0.467
INRH-MO-L-256	TRAP	4/5/15	35.12	-6.28	2	SE_ATL	0.011
INRH-MO-L-257	TRAP	4/5/15	35.12	-6.28	2	SE_ATL	0.083
INRH-MO-L-258	TRAP	4/5/15	35.12	-6.28	2	SE_ATL	0.316
INRH-MO-L-259	TRAP	4/5/15	35.12	-6.28	2	SE_ATL	0.209
INRH-MO-L-260	TRAP	4/5/15	35.12	-6.28	2	SE_ATL	0.667
INRH-MO-L-261	TRAP	4/5/15	35.12	-6.28	2	SE_ATL	0.010
INRH-MO-L-262	TRAP	5/5/15	35.12	-6.28	2	SE_ATL	0.061
INRH-MO-L-263	TRAP	5/5/15	35.12	-6.28	2	SE_ATL	0.170
INRH-MO-L-264	TRAP	5/5/15	35.12	-6.28	2	SE_ATL	0.461
INRH-MO-L-265	TRAP	5/5/15	35.12	-6.28	2	SE_ATL	0.179
INRH-MO-L-266	TRAP	5/5/15	35.12	-6.28	2	SE_ATL	0.683
INRH-MO-L-267	TRAP	5/5/15	35.12	-6.28	2	SE_ATL	0.034
INRH-MO-L-268	TRAP	5/5/15	35.12	-6.28	2	SE_ATL	0.170
INRH-MO-L-269	TRAP	5/5/15	35.12	-6.28	2	SE_ATL	0.167
INRH-MO-L-270	TRAP	5/5/15	35.12	-6.28	2	SE_ATL	0.373
INRH-MO-L-271	TRAP	5/5/15	35.12	-6.28	2	SE_ATL	0.103
INRH-MO-L-272	TRAP	5/5/15	35.12	-6.28	2	SE_ATL	0.044
INRH-MO-L-273	TRAP	5/5/15	35.12	-6.28	2	SE_ATL	0.846
INRH-MO-L-274	TRAP	5/5/15	35.12	-6.28	2	SE_ATL	0.034
INRH-MO-L-275	TRAP	9/5/15	35.12	-6.28	2	SE_ATL	0.894
INRH-MO-L-276	TRAP	9/5/15	35.12	-6.28	2	SE_ATL	0.065
INRH-MO-L-277	TRAP	9/5/15	35.12	-6.28	2	SE_ATL	0.891
INRH-MO-L-278	TRAP	9/5/15	35.12	-6.28	2	SE_ATL	0.629
INRH-MO-L-279	TRAP	9/5/15	35.12	-6.28	2	SE_ATL	0.902
INRH-MO-L-280	TRAP	9/5/15	35.12	-6.28	2	SE_ATL	0.188
INRH-MO-L-281	TRAP	9/5/15	35.12	-6.28	2	SE_ATL	0.891
INRH-MO-L-282	TRAP	9/5/15	35.12	-6.28	2	SE_ATL	0.379

INRH-MO-L-283	TRAP	9/5/15	35.12	-6.28	2	SE_ATL	0.749
INRH-MO-L-284	TRAP	9/5/15	35.12	-6.28	2	SE_ATL	0.175
INRH-MO-L-285	TRAP	9/5/15	35.12	-6.28	2	SE_ATL	0.731
INRH-MO-L-286	TRAP	9/5/15	35.12	-6.28	2	SE_ATL	0.503
INRH-MO-L-287	TRAP	9/5/15	35.12	-6.28	2	SE_ATL	0.610
INRH-MO-L-288	TRAP	9/5/15	35.12	-6.28	2	SE_ATL	0.291
INRH-MO-L-289	TRAP	9/5/15	35.12	-6.28	2	SE_ATL	0.264
INRH-MO-L-290	TRAP	9/5/15	35.12	-6.28	2	SE_ATL	0.916
INRH-MO-L-291	TRAP	9/5/15	35.12	-6.28	2	SE_ATL	0.257
INRH-MO-L-292	TRAP	9/5/15	35.12	-6.28	2	SE_ATL	0.012
INRH-MO-L-293	TRAP	9/5/15	35.12	-6.28	2	SE_ATL	0.102
INRH-MO-L-294	TRAP	9/5/15	35.12	-6.28	2	SE_ATL	0.051
INRH-MO-L-295	TRAP	9/5/15	35.12	-6.28	2	SE_ATL	0.876
INRH-MO-L-296	TRAP	9/5/15	35.12	-6.28	2	SE_ATL	0.304
IEO-CI-L-90	BB	9/3/15	28.27	-16.98	1	SE_ATL	0.165
IEO-CI-L-91	BB	9/3/15	28.27	-16.98	1	SE_ATL	0.233
IEO-CI-L-92	BB	9/3/15	28.27	-16.98	1	SE_ATL	0.384
IEO-CI-L-93	BB	9/3/15	28.27	-16.98	1	SE_ATL	0.556
IEO-CI-L-94	BB	9/3/15	28.27	-16.98	1	SE_ATL	0.024
IEO-CI-L-95	BB	12/3/15	28.27	-16.98	1	SE_ATL	0.353
IEO-CI-L-96	BB	12/3/15	28.27	-16.98	1	SE_ATL	0.181
IEO-CI-L-97	BB	13/3/15	28.27	-16.98	1	SE_ATL	0.067
IEO-CI-L-98	BB	13/3/15	28.27	-16.98	1	SE_ATL	0.280
IEO-CI-L-99	BB	16/3/15	28.27	-16.98	1	SE_ATL	0.388
IEO-CI-L-100	BB	16/3/15	28.27	-16.98	1	SE_ATL	0.106
IEO-CI-L-101	BB	16/3/15	28.27	-16.98	1	SE_ATL	0.549
IEO-CI-L-102	BB	16/3/15	28.27	-16.98	1	SE_ATL	0.025
IEO-CI-L-103	BB	17/3/15	28.27	-16.98	1	SE_ATL	0.348
IEO-CI-L-104	BB	17/3/15	28.27	-16.98	1	SE_ATL	0.465
IEO-CI-L-105	BB	17/3/15	28.27	-16.98	1	SE_ATL	0.505
IEO-CI-L-106	BB	17/3/15	28.27	-16.98	1	SE_ATL	0.316
IEO-CI-L-107	BB	16/3/15	28.27	-16.98	1	SE_ATL	0.887
IEO-CI-L-108	BB	16/3/15	28.27	-16.98	1	SE_ATL	0.785
IEO-CI-L-109	BB	16/3/15	28.27	-16.98	1	SE_ATL	0.828
IEO-CI-L-110	BB	16/3/15	28.27	-16.98	1	SE_ATL	0.060
IEO-CI-L-111	BB	16/3/15	28.27	-16.98	1	SE_ATL	0.015
IEO-CI-L-112	BB	16/3/15	28.27	-16.98	1	SE_ATL	0.044
IEO-CI-L-113	BB	9/3/16	27.83	-16.92	1	SE_ATL	0.071
IEO-CI-L-114	BB	9/3/16	27.83	-16.92	1	SE_ATL	0.140
IEO-CI-L-115	BB	9/3/16	27.83	-16.92	1	SE_ATL	0.023
IEO-CI-L-116	BB	9/3/16	27.83	-16.92	1	SE_ATL	0.023
IEO-CI-L-117	BB	9/3/16	27.83	-16.92	1	SE_ATL	0.025
IEO-CI-L-118	BB	10/3/16	27.83	-16.92	1	SE_ATL	0.485
IEO-CI-L-119	BB	10/3/16	27.83	-16.92	1	SE_ATL	0.300

IEO-CI-L-120	BB	10/3/16	27.83	-16.92	1	SE_ATL	0.090
IEO-CI-L-121	BB	11/3/16	27.83	-16.92	1	SE_ATL	0.114
IEO-CI-L-123	BB	11/3/16	27.83	-16.92	1	SE_ATL	0.086
IEO-CI-L-124	BB	11/3/16	27.83	-16.92	1	SE_ATL	0.288
IEO-CI-L-125	BB	14/3/16	27.83	-16.92	1	SE_ATL	0.708
IEO-CI-L-126	BB	14/3/16	27.83	-16.92	1	SE_ATL	0.082
IEO-CI-L-127	BB	14/3/16	27.83	-16.92	1	SE_ATL	0.361
IEO-CI-L-128	BB	14/3/16	27.83	-16.92	1	SE_ATL	0.282
IEO-CI-L-130	BB	11/3/16	27.83	-16.92	1	SE_ATL	0.034
IEO-CI-L-131	BB	11/3/16	27.83	-16.92	1	SE_ATL	0.449
IEO-CI-L-133	BB	21/3/16	27.83	-16.92	1	SE_ATL	0.010
IEO-CI-L-134	BB	21/3/16	27.83	-16.92	1	SE_ATL	0.230
IEO-CI-L-135	BB	21/3/16	27.83	-16.92	1	SE_ATL	1.000
IEO-CI-L-136	BB	21/3/16	27.83	-16.92	1	SE_ATL	0.246
IEO-CI-L-137	BB	11/3/16	27.83	-16.92	1	SE_ATL	0.046
IEO-CI-L-139	BB	11/3/16	27.83	-16.92	1	SE_ATL	0.055
IEO-CI-L-140	BB	11/3/16	27.83	-16.92	1	SE_ATL	0.245
IEO-CI-L-141	BB	16/3/16	27.83	-16.92	1	SE_ATL	0.273
IEO-CI-L-142	BB	16/3/16	27.83	-16.92	1	SE_ATL	0.821
IEO-CI-L-143	BB	16/3/16	27.83	-16.92	1	SE_ATL	0.557
IEO-CI-L-144	BB	16/3/16	27.83	-16.92	1	SE_ATL	0.824
IEO-CI-L-145	BB	11/3/16	27.83	-16.92	1	SE_ATL	0.112
IEO-CI-L-146	BB	11/3/16	27.83	-16.92	1	SE_ATL	0.103
IEO-CI-L-147	BB		27.83	-16.92	1	SE_ATL	0.156
IEO-CI-L-148	BB	9/3/16	27.83	-16.92	1	SE_ATL	0.064
IEO-CI-L-149	BB	11/3/16	27.83	-16.92	1	SE_ATL	0.628
IEO-CI-L-151	BB	11/3/16	27.83	-16.92	1	SE_ATL	1.000
IEO-CI-L-152	BB	11/3/16	27.83	-16.92	1	SE_ATL	1.000
IEO-CI-L-153	BB	16/3/16	27.83	-16.92	1	SE_ATL	0.120
IEO-CI-L-154	BB	11/3/16	27.83	-16.92	1	SE_ATL	0.981
IEO-CI-L-155	BB	9/3/16	27.83	-16.92	1	SE_ATL	0.783
IEO-CI-L-157	BB	16/3/16	27.83	-16.92	1	SE_ATL	0.926
IEO-CI-L-158	BB	16/3/16	27.83	-16.92	1	SE_ATL	0.308
IEO-CI-L-159	BB	16/3/16	27.83	-16.92	1	SE_ATL	0.456
IEO-CI-L-160	BB	16/3/16	27.83	-16.92	1	SE_ATL	0.452
IEO-CI-L-161	BB	16/3/16	27.83	-16.92	1	SE_ATL	0.063
IEO-CI-L-162	BB	16/3/16	27.83	-16.92	1	SE_ATL	0.546
NRIF-CA-M-96	LL	14/10/14	59.00	-18.00	4	NE_ATL	0.107
NRIF-CA-M-97	LL	15/10/14	59.00	-18.00	4	NE_ATL	0.164
NRIF-CA-M-98	LL	15/10/14	59.00	-18.00	4	NE_ATL	0.048
NRIF-CA-M-99	LL	19/10/14	59.00	-18.00	4	NE_ATL	0.848
NRIF-CA-M-100	LL	30/10/14	59.00	-18.00	4	NE_ATL	0.396
NRIF-CA-M-101	LL	25/10/14	45.00	-48.00	4	W_ATL	0.148
NRIF-CA-L-1226	LL	15/9/14	59.00	-22.00	4	NE_ATL	0.949
NRIF-CA-L-1227	LL	26/8/14	45.00	-42.00	3	NE_ATL	0.207

NRIF-CA-L-1228	LL	26/8/14	45.00	-42.00	3	NE_ATL	0.208
NRIF-CA-L-1233	LL	28/8/14	44.00	-48.00	3	W_ATL	0.408
NRIF-CA-L-1244	LL	2/9/14	45.00	-48.00	4	W_ATL	0.718
NRIF-CA-L-1251	LL	6/9/14	45.00	-48.00	4	W_ATL	0.406
NRIF-CA-L-1254	LL	6/9/14	45.00	-48.00	4	W_ATL	0.043
NRIF-CA-L-1255	LL	6/9/14	45.00	-48.00	4	W_ATL	0.107
NRIF-CA-L-1257	LL	7/9/14	45.00	-48.00	4	W_ATL	0.169
NRIF-CA-L-1258	LL	8/9/14	45.00	-48.00	4	W_ATL	0.058
NRIF-CA-L-1261	LL	9/9/14	45.00	-48.00	4	W_ATL	0.958
NRIF-CA-L-1263	LL	10/9/14	44.00	-48.00	4	W_ATL	0.682
NRIF-CA-L-1265	LL	13/9/14	45.00	-48.00	4	W_ATL	0.179
NRIF-CA-L-1271	LL	14/9/14	44.00	-48.00	4	W_ATL	0.026
NRIF-CA-L-1274	LL	15/9/14	44.00	-48.00	4	W_ATL	0.973
NRIF-CA-L-1280	LL	5/10/14	44.00	-47.00	4	W_ATL	0.533
NRIF-CA-L-1281	LL	17/10/14	42.00	-51.00	4	W_ATL	0.988
NRIF-CA-L-1286	LL	11/11/14	42.00	-52.00	4	W_ATL	0.234
NRIF-CA-L-1289	LL	12/10/14	59.00	-19.00	4	NE_ATL	0.062
NRIF-CA-L-1296	LL	12/10/14	59.00	-19.00	4	NE_ATL	0.181
NRIF-CA-L-1303	LL	13/10/14	59.00	-18.00	4	NE_ATL	0.155
NRIF-CA-L-1306	LL	13/10/14	59.00	-18.00	4	NE_ATL	0.058
NRIF-CA-L-1308	LL	14/10/14	59.00	-18.00	4	NE_ATL	0.053